METABOLIC ENGINEERING OF YEAST STRAINS FOR RENEWABLE BIOMASS UTILIZATION AND VALUABLE CHEMICAL PRODUCTION

BY

HEEJIN KIM

DISSERTATION

Submitted in partial fulfillment of the requirements
for the degree of Doctor of Philosophy in Food Science and Human Nutrition
with a concentration in Food Science
in the Graduate College of the
University of Illinois at Urbana-Champaign, 2017

Urbana, Illinois

Doctoral Committee:

Associate Professor Michael J. Miller, Chair
Associate Professor Yong-Su Jin, Director for Research
Associate Professor Manabu T. Nakamura
Professor Christopher Rao

ABSTRACT

The overall goal of this thesis study is to use metabolic engineering and biotechnology tools for developing optimal yeast strains capable of utilizing various sugars derived from renewable biomass and produce valuable chemicals. Sugars derived from lignocellulosic biomass, mainly cellobiose and xylose, cannot be assimilated by the industrial microorganisms, such as yeast *Saccharomyces cerevisiae.* To utilize cellobiose or xylose for the fuels and chemicals production by *S. cerevisiae* strains, heterologous expression of cellobiose or xylose metabolizing genes are required. The first part of this dissertation focuses on developing optimal yeast strains for utilizing renewable sugars, cellobiose, xylose and galactose, and understanding underlying mechanism for improvement on lignocellulosic sugar utilization.

Initially, cellobiose fermenting *S. cerevisiae* was developed by expressing *Neurospora crassa* cellodextrin transporters (CDT-1 and CDT-2) and β-glucosidase (BGL) or cellobiose phosphorylase (CBP) to breakdown cellobiose into hexose units. In various cellobiose fermentation conditions, the strains expressing CDT-1 showed efficient fermentation compared to the strains expressing CDT-2. Also, strains expressing BGL had better cellobiose fermentation compared to CBP. However, I hypothesized expressing CDT-2 and CBP might have a beneficial effect under energy-limiting conditions (such as industrial fermentation environment) due to minimal ATP requirement compare to pairing with/or CDT-1 and BGL. Because the rate of cellobiose fermentation with CDT-2 and CBP were very inefficient, laboratory evolution approach was employed to enhance cellobiose utilization. I isolated an evolved strain that harbored one SNP change in CDT-2 that is responsible for enhanced cellobiose utilization. With evolved CDT-2 and CBP, cellobiose fermentation rate improved drastically.

Previous studies successfully developed xylose-utilizing *S. cerevisiae* strain. However, the overall fermentation efficiency of the strain is relatively poor. Additionally, using different strain backgrounds resulted in various patterns of the xylose utilization. This variation is presumably caused by the genotype differences among the strains. Thus, I hypothesized the xylose-utilizing trait is a complex trait which phenotypes result from a multiple genes interaction. Quantitative Trait Locus (QTL) mapping strategy was used to identify 'hotspots' in the genome responsible for enhanced xylose utilization. The identified QTLs reveal that enhanced xylose fermentations are likely very complex due to many detected QTL. Also, previously reported

gene targets that may improve xylose fermentation was not detected. This result indicates complex genetic interactions are responsible for xylose fermentation. Although specific genetic targets were not identified, our results show genome shuffling of two highly variable strains is a very effective methodology to obtain an efficient xylose-fermenting strain with minimal genetic engineering.

Galactose is abundantly found in marine biomass and hemicellulose from plant cell wall. Although yeast can naturally metabolize galactose, consumption rate and overall ethanol yield are usually lower compared to glucose. While screening various gene targets related glucose sensing, regulation and metabolism, *TPS1* deletion expressed with mutant *HXK2* allowed enhanced glucose or galactose fermentation. Because *HXK2* also has a role in glucose signaling and repression, a mutation caused a change in this property. By deleting *TPS1* and expressing mutant *HXK2,* yeast effectively utilized glucose and galactose under mixed sugar condition whereas wild-type strain could not consume galactose in the presence of glucose.

Following renewable sugar utilization by engineered strain, the second part of this dissertation investigates on chemical production by engineered yeast. To replace current chemical production system, diversification of product formation by the microbial system is necessary. I identified 2-isopropylmalate (2-IPM), and intermediate of leucine biosynthesis, as a target chemical production in yeast. The dicarboxylic organic acids are favorable for production due to possible bio-based polymer synthesis. I observed 2-IPM accumulation by deleting *LEU1* and further optimized the strain by removing nitrogen catabolite repression (Δ*URE2*), leucine feedback inhibition (mutant *LEU4*) and increase pyruvate flux to leucine biosynthetic pathway (*Bacillus subtilis AlsS*). Also, fermentation media optimization was performed. From no accumulation of 2-IPM by wildtype yeast, 0.033 g/g yield was achieved by optimizing strain and fermentation condition. At scale-up fermentation, 2-IPM titer reached 25 g/L by glucose-limited fed-batch strategy. After 2-IPM overproduction had been achieved, various prospective applications were explored. First, polymer synthesis derived from 2-IPM was investigated. By converting 2-IPM to anhydride form then reaction with epoxide yielded biodegradable elastomer. Also, taking advantage of the organic acid identity of 2-IPM and skin-whitening effect by inhibiting melanin formation was investigated.

In summary, this research demonstrates effective metabolic strategy employed for developing yeast strains capable of fermenting lignocellulosic sugars and diversified chemical production by discovering new target chemical with many projected applications.

ACKNOWLEDGEMENT

I would like to thank my advisor Dr. Yong-Su Jin for his guidance, training, and patience to my endless drafts. I would also like to thank my committee members Drs. Dawn M. Bohn, Hao Feng, Youngsoo Lee, Michael Miller, Manabu T. Nakamura and Christopher Rao. They served as a committee on my qualifying exam, preliminary exam, and defense. Especially, Drs. Michael Miller, Manabu T. Nakamura and Christopher Rao served on my preliminary exam and final defense and gave valuable advice, scientific insights, and guidance.

I would also like to thank all former and current colleagues in Dr. Jin's Lab. All of them were very kind it was a privilege to work with them. Especially, I would like to express great appreciation to Drs. Suk-Jin Ha, Won-Heong Lee, Jin-Ho Choi, Hyo-Jin Kim, Soo Rin Kim and Eun Joong Oh. They not only trained me when I started as an undergraduate researcher, but have been patient with me and encouraged me through the times when I struggled. They have been great mentors throughout my graduate years, and I owe the success of this dissertation to them. Also, I would like to thank many collaborators in various places: Drs. Jamie Cate (UCB), Adam Arkin (UCB), Jeff Skerker (UCB), Matthew Maurer (UCB), Kyung Heon Kim (KU), Eun-Ju Yun (KU), Damien Guironnet (UIUC), and Camille Boucher (UIUC). This study would not have been possible without generous funding from the Energy Biosciences Institute (EBI) and encouragement from Dr. Isaac Cann.

Next, I would like to thank all my friends and family. My parents had supported and encouraged me unconditionally through all times. I also would like to thank my friend, Seunghwi Kim for his support and encouraging me to dream big. Although our fields of study are very different, by numerous discussions, debates, and informative conversations, it broadened my knowledge and view and helped to embody my dreams.

TABLE OF CONTENTS

CHAPTER I: Introduction to Microbial Engineering for Sustainable Fuels and Chemical Production Process 1

CHAPTER II: Analysis of Cellodextrin Transporters from *Neurospora Crassa* in *Saccharomyces cerevisiae* for Cellobiose Fermentation 13

CHAPTER III: Enhanced Cellobiose Fermentation by Engineered *Saccharomyces cerevisiae* Expressing a Mutant Cellodextrin Facilitator and Cellobiose Phosphorylase 29

CHAPTER IV: QTL Mapping Analysis for Enhanced Xylose Utilization in Engineered *Saccharomyces cerevisiae* 47

CHAPTER V: Enhanced Glucose and Galactose Fermentation by Engineered Yeast Harboring *TPS1* Deletion and Mutant *HXK2* 64

CHAPTER VI: Yeast to Rubber: Sustainable Production of Novel Polymers from Novel Molecule 84

CHAPTER VII: Potential Applications of 2-IPM: Novel Skin-Brightening Agent 102

CHAPTER VIII: Summary and Future Studies 111

REFERENCE 114

CHAPTER I: Introduction to Microbial Engineering for Sustainable Fuels and Chemical Production Process

1.1 General Introduction

As human society and population have grown, the demand of commodity fuels and chemicals also increased. To supply the increasing demands, utilization energy sources such as fossil fuels prospered. Most of current fuels and chemicals production directly or indirectly utilizes non-renewable and unsustainable fossil fuel resources. For example, predominant fuels such as gasoline and jet fuels are processed directly from fossil fuels. Also, chemicals such as olefins and aromatics, widely used across all industries, are petrochemicals [1, 2]. Fossil fuels became an essential energy source, and humans rely heavily on making up approximately 80% of overall energy needs [2, 3]. Although fossil fuel-based fuels and chemical productions are well-established, the current process is frequently challenged for its sustainability for the future [1].

There are two primary problems that fossil fuels disqualify for future resources. Fossil fuels are resources that formed around 370 million years ago during the Carboniferous age. Because fossilization process takes millions of years, fossil fuel based resources are considered finite. However, the current rate of fossil fuel usage greatly outpaces the rate of its formation. At the current rate of fossil fuel usage, fossil fuels are likely to go extinct in 40-50 years [4]. Fossil fuels are simply non-renewable and unsustainable resources for the future. Secondly, fossil fuels cause a detrimental effect on the environment. When fossil fuels are burnt, major air pollutants are produced. Among pollutant, production of carbon dioxide, one of the greenhouse gasses, became a strong concern due to its major responsibility of causing climate change and global warming [4-7].

Many alternative solutions have been proposed to resolve the current issue faced by fossil fuels. Among many proposed solutions, synthesis of bio-based and renewable products have gained global interest [8]. Prominently, production of fuels and chemicals using microbes expanded rapidly over the last few decades gradually replacing current petroleum refineries [9, 10]. For example, bioethanol production by yeast fermenting corn or sugarcane-derived sugars are widely accepted in the society [11]. Despite the successfulness of bioethanol production by

yeast, however, its production from food crops are highly controversial due to limited arable land and increasing food scarcity [2, 12, 13]. Additionally, production of bioethanol only can replace a small fraction of current fossil fuel based chemical production [14, 15]. Thus, to overcome major challenges for microbial synthesis of fuels and chemicals, at least three specific characteristics should be considered: 1) capable of metabolizing non-food and renewable resources *efficiently* and *rapidly*, and 2) capable of producing targeted chemicals. To address the challenges by current microbial synthesis, methodologies from metabolic engineering and synthetic biology have been employed.

1.2 Microbial fermentation with renewable resources

Current biorefineries producing fuels and chemicals by microbial fermentations require fermentable substrates (feedstock). Commonly, sugars derived from sugarcane or corn starch have been used for a long time as the fermentable resources [16, 17]. Glucose and fructose are the major sugars derived from sugarcane and corn and fermented by *Saccharomyces cerevisiae*, traditional industrial yeast. However, recent ethical criticism of using food resources for fuels and chemical production directed researchers to find alternate non-nutritious feedstocks [18]. Also, utilizing sugarcane and corn feedstocks is unsustainable because the current production of these crops is limited for replacing all fuels and chemical needs as well as using as a food source [18]. Thus, utilizing non-food, sustainable and renewable sources such as lignocellulosic biomass from agricultural residues, wood wastes, or energy crops and marine biomass from red seaweed has been proposed replacing the feedstock from sugarcane and corn [13, 19-21].

Lignocellulosic biomass is composed of carbohydrate polymers (cellulose and hemicellulose), that are tightly bound to lignin. Thus, pretreatment and hydrolysis of lignocellulosic biomass are necessary to release fermentable sugars. During hydrolysis process, both hexose and pentose sugars are released, among which glucose and xylose are major sugars [22]. Then glucose and xylose can be utilized as a substrate for microbial fermentations. In the case of marine macroalgae, galactose is major hexose sugar obtained from hydrolysis process that can be used as the substrate [13, 23]. Therefore, efficient utilization of renewable

sugars in the placement of glucose from sugarcane or corn is the key to establishing a feasible and sustainable process for the fuel and chemical production.

Xylose utilization by *S. cerevisiae*

At industrial scale production of fuels and chemicals, host microorganisms should be able to metabolize the given substrates and produce the target chemicals efficiently and productively [24]. *Saccharomyces cerevisiae*, a robust and efficient yeast strain capable of converting glucose to ethanol, is commonly used for microbial fermentations due to its capacity at an industrial scale. However, native *S. cerevisiae* lacks metabolic pathways to utilize xylose. Therefore, the species cannot metabolize xylose to produce a target chemical. To allow xylose fermentation by *S. cerevisiae*, a xylose assimilation pathway should be introduced to the strain.

Numerous studies attempted to engineer the *S. cerevisiae* strain capable of fermentation xylose during last decade [25-30]. Commonly, the xylose-fermenting *S. cerevisiae* strains are developed by heterologous expression of fungal xylose reduction-oxidation (XR/XDH) pathway or bacterial xylose isomerization (XI) pathway. The XR/XDH pathway taken from native xylose-fermenting yeast such as *Scheffersomyces stipitis* consists of expressing three primary genes, *XYL1, XYL2* and *XYL3* encoding xylose reductase, xylitol dehydrogenase and xylulokinase, respectively (Figure 1.2A) [28, 30-32]. Xylose is reduced to xylitol by XR with cofactor NAD(P)H followed by oxidation of xylitol to xylulose by XDH with cofactor NAD^+. Xylulose is phosphorylated to xylulose-5-phosphate by XK then metabolized further via pentose phosphate pathway that is native to *S. cerevisiae*. Although native xylulokinase (encoded by *XKS1*) exists in *S. cerevisiae*, often XK from *S. stipitis* is co-expressed with XR and XDH for optimized expression with *XYL1* and *XYL2* [29, 30]. The heterologous expression will allow xylose fermentation in engineered *S. cerevisiae*. However, the introduction of enzymes requiring additional cofactors breaks the natural cofactor balance allowing intermediate product accumulation, especially xylitol [25, 33]. Unfavorable intermediate accumulation reduces the efficiency of the designed pathway and creates a cost-ineffective process. Also, cofactor imbalance can affect the efficiency of the pathway, reducing the xylose consumption rate [33, 34]. On the other hand, the XI pathway typically taken from *Piromyces* sp. consists of *xylA* encoding for xylose isomerase and overexpression of xylulokinase [35-37]. Xylose isomerase allows direct conversion of xylose to xylulose and converts to xylulose-5-phosphate by either heterologous or native XK expression. Unlike XR/XDH pathway, XI pathway does not require

additional cofactors. Thus, efficient xylose fermentation under anaerobic conditions and higher ethanol yield is permitted.

Despite the extensive research to enable efficient xylose fermentation with engineered yeast, fermentative yield and productivity using either XR/XDH or XI pathway have not reached the level of glucose fermentation. Thus, several researchers directed their efforts to identify and resolve the bottlenecks of efficient xylose fermentation. Initially, the effective of overexpression of pentose phosphate enzymes was investigated. In general, overexpression helped to increase xylose fermentation capability [37-40]. Specifically, overexpression of *TAL1*, encoding transaldolase converting sedoheptulose 7-phosphate and glyceraldehyde 3-phosphate to erythrose 4-phosphate and fructose 6-phosphate, have shown to increase the efficiency of xylose fermentation significantly [16]. Still, however, xylose fermentation is not comparable to glucose fermentation in yeast. Further elucidation of xylose metabolism in yeast remains unsolved.

Advantage and remaining challenges of using cellobiose as a fermentable sugar

The cellulose component from lignocellulose is primarily composed of glucose units bound by a strong β(1→4) glycosidic linkages. Saccharification of cellulose requires groups of cellulose enzymes, commonly endo-and exoglucanases for hydrolyzing cellulose to cellodextrins and β-glucosidase for hydrolysis of cellodextrin to glucose. However, saccharification of cellulose by a mixture of cellulolytic enzymes can be challenging. As the β-glucosidase activity of fungal cellulolytic enzymes is weak, intermediates of cellulose hydrolysis cellobiose (and cellodextrins) will accumulate to inhibit cellulolytic enzymes. Also, end-product glucose will inhibit overall enzymatic activity lowering the overall efficiency of saccharification process.

Another critical barrier to using lignocellulosic hydrolysate is glucose repression exerted by end-product of cellulose saccharification. As mentioned earlier, main monomeric sugars derived from lignocellulose are glucose and xylose. In the end, microorganisms should be able to consume both sugars simultaneously to allow efficient bioconversion. However, in the presence of glucose, cells prioritize utilization of glucose then consume other sugars only after glucose is depleted from the media. This sequential utilization of sugars is a significant barrier to maximize the efficiency of lignocellulosic hydrolysates.

To bypass both inefficient saccharification process and bottlenecks caused by glucose repression, utilization of cellobiose have been proposed [41]. Cellobiose is a dimer of two glucose units bound by β(1→4) glycosidic linkages and shortest cellodextrin unit from saccharification process without β-glucosidase activity. Hence, cellobiose metabolism mainly will be done by native pathway glycolysis. However, though *S. cerevisiae* is an excellent glucose fermentor, they cannot assimilate cellobiose. Thus, metabolic engineering of *S. cerevisiae* is necessary to enable cellobiose fermentation.

Cellobiose fermentation in *S. cerevisiae* essentially require two additional heterologous expressions: 1) cellodextrin transporter to transport cellobiose into the cell and 2) hydrolyzing enzyme to break cellobiose to monomeric sugar (Figure 1.2B). Previous studies have shown expression of both cellodextrin transporter and hydrolyzing enzyme allows successful cellobiose fermentation in yeast [41-43]. The rate of cellobiose utilization, ethanol yield and productivity and cell growth on cellobiose differs by which transporter is expressed as well as which hydrolyzing enzyme it is co-expressed. There has been considerable debate on which pair of the transporter and the hydrolyzing enzyme is most efficient for yeast cellobiose fermentation.

For cellodextrin transporters, two fungal cellodextrin transporters such as CDT-1(NCU00801) and CDT-2 (NCU08114) from *Neurospora crassa* have been studied extensively [41-46]. CDT-1 was determined to be an active transporter (proton symporter, specifically) and CDT-2 was determined to be a facilitator transporting cellobiose via diffusion [43]. In general, CDT-1 had a superior cellobiose transportation compared to CDT-2. Being a proton symporter, CDT-1 co-transports one proton ion per cellobiose transport. Then yeast cells will pump out extra proton ion via Pma1p to maintain intracellular pH homeostasis and plasma membrane potential. This process requires energy and need extra ATP to use cellobiose as a substrate. On the other hand, CDT-2 does not require proton cotransport allowing no disturbance of intracellular pH homeostasis, therefore, does not require extra energy for cellobiose fermentation. For this reason, regardless of its superior cellobiose transport capability, there has been a significant debate on which transporter, CDT-1 or CDT-2, is more suitable for cellobiose fermentation.

Once cellobiose in transported into the cell, either β-glucosidase (BGL) or cellobiose phosphorylase (CBP) can be used for hydrolysis of cellobiose. The BGL from *N. crassa* can be intracellularly expressed and hydrolyze cellobiose into two units of glucose, then metabolized

via glycolysis. The BGL coupled with CDT-1 or CDT-2 generally have higher cellobiose consumption rate compared to CBP [43]. However, ethanol yield from cellobiose fermentation with BGL is lower. During cellobiose utilization, BGL is very efficient hydrolyzing cellobiose into two glucose units, but also promote transglycosylation activity [47]. Thus, glucose units can bind to cellobiose and create undesired cellodextrins (cellotriose and cellotetraose). In comparison, the CBP from *Saccharophagus degradans* bypasses transglycosylation activity. The CBP directly phosphorylates one of the glucose units from cellobiose yielding one glucose-1-phosphate and one glucose. Then glucose-1-phosphate and glucose can be metabolized by glycolysis [45]. Accordingly, cellobiose fermentation with CBP yields higher ethanol yield. However, the rate of cellobiose conversion by CBP is comparably slower than conversion by BGL. While successful cellobiose fermentation can be achieved by expression CDT-1 or CDT-2 and CBP or BGL, the best system to utilize cellobiose remains problematic.

Galactose utilization by *S. cerevisiae*

Galactose is a monosaccharide sugar abundantly derived from marine biomass such as macroalgae and industrial waste such as cheese whey [48, 49]. Native *S. cerevisiae* can utilize this sugar by Leloir pathway. Galactose is utilized by converting to glucose-6-p in few enzymatic steps, then metabolized via glycolysis (Figure 1.2C). However, due to a tight regulation of if Leloir pathway, specific galactose uptake rates and ethanol yields are significantly lower than glucose [50, 51]. Thus, previous studies attempted to improve galactose utilization by yeast by employing various strategies. For example, Ostergaard et. al. modified expression of galactose metabolic enzymes by deleting negative transcription regulators (*GAL6, GAL80,* and *MIG1*) and overexpressing transcription activator (*GAL4*) [52]. Additionally, *SNR84* (encoding small nuclear RNA), *TUP1* (general transcription repressor), and *RAS2* (encoding for GTP-binding protein) [53, 54] were identified as gene targets affecting galactose metabolism. Despite many efforts of previous studies to improve galactose fermentation in *S. cerevisiae,* clear galactose metabolism governing mechanisms have not been elucidated that is necessary to improve galactose fermentation in yeast can be achieved.

1.3 Value-added product formation by engineered yeast

Many of current chemical production rely on fossil-fuel derived resources such as petroleum. These petrochemicals include major chemical classes of olefins (i.e. ethylene, propylene) and aromatics (i.e. benzene, toluene) [55]. These olefins and aromatic chemical compounds are industrially significant and highly demanded due to its wide range of usage, from the synthesis of solvents, detergents, and adhesives. Especially, olefins serve as building blocks for synthesizing polymers used for the synthesis of plastics, fibers, rubber, gels, etc. [55, 56]. Considering current usage and production of even plastics alone (produced over 300 million metric tons annually) [57], petrochemicals are an absolute necessity for modern society. However, due to the unsustainability of fossil fuels, petrochemicals are subjected to be replaced by a sustainable system.

The microbial fermentation system can be a sustainable option to replace current petrochemicals production. By engineering microbes and fermentation processes, I can manipulate the produced metabolite to our favor. Often, utilizing microbes for chemical production can be highly advantageous because complex bioconversion is readily performed [9]. Thus, increasing number of chemical production are attempted to be transferred to the microbial production platform.

Among many targeted chemicals for microbial production, organic acids have been gaining increasing attention from many industries. In general, organic acid, due to its carboxylic group with carbon chain and reactivity, holds great potential to serve as building blocks for synthesizing polymeric compounds [58]. For example, lactic acid can be produced by engineered *S. cerevisiae* with the introduction of heterologous enzyme lactate dehydrogenase [59, 60]. Then, produced lactic acid can go under few chemical reactions to produce polylactic acid (PLA). PLA is renewable and biodegradable plastic and already commercialized for producing various products such as plastic dining utensils [61].

Succinic acid is another valued product that can be overproduced by engineered *S. cerevisiae* [62-64]. Because native *S. cerevisiae* can produce succinic acid under the aerobic condition without any genetic perturbation, succinic consuming reactions are removed by deleting genes such as *SHD3, SER3,* and *SER33 [64]*. Although resulting engineered strains displayed great improvement of succinic acid yield, on-going studies are focusing on improving

the yield to reach closer to the theoretical maximum. Also, despite the successfulness of few chemical production with the microbial platform, challenges of replacing all petrochemicals remains to be overcome. The various product formation from petrochemical makes difficult for microbial systems to replace all effectively. Thus, more microbial platform-based chemical synthesis should be discovered.

1.4 Recent advances in biotechnology and metabolic engineering

Metabolic engineering is a practice of optimizing genetic and regulatory systems within a cell to increase the productivity of chemical production via recombinant DNA technology [65]. It is a strategic and directed approach for the strain improvement thus requires a thorough understanding of the cellular system. Current cutting-edge technology development and advancement such as clustered regularly interspaced short palindromic repeats (CRISPR) and the CRISPR-associated proteins (Cas) system [11, 66, 67], global metabolite profiling [68, 69] and whole genome sequencing extended the limits of modification and analysis of the cellular system. This advancement allows rapid development of industrial yeast strains that can produce value-added chemicals efficiently and productively.

A rational design of metabolic engineering takes a systematic approach to design the pathway for the most efficient production of the target chemical carefully. This method requires careful examination of target pathway stoichiometry, regulatory systems, and metabolic fluxes, thus requiring extensive prior knowledge of the cellular system [70]. Based on the rational design, necessary genetic changes are made such as the amplification and deletion of the native genes and the introduction of heterologous genes [71, 72]. The introduction of xylose and cellobiose metabolic pathway in *S. cerevisiae* is an example of the systematic approach. For *S. cerevisiae* to ferment xylose, the most plausible design is to adapt and introduce a pathway that converts xylose to xylulose-5-phosphate from other native cellular systems. Subsequently, native *S. cerevisiae* strains can utilize xylulose-5-phosphate via the pentose phosphate pathway. In the case of cellobiose utilization, cellobiose transporter and cellobiose hydrolyzing enzymes are introduced to convert cellobiose into glucose units. However, the rational design of metabolic engineering can be an effective approach to some extent; there are several limitations. Often, conducted pathway manipulations based on prior knowledge and careful design may result in unexpected results such as no phenotypic change and adverse effects on cellular functions [73]. Also, lack of available information on the cellular system can halt from

designing an effective pathway [74]. Likewise, engineered *S. cerevisiae* strain with xylose or cellobiose metabolism pathway allow the utilization of the sugars. However, the efficiency of the pathway was very low compared to the primary sugar metabolism such as glucose.

To complement the limitations of a systematic approach, a combinatorial approach to metabolic engineering can be used. In contrast to the systematic approach that requires a thorough understanding of the cellular system, the combinatorial approach requires minimum prior knowledge of the cellular system. Instead of rational genetic perturbation then evaluating the phenotypes of the newly engineered strains, the combinatorial approach rather takes an inverse experimental flow. Random genetic changes are made, and cells that harbor useful phenotypes are screened and selected [75]. Construction of mutant strains with random genetic perturbation can be developed using tools such as a random mutagenesis, genomic library, and randomized gene knockout library. The pool of mutants can be screened and selected by high-throughput screening tools such as flow cytometry or microfluidics devices [76]. Then, the beneficial mutations accumulated are identified by high-throughput sequencing. An example of combinatorial metabolic engineering is laboratory evolution. This strategy allows cells that make random genetic mutations that increase the growth and survival under the selective pressure. Several studies report the successfulness of laboratory evolution to obtain enhanced yeast strain.

Both rational and traditional combinatorial metabolic engineering allows developing a strain with improved properties [77]. Many previous studies reported the successful application of both metabolic engineering approaches [78, 79]. Methodologies are often optimized for the monogenic effect of a phenotype that is affected by a single or a few genes. However, many observed phenotypes are often caused by the interaction of many genes, and underlying genetic network and mechanisms are complex. Thus, tools such as Quantitative Trait Locus (QTL) mapping analysis particularly or statistical analysis of the genome are often applied.

Quantitative traits are a result of many interactions of the genes or a polygenic effect to the phenotype. Examples of the quantitative traits include industrially favorable phenotypes such as efficiency and productivity of the pathway, robustness, and resistances to stressful conditions. Thus, it is crucial to consider quantitative traits for engineering microbes for improved features. Traditional methodologies for identifying quantitative traits are depended on the two major factors: phenotypic (trait) evaluation and genotypic (genetic sequences)

evaluation. Quantitative Trait Locus (QTL) mapping analysis is a widely accepted analysis used in various fields of study such as plant biology, medicine, and microbiology [80]. Many studies in metabolic engineering of microbes performed QTL mapping analysis that allowed identification genetic targets for strain improvement [81-89]. The analysis allows linking statistically phenotypic and genotypic data for determining the genetic basis of the trait of interest.

1.5 Motivations and research objectives

Owing to tremendous advances in metabolic engineering and biotechnology, the microbial production of fuels and chemicals envisioned to replace the current unsustainable fossil-fuel-based system. While several successful transitions to microbial system lay the foundation of the renewable process to produce fuels and chemicals, many barriers remain to be solved. For example, utilization of lignocellulosic sugars (xylose and cellobiose) in engineered *S. cerevisiae* strain allowed to move away from food-derived substrates (glucose and sucrose). However, lower efficiency of lignocellulosic sugar utilization is a major hindrance to replace the current system. Also, current chemical production with microbial fermentation cannot cover the current diverse petroleum-derived chemical production making microbial chemical production less practical.

Thus, this dissertation addresses the development of optimal yeast strains for utilizing lignocellulosic sugars, elucidation of underlying mechanisms related to carbon metabolism and extension of chemical production by engineered yeast. Specific objectives include: 1) Evaluation of cellobiose transporter for enhanced cellobiose fermentation, 2) investigate synergistic effect cellobiose transporter and hydrolyzing enzyme, 3) Investigate complex metabolic system for xylose metabolism, 5) genetic engineering for enhanced galactose fermentation, 5) produce novel chemicals, 2-isopropylmalate, by engineered yeast, and 6) prospective applications of 2-isopropylmalate. In the future, I anticipate the outcome of these studies will have positive impacts on the advance in the microbial production of value-added fuels and chemicals.

1.6 Figures and tables

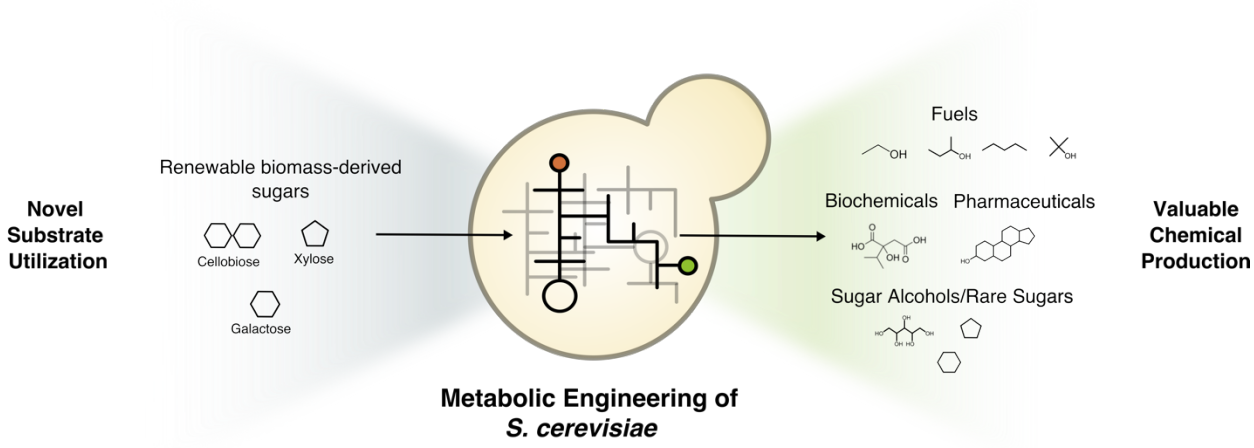

Figure 1.1 Schematic diagram of metabolic engineering of *S. cerevisiae.* Metabolic engineering strategy is used to enable novel substrate utilization and valuable chemical production in *S. cerevisiae*.

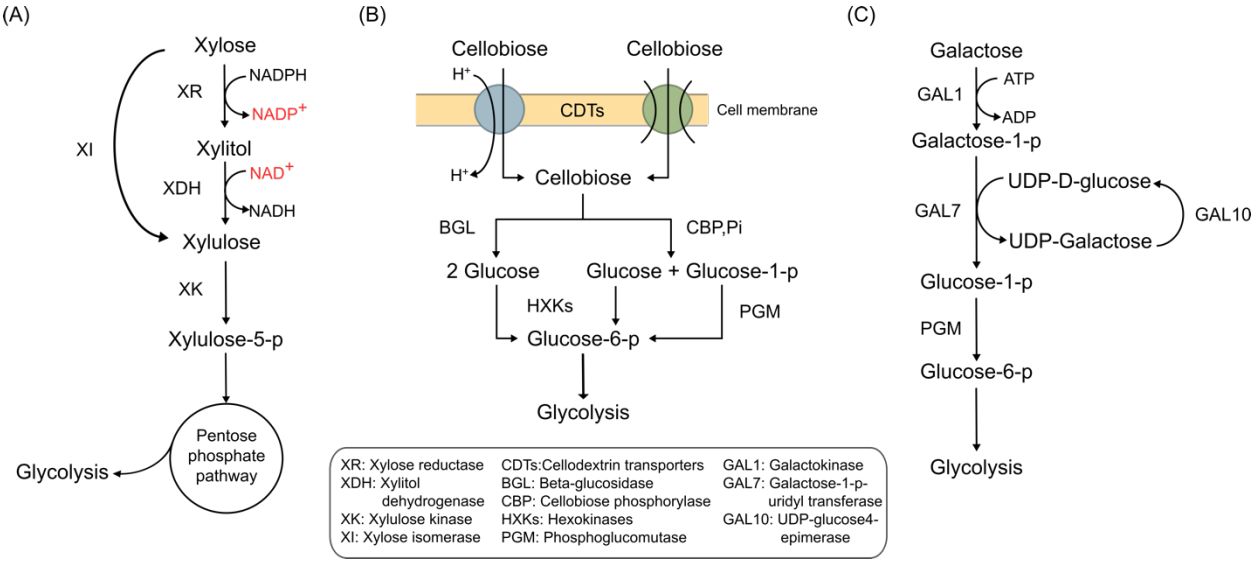

Figure 1.2 Xylose, cellobiose and galactose metabolic pathway. Xylose and cellobiose are the major sugars found in lignocellulosic hydrolysates and galactose are abundant in marine biomass. (A) To utilize xylose, yeast requires several heterologous enzymes to convert xylose to xylulose-5-p. Xylose can be converted to xylulose by xylose isomerases (XI), or converted to xylitol by xylose reductase (XR) then to xylulose by xylitol dehydrogenase (XDH). Xylulose can be phosphorylated by xylulose kinase (XK) then utilized by pentose phosphate pathway. (B) To utilize cellobiose, cellodextrin transporter is required to transport cellobiose into the cell via active transport or diffusion. Then cellobiose can be hydrolyzed by beta-glucosidase (BGL) or phosphorylated by cellobiose phosphorylase (CBP). Resulting glucose or glucose-1-p can be converted to glucose-6-p by hexokinases and/or phosphoglucomutase (PGM) and further metabolized via glycolysis. (C) Native *S. cerevisiae* can metabolize galactose in several steps. Galactose is converted to galactose-1-p (GAL1), glucose-1-p (GAL7) and glucose-6-p (PGM) then further metabolized by glycolysis.

CHAPTER II: Analysis of Cellodextrin Transporters from *Neurospora Crassa* in *Saccharomyces cerevisiae* for Cellobiose Fermentation [1]

2.1 Introduction

Saccharomyces cerevisiae has been widely used to produce ethanol from sugars derived from sugarcane and corn [90]. To avoid further impacting the food and feed markets, producing ethanol from non-edible crops has been proposed [91]. However, saccharification of cellulose into glucose requires substantial amounts of cellulolytic enzymes due to the presence of strong β(1→4) glycosidic linkages and the crystalline structure of cellulose, which makes cellulose relatively inaccessible to cellulolytic enzymes. Saccharification of cellulose mainly consists of two reactions: 1) hydrolysis of cellulose to cellobiose (and cellodextrins) by endo- and exoglucanases and 2) saccharification of cellobiose to glucose by β-glucosidase [92]. Because the main intermediates of cellulose hydrolysis (cellobiose and cellodextrins) strongly inhibit cellulolytic enzymes, rapid degradation of cellobiose into glucose is essential for efficient hydrolysis of cellulose. However, most cellulose mixtures obtained through cellulolytic fungal cultures exhibit low β-glucosidase activity as compared with their endo and exo-glucanases activity. Thus, supplementation with additional β-glucosidase is often necessary during the saccharification of cellulose into glucose. This may significantly increase the costs of the process, as enzymes constitute a considerable portion (40-50%) of total costs for ethanol production from cellulose [93-95].

To overcome the feedback inhibition by cellobiose on cellulases and relieve high enzyme cost, *S. cerevisiae* has been engineered to ferment cellobiose directly through the introduction of two heterologous genes that allow transport of cellobiose (and cellodextrin) and intracellular hydrolysis of cellobiose (and cellodextrin) to glucose [41]. Direct cellobiose fermentation via intracellular transport and hydrolysis will lead to the elimination of cellobiose in

[1] This chapter appeared in its entirely in *Applied Microbiology and Biotechnology*. **Kim H**, Lee W-H, Galazka JM, Cate JH, Jin Y-S (2014) Analysis of cellodextrin transporters from *Neurospora crassa* in *Saccharomyces cerevisiae* for cellobiose fermentation. *Applied Microbiology and Biotechnology* 98(3):1087-1094. This article is reprinted with slight modifications for consistency with other chapters and formatting purposes and the permission of the publisher was granted. I performed the research with help from co-authors and Dr. Yong-Su Jin was the director of the research.

the cultures and efficient cellulose degradation without requiring β-glucosidase supplementation.

Previously, several genes coding for putative cellobiose transporters including cellodextrin transporters (cdt-1 and cdt-2) from *Neurospora crassa* [41], lactose transporters (*LAC1, LAC2, and LAC3*) from *Kluyvergomyces lactis*, and putative hexose transporter (*HXT2.1, HXT2.3, HXT2.4, HXT2.5*, and *HXT2.6*) from *Pichia stipitis* [45] were identified. However, the exact mechanisms of cellobiose transport by those transporters have not been fully studied despite these transporters having exhibited diverse patterns of cellobiose utilization when expressed in *S. cerevisiae* by pairing with intracellular β-glucosidase(GH1-1) from *N. crassa*. In particular, different patterns of cell growth on cellobiose condition (including cellotriose and cellotetraose conditions) were observed between engineered *S. cerevisiae* expressing CDT-1 and CDT-2 from *N. crassa*, although both transporters were reported to have a very similar affinity to cellobiose [41]. As detailed biochemical characteristics of CDT-1 and CDT-2 have not been reported yet, this study was undertaken to investigate characteristics of engineered *S. cerevisiae* expressing CDT-1 or CDT-2 with GH1-1 for cellobiose fermentation. The mechanism of cellobiose transport by CDT-1 and CDT-2 was investigated, and profiles of sugar utilization by engineered *S. cerevisiae* during cellobiose fermentation were also investigated.

2.2 Materials and methods

Strains, plasmids, and culture conditions

In the previous studies, cellobiose transporter genes from *N. crassa* FGSC 2489, NCU00801 and NCU08114 (*cdt-1* and *cdt-2*), and an intracellular β-glucosidase gene (*gh1-1*) from *N. crassa* were cloned into a pRS426 plasmid (*URA3*, PGK1 promoter, CYC1 transcriptional terminator) and a pRS425 plasmid (*LEU2*, PGK1 promoter, CYC1 transcriptional terminator), respectively [41]. The resulting plasmids were pRS426-*cdt-1*, pRS426-*cdt-2*, and pRS425-*gh1-1*. *S. cerevisiae* YPH499 (*MATa ura3-52 lys2-801_amber ade2-101_ochre trp1-Δhis3-Δ200 leu2-Δ1*) [96] was used for the cellobiose transport assay. *S. cerevisiae* D452-2 (*MATα leu2 his3 ura3 can1*) [97] was used for characterization of cellobiose transporters after expressing CDT-1 or CDT-2 along with GH1-1 under various fermentation conditions. All strains

and plasmids used in this study are listed in Table 2.1. Synthetic complete (SC) medium (6.7 g/L yeast nitrogen base without amino acids, 20 g/L glucose, and 0.625 g/L complete supplement mixture (CSM) without leucine, tryptophan, and uracil) (Bio 101, Vista, CA) with appropriate nucleotides and amino acids was used for selection of the transformants.

Cellobiose transport assay

To determine the sensitivity of cellobiose transport by CDT-1 or CDT-2 to the strength of the plasma membrane proton gradient, strains expressing *cdt-1* or *cdt-2* were grown to OD600 of 1.5 to 3.0 in selective media, washed three times with assay buffer (30 mM MES (2-(N-morpholino) ethane sulfonic acid)-NaOH [pH 5.6] and 50 mM ethanol), and resuspended to an OD600 of 20 (Arendt et al. 2007). Then, 350 µL aliquots of cells were held on ice. To assay, the transport rate at a given concentration of carbonyl cyanide m-chlorophenyl hydrazine (CCCP), 0.35 µL of a 1,000× CCCP stock made in 100 % ethanol was added to a single 350 µL aliquot of cells. This aliquot of cells was then incubated for 10 min in a room temperature water bath. After incubation, a transport assay was performed by adding 50 µL of cells to 50 µL of buffered [3H]-cellobiose with an appropriate concentration of CCCP that was layered above 100 µL of silicone oil. The same process was repeated sequentially for each tested concentration of CCCP. Controls with no CCCP were incubated for 10 min with 0.35 µL of 100 % ethanol.

Fermentation experiments

A single colony after transformation was picked and grown in YP medium (10 g/L yeast extract and 20 g/L peptone) with 20 g/L of cellobiose at 200 rpm and 30 °C to prepare inocula (L) for cellobiose fermentation experiments. Yeast cells at their mid-exponential phase were harvested by centrifugation and washed with sterilized water before inoculations. Fermentation experiments were performed in YP (10 g/L yeast extract and 20 g/L peptone) or SC (6.7 g/L of yeast nitrogen base, 0.42 g/L of Tween 80, and 0.01 g/L of ergosterol with CSM or without CSM, pH 6.0) media in an oxygen-limited condition or anoxic condition. Appropriate concentrations of cellobiose (20, 40, or 80 g/L) were used. Oxygen-limited fermentation experiments were performed in 25 mL culture using a 125 mL Erlenmeyer flask tightly covered by aluminum foil at 30 °C and an agitation speed of 100 rpm. Anaerobic fermentation was done by 20 mL culture using a 100-mL serum vial sealed with a rubber cap and nitrogen purged for 5 min with gentle swirling. Vials were incubated at 30 °C at 100 rpm as well. Initial cell densities of

all fermentation experiments were adjusted to OD600 of 1. All fermentation experiments were performed in duplicates.

Analytical methods

Cell growth was monitored by measuring optical density at 600 nm using a UV-visible spectrophotometer (Biomate5, Thermo, Rochester, NY). Cellobiose, glycerol, acetate, ethanol, and cellodextrin concentrations were determined by high-performance liquid chromatography (Agilent Technologies 1200 Series, Mississauga, CA) equipped with a refractive index detector using a Rezex ROA-Organic Acid H^+ (8 %) column (Phenomenex Inc., Torrance, CA). The column was eluted with 0.005 N of H_2SO_4 at a flow rate of 0.6 ml/min at 50 °C.

2.3 Results

Determination of a mode of transportation through cellobiose transport assay

As observed in previous studies (Galazka et al. 2010), cellodextrin transporters in *N. crassa* (CDT-1 and CDT-2) with high affinity to cellobiose were selected for further characterization in *S. cerevisiae*. When the cellodextrin transporters were expressed with GH1-1 in *S. cerevisiae* strains, the resulting engineered strains were able to utilize and grow with cellodextrin as the sole carbon source [41, 98].

To characterize the mechanism of transport by CDT-1 and CDT-2, their sensitivities to increasing concentrations of CCCP was measured. CCCP is a proton gradient uncoupler, which increases the proton permeability of the plasma membrane. The sensitivity of cellobiose transport by CDT-1 and CDT-2 to CCCP should, therefore, indicate whether or not either transporter utilizes the plasma membrane proton gradient during transport of cellobiose. *S. cerevisiae* YPH499 strains expressing *cdt-1* or *cdt-2* were incubated with different concentrations of CCCP and cellobiose transport rates were measured. As shown in Figure 2.1, the cellobiose transport rate of the *S. cerevisiae* strain expressing *cdt-1* was reduced as CCCP concentration increased. However, the strains expressing *cdt-2* showed a constant rate of cellobiose transportation regardless of CCCP concentrations. These results suggested that CDT-1 is proton symporter and that CDT-2 does not utilize the plasma membrane proton gradient.

Comparison of cellobiose fermentation characteristics of engineered *S. cerevisiae* expressing CDT-1 and CDT-2

CDT-1 and CDT-2 from *N. crassa* were further studied for the performance of cellobiose fermentation when they are co-expressed with GH1-1 in *S. cerevisiae*. Two strains (DBT-1 and DBT-2) overexpressing *gh1-1* and *cdt-1* or *cdt-2* under the control of a strong constitutive promoter were developed. The resulting strains were then evaluated for their fermentation capability using cellobiose as a sole carbon source under various fermentation conditions.

Cellobiose fermentation under oxygen-limited conditions

Both the DBT-1 (with CDT-1) and DBT-2 (with CDT-2) strains were cultured in YP medium with 40 g/L of cellobiose under an oxygen-limited condition. As shown in Figure 2.2A, both strains were able to grow and ferment all 40 g/L of cellobiose and produce ethanol. However, the DBT-1G strain had a twofold faster growth and cellobiose consumption rate and about three to fivefold higher ethanol productivity when compared to the DBT-2 strain (Table 2.2). Also, the DBT-1G strain was able to consume all cellobiose and reutilize cellodextrins (cellodextrins accumulate due to the transglycosylation activity GH1-1) within 36 h whereas the DBT-2 strain took about 72 h to utilize all cellodextrins. The DBT-1 strain correspondingly had a higher ethanol yield as compared to DBT-2 (Table 2.2; 0.42 g ethanol/g cellobiose vs. 0.31 g ethanol/g cellobiose). Interestingly, the DBT-2 produced 25% more biomass (OD_{600} = ~17 vs. OD_{600} = ~22) as compared to the DBT-1 strain at the end of fermentation, indicating that the DBT-2 strain directed more cellobiose consumption to yield biomass than the DBT-1 strain.

Because transport assay data suggests that CDT-2 is a simple facilitator, I hypothesized that CDT-2 might work better when the cellobiose concentration is high. Therefore, cellobiose fermentation rates using 80 g/L of cellobiose were also examined (Figure 2.2B). However, similar fermentation profiles were observed as compared when 40 g/L of cellobiose was used. The DBT-1 still showed higher cellobiose consumption rate and produced ethanol with a higher yield than the DBT-2 strain. The DBT-1 consumed all cellobiose within 36 h and produced ethanol with a yield of 0.39 g ethanol/g cellobiose (Table 2.2) whereas the DBT-2 failed to utilize all of the cellobiose. The DBT-2 strains consumed only 60 g/L of cellobiose in 62 h and stopped using cellobiose when 20 g/L cellobiose and 25 g/L cellodextrin were left in the medium. Also, less biomass formation and ethanol production were observed in DBT-2 strain.

Because YP media is composed of many nutrients such as peptides and amino acids that can be used as a source for ATP generation in the *cdt-1* expressing strain, cellobiose utilization of the strains expressing *cdt-1* and *cdt-2* along with gh1-1 in a minimal media were also examined (Figure 2.3). However, fermentation profiles in a minimal (SC) medium with 20 g/L cellobiose were consistent with the profiles obtained from the YP media. The DBT-1 strain still showed a faster fermentation rate than the DBT-2 strain regardless of the media conditions. Furthermore, the DBT-2 strain was not able to consume all cellobiose in the minimal media and produced low amounts of ethanol even though a lower concentration of initial cellobiose was loaded. Notably, in minimal media conditions, the differences in fermentation rates between the two strains was exacerbated compared the case in YP media due to the fact that DBT-2 had much lower cellobiose consumption rate and almost no ethanol production.

Cellobiose fermentation under anaerobic conditions

In a parallel set of experiments, cellobiose fermentations by two strains under anaerobic conditions were also examined to investigate whether or not the minimized ATP synthesis that occurs under anaerobic conditions might affect cellobiose fermentation by the *cdt-1* and *cdt-2* expressing strains. Both complex and minimal media was used for this comparison. Profiles of cellobiose fermentation of DBT-1 and DBT-2 under anaerobic conditions are illustrated in Figs. 4 and 5. In the YP media with cellobiose concentrations (40 and 80 g/L; Figure 2.4), the DBT-1 strain still had a significantly higher fermentation rate compared to the DBT-2 strain. In the minimal media (SC, with or without CSM) with 20 g/L cellobiose (Figure 2.5), the DBT-1 strain still showed a higher cellobiose fermentation rate and substantially more ethanol production.

Taken together, the better cellobiose fermentation capability of the DBT-1 strain, when compared to the DBT-2 strain, was observed regardless of the fermentation conditions, resulting in both a higher yield and productivity for ethanol (Table 2.2). While CDT-2 may have energetic benefits, the expression levels and kinetic properties of CDT-2 in *S. cerevisiae* might not be optimum for cellobiose fermentation. These results suggest CDT-1 is a more effective cellobiose transporter than CDT-2 for engineering *S. cerevisiae* to ferment cellobiose.

2.4 Discussion

Traditionally, additional β-glucosidase prepared by extra fungal or bacterial fermentation has been added to allow efficient hydrolysis of cellulose to glucose. However, this may increase

the enzyme cost and risk of contamination by bacteria during the saccharification step. To overcome this problem, fungal cellobiose transporters and intracellular β-glucosidase were expressed in *S. cerevisiae* for direct fermentation of cellodextrins [41]. However, the detailed mechanisms and characteristics of these cellobiose transporters have not been investigated systematically. Among the cellobiose transporters discovered previously, CDT-1 or CDT-2 along with GH1-1 expressing strains were able to grow on cellobiose as a sole carbon source, and both transporters had a similar affinity (Km≈3–4 μM) for cellobiose. However, the rates of cellobiose consumption were very different [41]. Hence, this study was undertaken to verify the difference between CDT-1 and CDT-2 in terms of energy (proton gradient) dependence and cellobiose fermentation characteristics under various cultivation conditions when they are overexpressed in *S. cerevisiae*.

Generally, transport of a molecule across the plasma membrane can be mediated by two types of transporters: passive and active. Passive transport by a uniporter is driven only by the concentration gradient of the substrate, while active transport by a symporter (or antiporter) is also driven by the concentration of a second substrate. This second substrate is maintained out of equilibrium by the cell through an energy consuming process [99]. Some native transporters present in yeast, such as glucose transporters, transport glucose via facilitated diffusion [100]. On the other hand, yeast disaccharide transporters such as maltose and sucrose transporters transport substrates via active transport. Specifically, the maltose and sucrose transporters require the presence of a proton gradient to move their substrates across the membrane (proton symporter) [101, 102].

From the results of cellobiose transport assay, CDT-1 was concluded as a proton symporter and CDT-2 as a uniporter. This result suggests that the CDT-1 expressing strain may require more energy than the CDT-2 expressing strain during cellobiose fermentation. Consequently, I hypothesized that this difference in energy requirement would affect fermentation rates of these engineered strains.

As YP media is composed of rich nutrients that can allow generation of excess energy, cannot exclude that the considerable difference in fermentation rates between the two strains may be because CDT-1 was reported to have a two-fold higher V_{Max} than CDT-2 in a previous kinetic study [41]. Indeed, a faster fermentation rate was observed by DBT-1 in YP medium with 40 g/L (or 80 g/L) cellobiose under oxygen-limited conditions (Figure 2.2). In addition, I

anticipated that the DBT-2 might show an increased fermentation rate with an increased initial concentration of cellobiose (40 to 80 g/L); however, slower cellobiose consumption, less production of ethanol, and much higher accumulation of cellodextrin were observed in the DBT-2 fermentation with 80 g/L of cellobiose (Figure 2.2). This result is likely due to increased levels of intracellular cellobiose leads to transglycosylation of cellobiose in cellodextrins by GH1-1 rather than degradation to glucose. The transglycosylation reaction of GH1-1 occurs under kinetically controlled conditions; therefore, an increased level of intracellular cellobiose will favor formation of cellodextrin accumulation intracellularly [103, 104], along with some secretion via the transporters. It is also possible that, although GH1-1 was expressed intracellularly, a very small amount of GH1-1 might be secreted out via nonconventional protein secretion pathway [105, 106]. A previous study on fungal β-glucosidase suggests a small amount of GH1-1 can have transglycosylation activity with a high concentration of the substrate [47]. Thus, a small amount of GH1-1 secretion could result in significant cellodextrin accumulation. This explains why DBT-1 accumulated less cellodextrin than DBT-2. Because CDT-1 was reported to have higher V_{Max} for cellodextrin (cellotriose and cellotetraose) than CDT-2 [41], DBT-1 can re-assimilate cellodextrin faster than DBT-2.

I speculated that a similar or even better fermentation rate by the DBT-2 rather than the DBT-1 strain would occur if the fermentation was performed with the minimal medium because nutrients for energy generation can be limited in minimal media conditions. However, the DBT-2 strain showed the same pattern of fermentation profile as in YP media (Figure 2.3), and the DBT-1 strain was still more efficient for fermenting cellobiose than the DBT-2 strain. Under minimal media condition, there was negligible amount cellodextrin accumulation (<1 g/L; Figure 2.3). This result is consistent with the previous study on cellodextrin transporters [41] where no secretion of GH1-1 was confirmed under minimal media. It is possible that the leakage of GH1-1 occurs under certain culture conditions, such as complex media. Regardless of the cellodextrin accumulation mechanism, CDT-1 is more effective in transporting cellobiose in the presence of oxygen regardless of the nutrient availability.

In addition to nutrient availability, the presence of oxygen was also expected to influence the fermentation profile. Under the anaerobic condition, the TCA cycle will be fully inactivated, and ATP generation is limited, and I reasoned that CDT-1 expressing cells might not produce enough energy to maintain active transport of cellobiose [107]. However, overall, there was no

significant difference in the fermentation profile pattern of the two strains under anaerobic conditions. Again, the CDT-1 expressing strain showed faster cellobiose fermentation as compared to the CDT-2 expressing strain. These results show that CDT-1 mediates more efficient cellobiose transport, which in turn results in a higher yield and productivity than CDT-2 regardless of nutrient and oxygen availability. As the previous study indicates, both CDT-1 and CDT-2 had a high affinity to cellobiose, but CDT-1 had a higher V_{Max}. Superior cellobiose fermentation by strains expressing CDT-1 may be due to the V_{Max} difference in CDT-1 and CDT-2.

In conclusion, cellodextrin transporters (*cdt-1* and *cdt-2*) and intracellular ß-glucosidase (gh1-1) from *N. crassa* were introduced into *S. cerevisiae*. By introducing each cdt-1 and cdt-2 paired with ß-glucosidase, both engineered strains (DBT-1 and DBT-2) were able to utilize cellobiose as a sole carbon source and produce ethanol. The DBT-1 strain showed a more efficient cellobiose fermentation as compared to the DBT-2 strain regardless of oxygen levels and media conditions. This is likely to due to the V_{Max} difference between CDT-1 and CDT-2. It will be interesting to determine if the transport rate of CDT-2 may be improved through various engineering techniques and if this improvement may subsequently provide the dual advantages of higher energy levels and better fermentation parameters.

2.5 Figures and tables

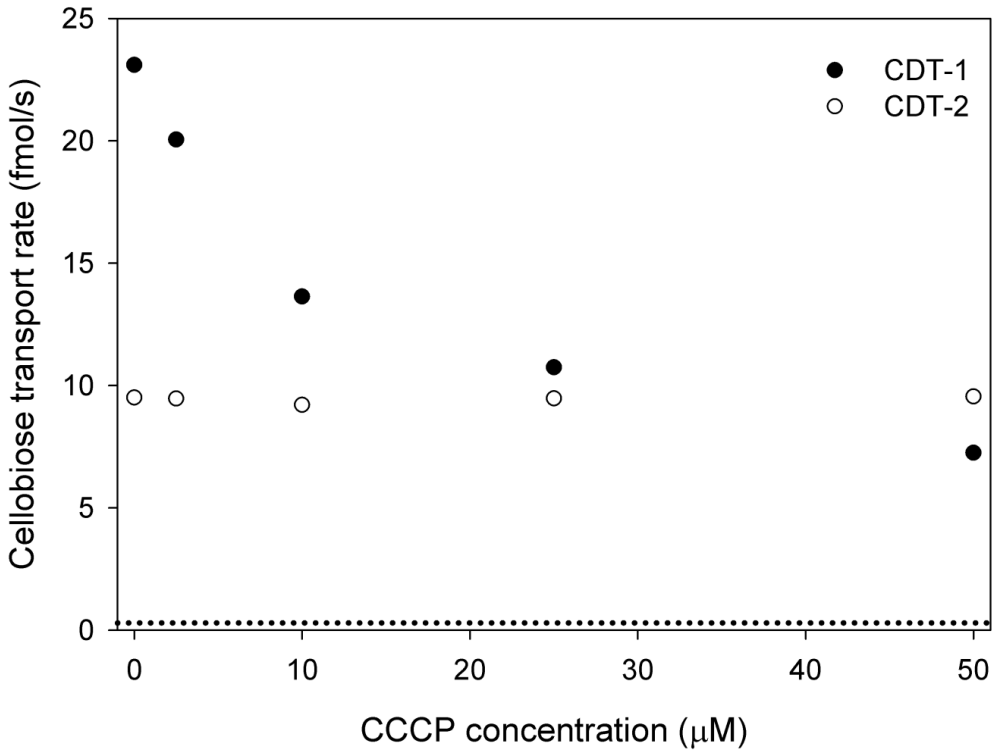

Figure 2.1 Sensitivity of cellobiose transport by CDT-1 and CDT-2 to the proton uncoupler, carbonyl cyanide m-chlorophenyl hydrazine (CCCP). *S. cerevisiae* strains expressing CDT-1 (*closed circle*) or CDT-2 (*open circle*) were incubated with the indicated concentration of CCCP for 10 minutes at room temperature. Then the rate at which these cells imported 0.25 μM [3H]-cellobiose was measured. The *dashed line* indicates the rate of transport by *S. cerevisiae* without CDT-1 or CDT-2 expression.

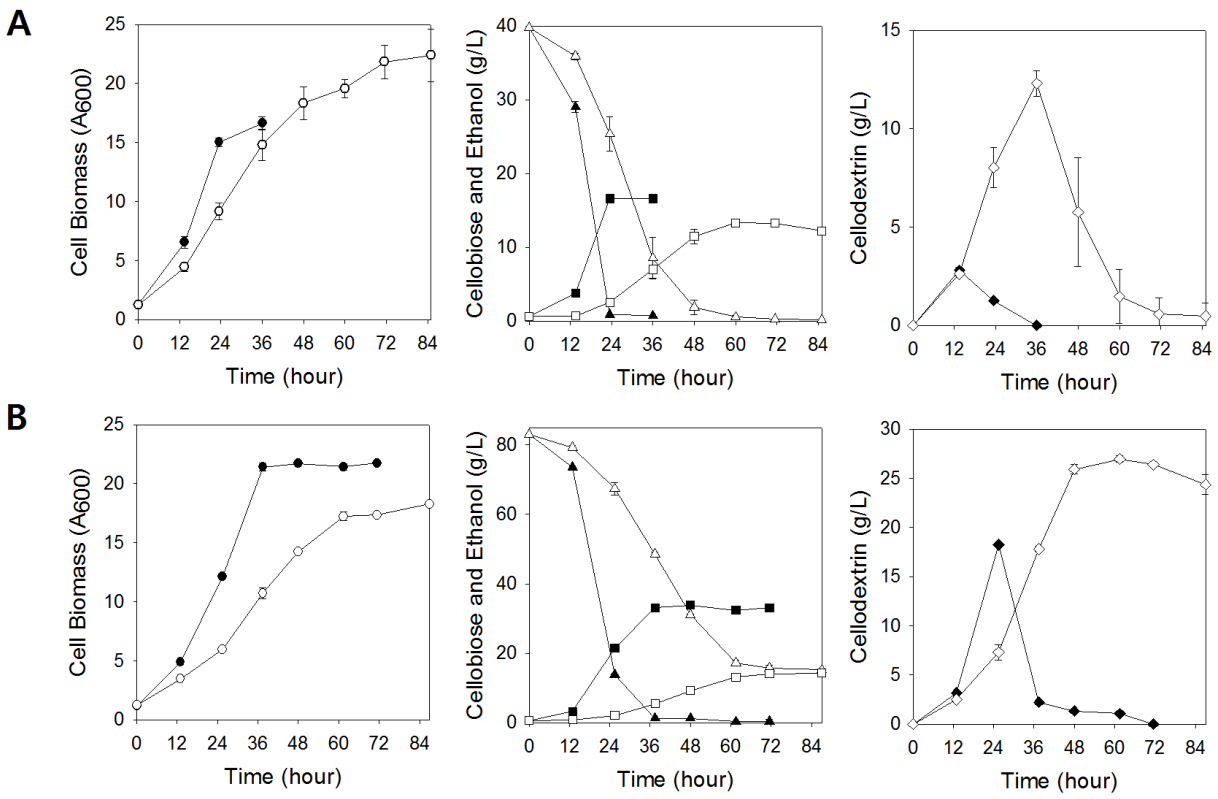

Figure 2.2 Fermentation profile comparisons between *S. cerevisiae* D452-2 *gh1-1* and *cdt-1* or *cdt-2* (DBT-1 and DBT-2, respectively) with rich media conditions and under oxygen-limited condition. Growth, cellobiose consumption, ethanol production and cellodextrin accumulations were compared as presented on the first, second and third column, respectively. (A) Fermentation profile under YP medium with 40 g/L cellobiose. (B) Fermentation profile under YP medium with 80 g/L cellobiose. Symbols: DBT-1 strain (*black*) DBT-2 (*white*), growth (*circle*), cellobiose (*triangle*), ethanol (*square*) and cellodextrin (*diamond*).

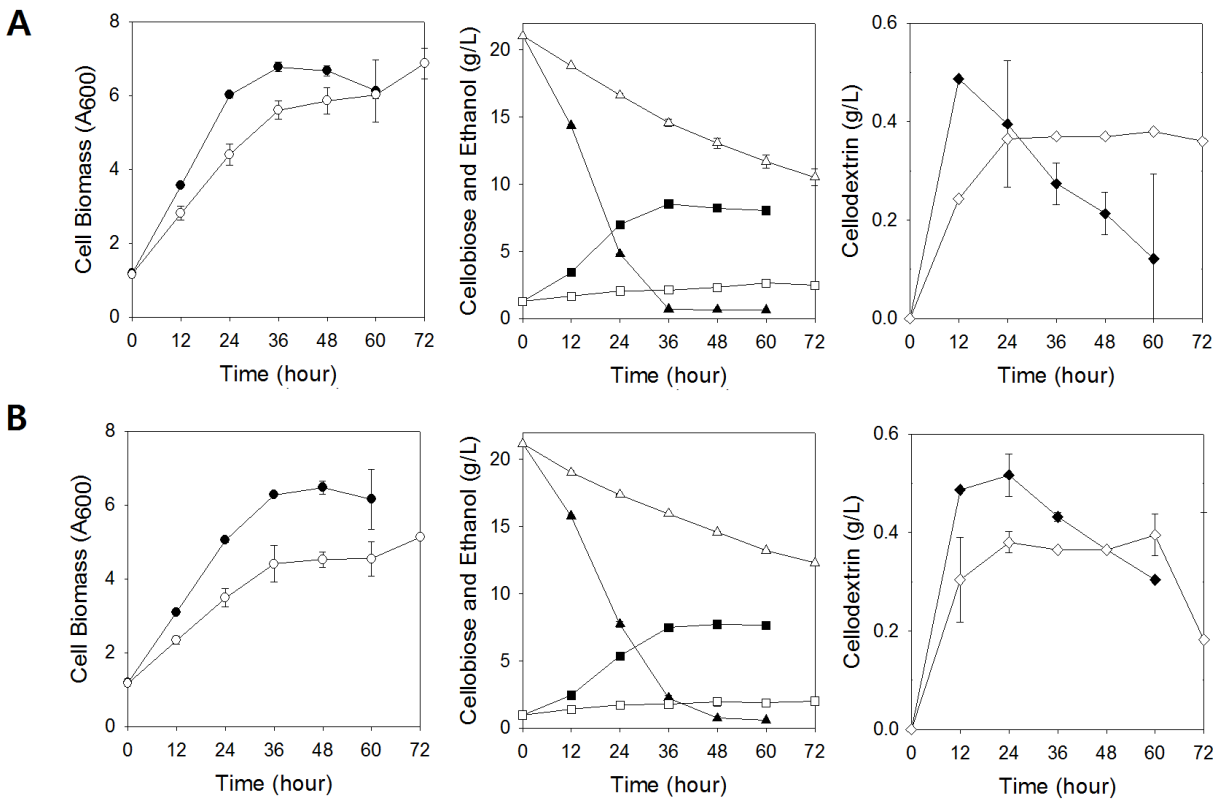

Figure 2.3 Fermentation profile comparisons between *S. cerevisiae* DBT-1 and DBT-2 with minimal medium and under oxygen-limited conditions. Growth, cellobiose consumption, ethanol production and cellodextrin accumulations were compared as presented in the first, second and third columns, respectively. (A) Fermentation profile under SC and CSM supplemented medium with 20 g/L cellobiose. (B) Fermentation profile under SC medium with 20 g/L cellobiose. Symbols: DBT-1 strain (*black*) DBT-2 strain (*white*), growth (*circle*), cellobiose (*triangle*), ethanol *(square*) and cellodextrin (*diamond*).

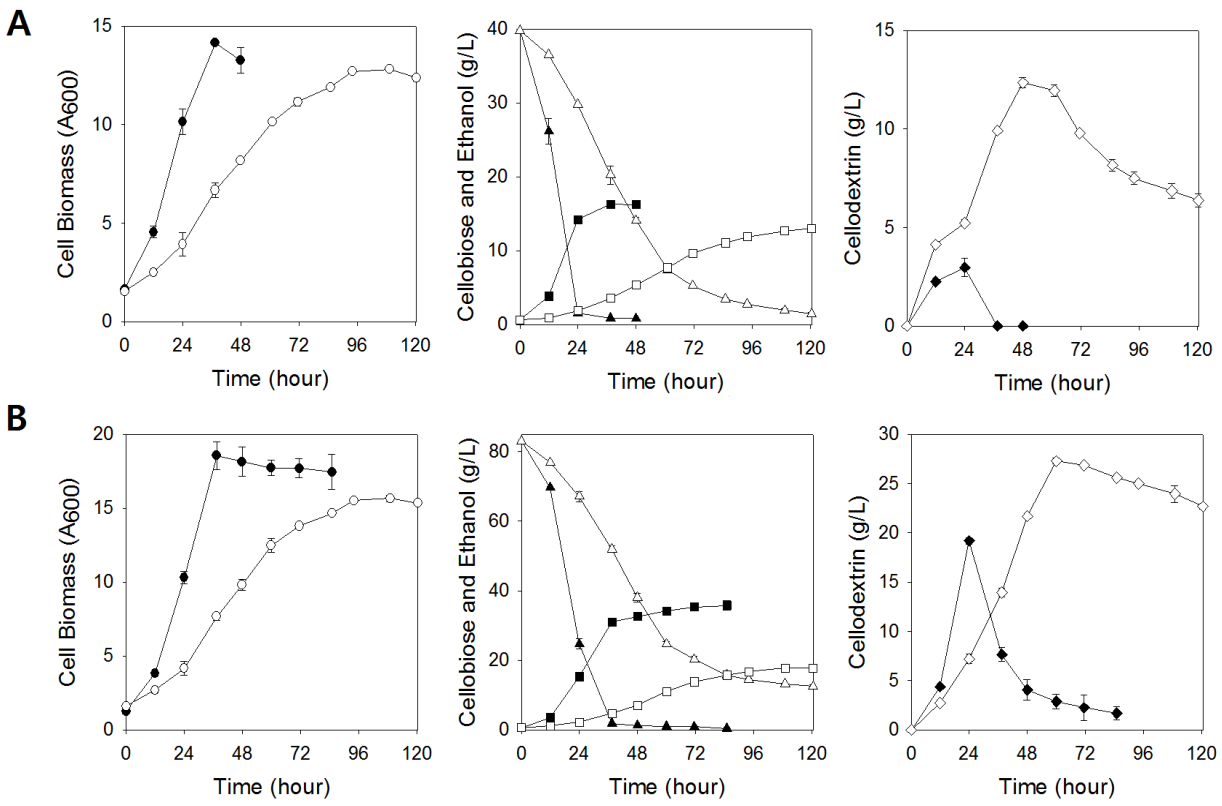

Figure 2.4 Fermentation profile comparisons between *S. cerevisiae* DBT-1 and DBT-2 with rich medium and under anaerobic conditions. Growth, cellobiose consumption, ethanol production and cellodextrin accumulations were compared as presented on the first, second and third column, respectively. (A) Fermentation profile under YP medium with 40 g/L cellobiose. (B) Fermentation profile under YP medium with 80 g/L cellobiose. Symbols: DBT-1 strain (*black*) DBT-2 strain (*white*), growth (*circle*), cellobiose (*triangle*), ethanol (*square*) and cellodextrin (*diamond*)

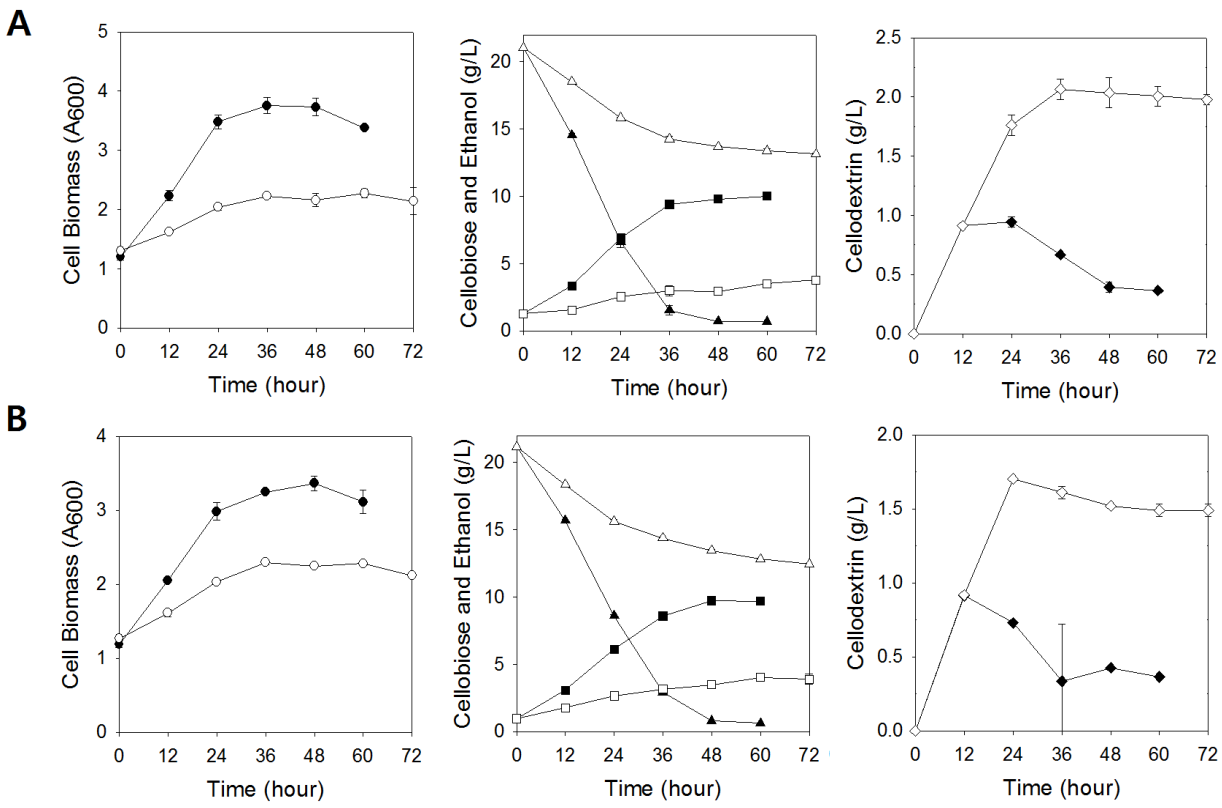

Figure 2.5 Fermentation profile comparisons between *S. cerevisiae* DBT-1 and DBT-2 with minimal medium and under anaerobic conditions. Growth, cellobiose consumption, ethanol production and cellodextrin accumulations were compared as presented in the first, second and third columns, respectively. (A) Fermentation profile under SC and CSM supplemented medium with 20 g/L cellobiose. (B) Fermentation profile under SC medium with 20 g/L cellobiose. Symbols: DBT-1 strain (*black*) DBT-2 strain (*white*), growth (*circle*), cellobiose (*triangle*), ethanol (*square*) and cellodextrin (*diamond*).

Table 2.1 The list of plasmids and *S. cerevisiae* strains used in this study

Plasmids and strains	Relevant features	Sources and references
Plasmids		
pRS425PGK	*LEU2*, P_{PGK} -MCS- T_{CYC}, 2μ origin, Amp^r	[41]
pRS426PGK	*URA3*, P_{PGK} -MCS- T_{CYC}, 2μ origin, Amp^r	[41]
pRS425-gh1-1	*LEU2*, P_{PGK}-*gh1-1*-T_{CYC}, 2μ origin, Amp^r	[41]
pRS426-cdt-1	*URA3*, P_{PGK}-*cdt-2*-T_{CYC}, 2μ origin, Amp^r	[41]
pRS426-cdt-2	*URA3*, P_{PGK}-*cdt-1*-T_{CYC}, 2μ origin, Amp^r	[41]
Strains		
YPH499	*MATa ura3-52 lys2-801_amber ade2-101_ochre trp1-Δhis3-Δ200 leu2-Δ1*	[96]
D452-2	*MATα leu2 his3 ura3 can1*	[97]
DBT-1	D452-2/ pRS425-gh1-1/pRS426-cdt-1	This study
DBT-2	D452-2/ pRS425-gh1-1/pRS426-cdt-2	This study

Table 2.2 Fermentation parameters of DCDT-1G and DCDT-2G under various media conditions and in oxygen-limited or anaerobic conditions

Conditions	Media	Strains	Y_{EtOH} [1)]	P_{EtOH} [1)]	RC [2)]
Oxygen-limited	YPC40 [3)]	DBT-1	0.42 ± 0.00	0.46 ± 000	0.73 ± 0.02
		DBT-2	0.31 ± 0.00	0.14 ± 0.00	0.17 ± 0.01
	YPC80 [4)]	DBT-1	0.39± 0.01	0.53± 0.01	0.39 ± 0.55
		DBT-2	0.19± 0.00	0.11± 0.00	15.3 ± 0.65
	SCC20 w/ CSM [5)]	DBT-1	0.39± 0.00	0.13± 0.00	0.63 ± 0.00
		DBT-2	0.23± 0.02	0.34± 0.00	10.5 ± 0.62
	SCC20 w/o CSM [6)]	DBT-1	0.37± 0.00	0.13± 0.00	0.60 ± 0.00
		DBT-2	0.23± 0.03	0.03± 0.00	12.3 ± 0.09
Anaerobic	YPC40	DBT-1	0.43± 0.01	0.35± 0.01	0.83 ± 0.00
		DBT-2	0.36± 0.00	0.09± 0.00	0.56 ± 0.16
	YPC80	DBT-1	0.42± 0.01	0.41± 0.02	0.35± 0.50
		DBT-2	0.28± 0.00	0.13± 0.00	11.7 ± 0.46
	SCC20 w/ CSM	DBT-1	0.49± 0.01	0.17± 0.00	0.71 ± 0.00
		DBT-2	0.48± 0.00	0.05± 0.00	13.1 ± 0.06
	SCC20 w/o CSM	DBT-1	0.47± 0.00	0.16± 0.00	0.61 ± 0.00
		DBT-2	0.45± 0.05	0.05± 0.01	12.5 ± 0.07

[1)]Fermentation parameters: Y_{EtOH}, ethanol yield (g ethanol g sugars^{-1}), P_{EtOH}, ethanol productivity (g ethanol L^{-1} h^{-1}).

[2)]Residual cellobiose concentration (g/L) at the end of fermentation.

[3)]YP medium containing 40 g/L of cellobiose, calculated at the end of fermentation.

[4)]YP medium containing 80g/L of cellobiose, calculated at the end of fermentation.

CHAPTER III: Enhanced Cellobiose Fermentation by Engineered *Saccharomyces cerevisiae* Expressing a Mutant Cellodextrin Facilitator and Cellobiose Phosphorylase [2]

3.1 Introduction

There have been extensive efforts to engineer microorganisms to produce fuels and chemicals from renewable cellulosic biomass mainly composed of polymers of glucose and xylose [91]. *Saccharomyces cerevisiae,* a preferred industrial yeast to produce biofuels and chemicals, has been engineered for efficient fermentation of xylose [27, 36, 39, 108-110]. However, xylose cannot be consumed in the presence of glucose due to glucose repression. Thus, yeast will sequentially utilize glucose first then xylose during mixed sugar fermentation with low ethanol yield and productivity [72, 111].

To overcome sequential sugar utilization and increase the efficiency of the fermentation, cellobiose, a dimer of glucose linked by β-(1→4) bonds [112], has been noted as an alternative sugar to glucose [41, 45, 46, 113]. Previous studies demonstrated that cellobiose and xylose could be simultaneously utilized due to the absence of glucose catabolite repression. Therefore, overall ethanol yield and productivity was dramatically improved by co-fermentation of cellobiose and xylose compared to diauxic utilization of glucose and xylose [24, 98].

Researchers note that heterologous expression of a cellodextrin transporter and an intracellular cellobiose hydrolyzing enzyme is essential for *S. cerevisiae* to ferment cellobiose [41, 44, 46]. Previous studies identified cellodextrin transporters from *Neurospora crassa,* CDT-1 or CDT-2 coupled with a hydrolytic enzyme (intracellular β-glucosidase from *N. crassa*) or phosphorolytic enzyme (cellobiose phosphorylase from *Saccharophagus degradans*) can be introduced to *S. cerevisiae* for cellobiose fermentation [43, 45, 114]. Thus, four different types of cellobiose utilization can be available in engineered *S. cerevisiae* (Fig. 1). Cellobiose is transported across the membrane by either CDT-1 (active transporter consuming one ATP per cellobiose) or CDT-2 (energy-independent facilitator) [43]. Once cellobiose enters the cell, it can be cleaved by hydrolysis with intracellular β-glucosidase (GH1-1) or phosphorolysis with cellobiose phosphorylase (CBP). When cellobiose is cleaved by β-glucosidase, two moles of

[2] The content of this chapter is in preparation for submission. I performed the research with helps from Eun Joong Oh, Stephan Thomas Lane, Won-Heong Lee, Dr. Jamie H. D. Cate and Yong-Su Jin (director of the research).

glucose are generated and subsequently converted to two moles of glucose-6-phosphate by hexokinases with the expense of two moles of ATP. On the other hand, phosphorolysis generates one mole of glucose and one mole of glucose-1-phosphate, saving one mole of ATP as glucose-1-phosphate is simply isomerized to glucose-6-phosphate by phosphoglucomutase without spending ATP [45, 115]). Consequently, the yeast expressing CDT-1 and β-glucosidase spends more energy (2 moles of ATP) than the yeast expressing CDT- 2 and cellobiose phosphorylase when grown on cellobiose, which suggests that CDT-2 paired with cellobiose phosphorylase can provide energetic benefits to yeast during industrial scale fermentation as many stress-overcoming cellular processes require ATP. Additionally, strains expressing cellobiose phosphorylase do not accumulate cellodextrin whereas strains expressing β-glucosidase showed accumulation of significant amounts of extracellular cellodextrin that has caused inefficient cellobiose fermentation and reduction of ethanol productivity [43, 45].

However, we previously observed yeast expressing CDT-2 could not perform efficient cellobiose utilization compared with yeast expressing CDT-1 (Kim et al. 2014). Thus, this study was undertaken to improve transporting activity of CDT-2 via evolutionary engineering [74]. We imposed cellobiose as a selection pressure onto yeast expressing CDT-2 and the cellobiose phosphorylase. After nine rounds of serial subcultures on cellobiose, we isolated an evolved strain exhibiting significantly faster cellobiose assimilation and increased ethanol yields. Also, we report that change of single amino acid residue on CDT-2 is sufficient for drastic improvement of cellobiose utilization in engineered *S. cerevisiae*.

3.2 Materials and methods

Strains and plasmids

All strains and plasmids used in the study are listed in Table 3.1. Cellobiose transporter genes from *N. crassa* FGSC 2489, NCU 00801 (*cdt-1*) and NCU08114 (*cdt-2)* were cloned into a pRS426 plasmid (*URA3*, *PGK1* promoter, and *CYC1* transcriptional terminator), respectively. An intracellular β-glucosidase gene (*gh1-1*) from *N. crassa* was cloned into a pRS425 plasmid (*LEU2*, *PGK1* promoter, *CYC1* transcriptional terminator) [41]. A cellobiose phosphorylase gene (*SdCBP*) from *Saccharophagus degradans* was cloned into a pRS425 plasmid (*LEU2*, *PGK1* promoter, *CYC1* transcriptional terminator) [45]. To create *gfp* tagged CDT-2 transporter, *gfp*

gene was cloned into pRS426 *cdt-2*. *S. cerevisiae* D452-2 (*MATα leu2 his3 ura3 can1*) [97] was used for transformation of the plasmids and characterization of the cellobiose fermentation. Synthetic complete (SCD) medium (6.7 g/L yeast nitrogen base without amino acids, 20 g/L glucose and 0.625 g/L complete supplement mixture (CSM) without leucine, tryptophan and uracil) (Bio 101, Vista, CA) with appropriate nucleotides and amino acids was used for selection of the transformants.

Cellobiose fermentation experiments

A single colony after transformation was picked and grown in YP medium (10 g/L yeast extract and 20 g/L peptone) with 20 g/L of cellobiose at 250 rpm and 30°C to prepare inocula for fermentation experiments. Yeast cells at mid-exponential phase were harvested by centrifugation and washed with sterile water before inoculations. Fermentation experiments were performed in YP (10 g/L yeast extract and 20 g/L peptone) with 80 g/L of cellobiose in micro-aerobic condition or anaerobic condition. Micro-aerobic fermentation experiments were performed in 25 mL culture using a 125 mL Erlenmeyer flask tightly covered by aluminum foil at 30°C and 100 rpm. Anaerobic fermentation was performed by 20 mL culture using a 100-mL serum vial sealed with a rubber cap and nitrogen purged for 15 min with gentle swirling. Vials were incubated at 30 °C at 100 rpm as well. Initial cell densities of all fermentation experiments were adjusted to an OD_{600} of 1. All fermentation experiments were performed in duplicates.

Laboratory evolution and isolation of an evolved strain

For laboratory evolution, serial subcultures on cellobiose were conducted with an *S. cerevisiae* strain harboring pRS425 *cdt-2* and pRS426 *SdCBP.* Yeast inoculum was prepared by cultivating a single colony in 5mL YP medium with 20 g/L of cellobiose at 30°C and 250 rpm. Cells were harvested, and an initial cell density equal to an OD_{600} of 1 was inoculated in 25 mL of YP medium with 80 g/L of cellobiose using 125 mL Erlenmeyer flasks. When cellobiose concentration reached below 10 g/L, inoculum equivalent to an OD_{600} of 1 was collected and transferred to a new 25mL of YP medium with 80 g/L cellobiose. This step was repeated nine times, and a single colony from the culture was isolated. A single colony isolated was then evaluated to confirm improved phenotype and plasmids were extracted for Sanger sequencing.

Analytical methods

Cell growth was monitored by measuring optical density (OD) at 600 nm using a UV-visible spectrophotometer (Biomate5, Thermo, Rochester, NY). Cellobiose, cellodextrin, and ethanol concentrations were determined by high-performance liquid chromatography (HPLC, Agilent Technologies 1200 Series, Mississauga, CA) equipped with a refractive index detector using a Rezex ROA-Organic Acid H^+ (8%) column (Phenomenex Inc., Torrance, CA). The column was eluted with 0.005 N of H_2SO_4 at a flow rate of 0.6 ml/min at 50°C.

Transporter topology prediction of CDT-2

Homology model of CDT-2 was predicted by online web portal server Phyre2 (http://www.sbg.bio.ic.ac.uk/phyre2)[116] using intensive mode. 90% of the residues were modeled with >90% accuracy. Then VMD (Visual Molecular Dynamics, http://www.ks.uiuc.edu/Research/vmd/, [117]) program was used to visualize the resulting homology model (PDB entry 4GBZ).

Fluorescence measurement and intracellular cellobiose measurement

To measure fluorescence of gfp tagged transporters, *S. cerevisiae* harboring pRS425 *cdt-2-gfp* or pRS425 *cdt-2 N306I-gfp* were cultured in SCD medium without uracil at 30°C and 250 rpm. Cells were harvested at the late exponential phase and washed twice with sterile water. Cell density equal to an OD_{600} 5 were re-suspended in 300 μL of sterile water and transferred to a black 96 well plate for fluorescence measurement. To measure intracellular cellobiose, cells cultured in SCD medium without uracil were harvested at mid-exponential phase. Cells were washed twice with sterile water, transferred to YPC 20g/L medium and incubated at 30°C and 250 rpm. Cells were harvested by centrifugation and washed twice with ice-cold water at 15 hours of incubation which showed cellobiose concentration of both CDT-2 and CDT-2m expressing strain. Cell density equal to an OD_{600} 30 were re-suspended in 1 mL of < 40°C methanol with glass beads. After a vigorous vortexing for 3 minutes, samples were incubated in -80°C for 30 minutes. Supernatants were separated by centrifugation, and 900 μL were transferred to a microcentrifuge tube and allowed to evaporate. Then remaining solids were re-suspended in 300 μL of water to quantify cellobiose via HPLC.

3.3 Results

Comparison of cellobiose fermentation by engineered yeast with CDT-1 and CDT-2 coupled with phosphorylase

As I hypothesized that CDT-2 paired with SdCBP might have energetic benefits during fermentation, two yeast strains overexpressing *cdt-1* with *SdCBP* (DCT-1) and *cdt-2* with *SdCBP* (DCT-2) were compared for cellobiose fermentation capability under oxygen-limited conditions. As shown in Figure 3.2, both strains could grow on 80 g/L of cellobiose. As expected, cellodextrin accumulation was not observed in both DCT-1 and DCT-2 strains. However, DCT-2 showed poorer growth rate, cellobiose consumption and ethanol production compared to DCT-1. Because similar cellobiose fermentation patterns were already observed in yeast strains expressing CDT-1 and CDT-2 coupled with GH1-1 [43, 118], in general, CDT-2 is an inefficient cellobiose transporter regardless of pairing with hydrolytic or phosphorolytic enzymes.

Laboratory evolution of strain DCT-2 for improved cellobiose fermentation

To improve CDT-2 performance on cellobiose transportation, I performed serial subculture of DCT-2 with cellobiose. In this case, cellobiose is not only the major carbon source but also a selection pressure: the cells with beneficial mutations on cellobiose metabolism will become dominant during serial subculturing. Initially, cell inoculum equivalent to OD 1 was inoculated to YPC 80 g/L medium. Once cell growth was observed and cellobiose consumption was observed but before depleted, cell inoculum equivalent to OD 1 was transferred to fresh YPC 80 g/L media. I repeated subculturing successively as cellobiose utilization rate improved gradually and stopped when cellobiose utilization rate improvement ceased (total nine rounds of serial subculture on cellobiose). Then, single colonies from the last culture were isolated, and fermentation capability was compared with an original DCT-2 strain to confirm the improvement. As shown in Figure 3.3, all three isolated colonies from the evolved DCT-2 culture showed consistent and significant improvement in cellobiose fermentation compared to the original DCT-2 strain. While the original DCT-2 could not finish consuming cellobiose at 120 hours, three evolved colonies were able to complete fermenting all cellobiose within 36 hours with corresponding improvements in ethanol productivities.

A single nucleotide change in cdt-2 for improved cellobiose fermentation

To confirm whether mutations formed in either CDT-2 or SdCBP during serial subculture, both plasmids were rescued from all three isolates and sequenced along with wild-type CDT-2 and wild-type SdCBP plasmids. While no change of DNA sequence was observed on the rescued SdCBP, one mutation was observed on the all three rescued CDT-2. Base pair adenine was changed to thymine at position 917 (A917T), resulting in a change of protein sequence from asparagine to isoleucine at position 306 of CDT-2 (N306I) (Figure 3.4). To analyze the potential effects of this mutation, I predicted the structure of CDT-2 using the Phyre2 web portal [116]. The Phyre2 analysis used 20 templates that had 100% confidence of CDT-2 sequence covering protein sequence 14-525. Then, the mutant CDT-2 homology model was structurally aligned to *E. coli* XylE, xylose proton symporter bound to glucose (PDB entry 4GBZ, total 462 nucleotide alignment to CDT2) as other previous cellobiose transporter studies [119, 120]. As shown in Figure 3.4, mutation N309I occurred within a transmembrane α-helix domain. (Figure 3.4A). A mutation at such a location might enhance the cellobiose uptake rate of CDT-2 as observed in the previous report [118]. To examine if the N306I mutation influenced the expression level of the mutated CDT-2, expression levels of wild-type and mutant CDT-2 were monitored by tagging with GFP and measuring fluorescence (Figure 3.4B). Mutant CDT-2 showed about 2-fold higher fluorescence than wild-type CDT-2, indicating mutation increases expression level or stability of CDT-2. Next, yeast strains with only expressing CDT-2 and mutated CDT-2 (N309I) were incubated in YPC 20g/L medium to observe relative cellobiose transport activities. I observed intracellular cellobiose accumulation at 15h based where both CDT-2 and CDT-2m shows detectable and comparable cellobiose transportation. As expected, the engineered yeast expressing the N309I CDT-2 showed ~6 times higher intracellular cellobiose accumulation than the engineered yeast expressing CDT-2. These results confirm that the N309I mutation in CDT-2 may enhance expression and overall enhanced transporting capability in yeast (Figure 3.4C).

Comparison of phosphorolytic and hydrolytic pathways for cellobiose fermentation

After identifying the beneficial mutation (N309I) on CDT-2, I introduced the mutant CDT-2 into a wild-type *S. cerevisiae* along with SdCBP to verify that such an improvement of cellobiose fermentation is due solely to a mutation on cellodextrin transporter and not a genomic mutation in the yeast. As shown in Figure 3.5, the transformant expressing the mutant CDT-2 and SdCBP (DCT-2m) was able to consume cellobiose as fast as isolates from the serial

subculture (Figure 3.4B and C), suggesting that the single amino acid mutation on CDT-2 is to responsible for enhanced cellobiose fermentation capacity.

I suspected that the mutant CDT-2 might also improve cellobiose fermentation when paired with intracellular β-glucosidase. Thus, the mutant CDT-2 and GH1-1 genes were introduced into wild-type *S. cerevisiae* to enable cellobiose fermentation by the hydrolytic pathway (Figure 3.1). To compare fermentation capabilities of yeast the phosphorolytic pathway (yeast expressing CDT-2m and SdCBP; DCT-2m with yeast utilizing the hydrolytic pathway (yeast expressing CDT-2m and GH1-1; DBT-2m), DCT-2m and DBT-2m strains were cultured in YPC 80 g/L medium under oxygen-limited conditions. The DCT-2m strain was able to ferment cellobiose and produce ethanol at a faster rate than DBT-2m (Figure 3.5). While strain DCT-2m was able to completely consume 80 g/L of cellobiose within 48h without any accumulation of cellodextrin, strain DBT-2m consumed all cellobiose within 60h while accumulating significant amounts of cellodextrin (Figure 3.5D). Strain DCT-2m showed higher ethanol yield and productivity from cellobiose than strain DBT-2m (0.42 g/g ethanol yield and 0.70 g/L·h by the DCT-2m strain vs. 0.32 g/g ethanol yield and 0.36 g/L·h by DBT-2m strain, Table 3.2, second column).

To further validate the superiority of strain, I performed cellobiose fermentation (YPC 80 g/L) under the anaerobic condition where energy generation is limited. At the end of fermentation, ethanol yield and productivities were calculated (Table 3.2, third column). In general, all strains tested had slower cellobiose fermentation rate. DCT-2m strain highest ethanol yield (0.45 g/g) compared to DCT-1, DCT-2, DBT-2 and DBT-2m (0.44 g/g, 0.39 g/g, 0.29 g/g and 0.32 g/g, respectively. For ethanol productivity, however, DBT-2m produced ethanol at a higher rate compared to DCT-2m strain (0.21 g/L·h vs. 0.11 g/L·h). Still, DBT-2m had significantly lower ethanol yield (0.32 g/g) due to cellodextrin accumulation. Under anaerobic fermentation, β-glucosidase expressing strains (DBT-2 and DBT-2m) was not able to re-assimilate cellodextrin (data not shown).

3.4 Discussion

Fermentation of cellobiose (or cello-oligosaccharides from enzymatic cellulose hydrolysis) by engineered yeast has received strong attention as a promising strategy to replace

current corn starch fermentation. Heterologous expression of cellodextrin transporters and intracellular cellobiose hydrolyzing enzymes are necessary for *S. cerevisiae* to ferment cellobiose. Thus, previous reports identified several cellodextrin transporters and hydrolyzing enzymes from a variety of microorganism. Particularly, two cellodextrin transporters (CDT-1 and CDT-2) from *N. crassa* and two cellobiose hydrolyzing enzymes (GH1-1 from *N. crassa* and SdCBP from *S. degradans*) have been functionally expressed in yeast, leading to not only direct fermentation of cellobiose, but also co-fermentation of mixed sugars such as cellobiose/xylose and cellobiose/galactose [24, 44, 121]. Among the two cellodextrin transporters, yeast strains expressing CDT-1 showed better cellobiose fermentation than yeast strains expressing CDT-2 when paired with β-glucosidase [43]. I reason that the difference in cellobiose fermentation rate might be caused by different kinetic properties of CDT-1 and CDT-2. CDT-1 exhibits 2-fold higher V_{max} than CDT-2 while Michaelis constant (K_m) remains slightly higher than CDT-2 (4.0 μM vs. 3.2 μM). (Galazka et al. 2010). Also, CDT-1 is an active transporter requiring ATP to transport even low concentrations of cellobiose, but CDT-2 is a facilitator which depends on a cellobiose concentration gradient. While engineered yeast expressing CDT-1 showed faster cellobiose fermentation than engineered yeast expressing CDT-2, expression of CDT-2 in yeast might be more advantageous for large-scale production of ethanol because most industrial fermentations are performed under harsh conditions (i.e., ATP-limited conditions) caused by pretreatment of cellulosic biomass with acids or bases.

Despite the potential advantage of CDT-2, it is necessary to improve kinetic properties of CDT-2 for feasible cellobiose fermentation due to slower cellobiose fermentation compared to CDT-1. There have been efforts to improve the kinetic properties of CDT-2 through protein engineering and identification of mutants presenting enhanced cellobiose fermentation when paired with GH1-1 [118]. However, GH1-1 frequently causes the formation of undesirable by-products such as cellodextrin (a by-product from transglycosylation by β-glucosidase), resulting in inefficient cellobiose fermentation. Indeed, previous reports showed that accumulation of cellodextrins by the strains expressing intracellular β-glucosidase yielded less ethanol regardless of the type of transporter [43, 45]. As an alternative to β-glucosidase, cellobiose phosphorylase can be used to eliminate cellodextrin accumulation. Additionally, the phosphorolysis of cellobiose reaction will consume one less ATP per one cellobiose compared to the hydrolysis reaction. However, the catalysis by cellobiose phosphorylase is a thermodynamically unfavorable reaction ($\Delta G > 0$), contributing to inefficient cellobiose

fermentation by yeast strains expressing SdCBP compared with strains expressing GH1-1. To observe cellobiose fermentation pattern by DCT-2 in *S. cerevisiae*, fermentation experiments were conducted in YPC 80 g/L medium and under microaerobic condition. As a result, CDT-2 and SdCBP combination had the least efficient cellobiose fermentation compared to other transporter and hydrolyzing enzyme despite its potential advantages ([43], Figure 3.1). Thus, I hypothesized improvement of DCT-2 is necessary to benefit the potential energetic advantages of CDT-2 and SdCBP.

Previous studies show that kinetic properties of cellodextrin transporters were drastically changed by mutated cellodextrin transporters, thus an improvement on cellobiose fermentation [45]. Also, the mutated cellodextrin transporters have been obtained through laboratory evolution of yeast strains expressing cellodextrin transporters such as CDT-1 from *N. crassa* and HXT2.4 from *Pichia stipitis* [42, 118]. As such, I reasoned that transporting activity of CDT-2 might also be improved by modification of some amino acid residues on CDT-2, which would lead to enhanced cellobiose fermentation rate in engineered *S. cerevisiae*.

Based on the previous successes with laboratory evolution engineering approach, a similar strategy was adapted to improving DCT-2 strain, evolving under cellobiose-containing media. I hypothesized a significant selection pressure could stimulate the rate of cellobiose fermentation with 80 g/L of cellobiose in the media. From nine rounds of evolution, I identified a mutant CDT-2 (N306I) sufficient to significantly improve the rate of cellobiose fermentation and yield of ethanol. To visualize the single mutation on the protein structure, CDT-2 (N306I) homology model was created using Phyre2 and structurally aligning to *E. coli* XylE bound to glucose. From the alignment result, the local region of N306I mutation (Figure 3.4, left arrow) was located near the vicinity of the substrate binding site N294 of XylE (Figure 3.4, right arrow), possibly in the binding site for a substrate unit. Also, as a result of the mutation N306I, overall expression or stability and cellobiose transportation may have enhanced (Figure 3.4B and C).

I confirmed the beneficial effect of the mutant CDT-2 by re-constructing strain DCT-2m and fermenting 80 g/L of cellobiose under oxygen-limited conditions. Indeed, DCT-2m could consume cellobiose and produce ethanol at a faster rate and higher yield than both DCT-1 and DCT-2. In the most favorable condition, the ethanol yield and productivity of DCT-2m were approximately 2-fold and 10-fold higher than DCT-2, respectively (Table 3.2). When considering directed evolution of CDT-2 improved expression level as well as cellobiose uptake activity

(Figure 3.5), change of the kinetic properties, increase in the expression level, or enhanced the stability of mutant CDT-2 may explain the enhanced cellobiose fermentation of DCT-2m observed in this study.

I also investigated whether expression of the mutant CDT-2 with β-glucosidase in a wild-type yeast could also increase the rate of cellobiose consumption and ethanol yield. However, we did not observe a significant improvement of cellobiose consumption rate and ethanol yield in yeast expressing the mutant CDT-2 with GH1-1 as observed with yeast expressing the mutant CDT-2 with SdCBP. While DCT-2m showed 100% and 900% enhanced ethanol yield and productivity than DCT-2, DBT-2m showed 70% and 230% changes in ethanol yield and productivity than DBT-2. This effect may be caused by the incapability for mutant CDT-2 to transport cellodextrins formed by transglycosylation activity of GH1-1 as observed in the previous study [43] and shown in Fig. 3.5. Most likely, improvement of cellobiose fermentation in DBT-2m may be due to increased expression level, stability, and kinetic properties change specific to cellobiose but not cellodextrins. Correspondingly, DCT-2m, a strain which does not accumulate cellodextrins, showed enhanced performance in cellobiose fermentation and produced more ethanol at a faster rate than DBT-2m (0.42 g/g and 0.70 g/L· h in DCT-2m vs. 0.33 g/g and 0.36 g/L· h in DBT-2m). Additionally, cellodextrin accumulation is likely to require more ATP for re-assimilation, resulting in residual cellodextrin at the end of fermentation (Fig. 3.5D).

I further hypothesized that the energetic benefits of CDT-2 requiring less ATP might become maximized under energy-limited conditions. Anaerobic condition limits respiration of the yeast strains thus limit energy production. DCT-1, DCT-2, DCT-2m, DBT-2 and DBT-2m were compared for anaerobic cellobiose fermentation regarding ethanol yield and productivities (Table 3.2, third column). Like micro-aerobic condition, strains expressing CDT-2m showed improvement in cellobiose fermentation. Among all strains tested, the DCT-2m strain had the highest ethanol yield of the strains compared, even compared to micro-aerobic condition (0.45 g/g vs. 0.44 g/g). However, under anaerobic condition, I observed DBT-2m strains exhibited higher ethanol productivities but lower yield than DCT-2m strain (0.21 g/L· h vs. 0.11 g/L· h for productivity and 0.32 g/g vs. 0.45 g/g for yield). As mentioned above, it is likely due to efficient cellobiose conversion by GH1-1 but the accumulation of cellodextrin by trans-glycosylation activity. Under anaerobic condition, re-assimilation of cellodextrin might be even more

challenging due to limited energy production. In sum, improved cellobiose fermentation was only observed with strains expressing CDT-2m compared to CDT-2 regardless of the which hydrolyzing enzyme it is paired with. DCT-2m (CDT-2m with phosphorylase) showed the most efficient utilization of cellobiose especially under microaerobic cellobiose fermentation, proven by its ethanol yield and productivity.

In conclusion, the introduction of a mutated energy independent cellodextrin transporter (CDT-2) from *N. crassa* and cellobiose phosphorylase (SdCBP) from *S. degradans* into *S. cerevisiae* resulted in the fermentation of cellobiose as the sole carbon source without cellodextrin accumulation. An original strain expressing CDT-2 showed very inefficient cellobiose fermentation. However, a single nucleotide change in CDT-2 could improve the cellobiose fermentation significantly. Our mutant CDT-2 paired with phosphorylase may provide several advantages in the fermentation of cellulosic biomass by allowing energy conservation and better fermentation parameters.

3.5 Figures and tables

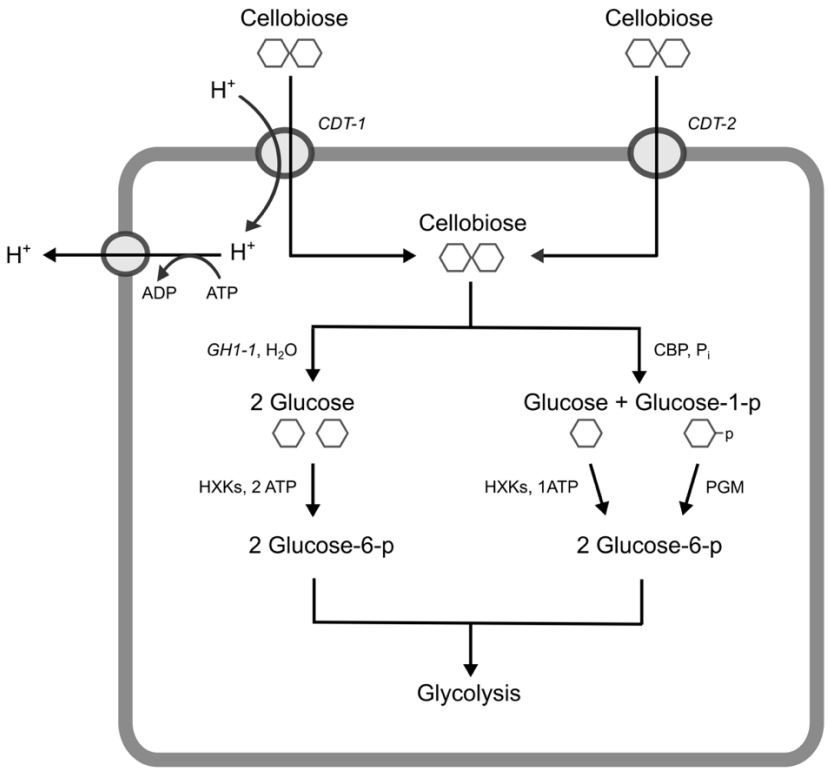

Figure 3.1 Possible cellobiose fermentation pathways with the combinatorial introduction of cellobiose transporters and cellobiose cleaving enzymes. Either Cdt-1 or Cdt-2 transport cellobiose across the membrane; then cellobiose is cleaved by either hydrolytic enzyme (intracellular β-glucosidase, GH1-1) or phosphorolytic enzyme (cellobiose phosphorylase, SdCBP). Cleaved cellobiose, generating two glucose or one glucose with one glucose-1-phosphate, is converted to glucose-6-phosphate via hexokinases (HXKs) and phosphoglucomutase (PGM) [45].

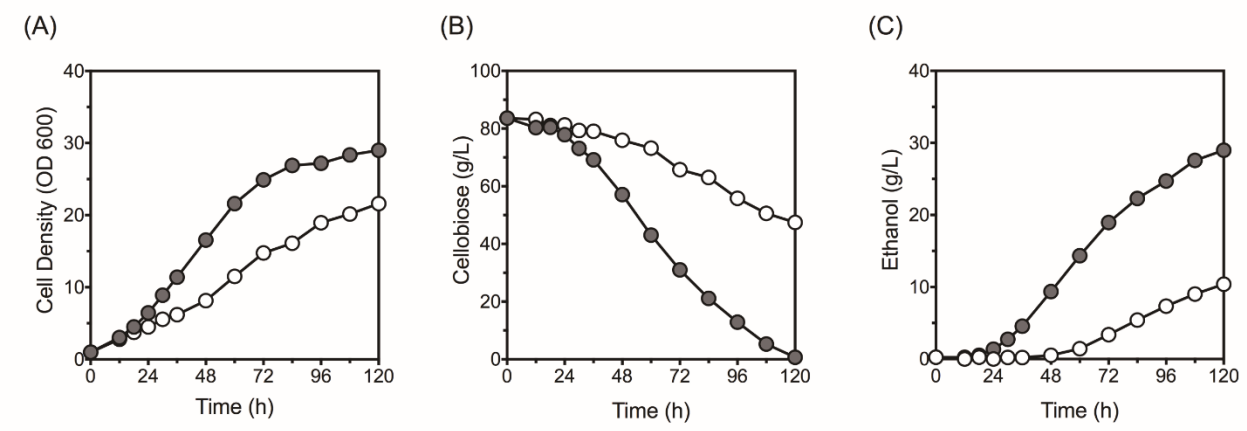

Figure 3.2 Comparison of fermentation profiles between *S. cerevisiae* DCT-1 expressing *cdt-1* and *SdCBP* and *S. cerevisiae* DCT-2 expressing *cdt-2* and *SdCBP* in YP media under oxygen-limited conditions. Cell growth (A), cellobiose consumption (B) and ethanol production (C) were compared. The DCT-1 is represented in the gray circle, and the DCT-2 strain is represented by the white circle.

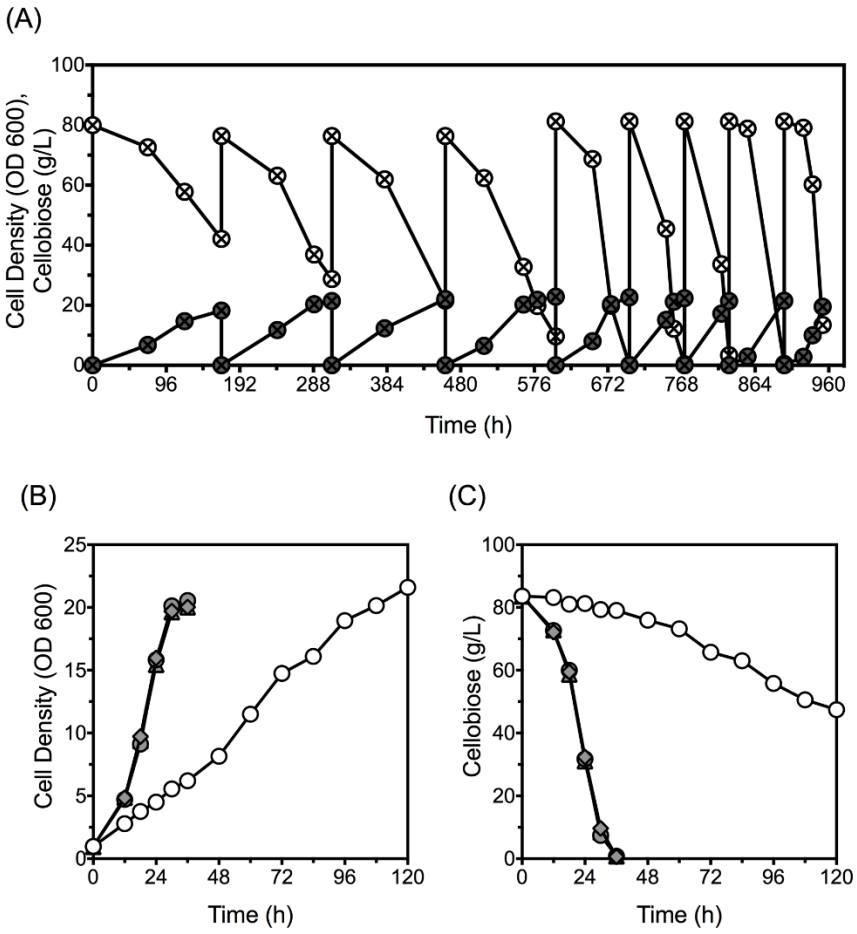

Figure 3.3 Serial subcultures of the DCT-2 strain on cellobiose and fermentation profile of the isolated colonies from the last enriched culture. Growth (gray circle with cross) and cellobiose consumption (white circle with cross) were measured (A). As growth rate and cellobiose consumption rate saturated at ninth transfer, single colonies were isolated. Cell growth and cellobiose consumption of the original DCT-2 and three single isolated colonies from the evolved DCT-2 were compared (B). Three single colonies of the evolved DCT-2, and the original DCT-2 are represented in the gray circle, gray diamond, gray triangle and white circle respectively.

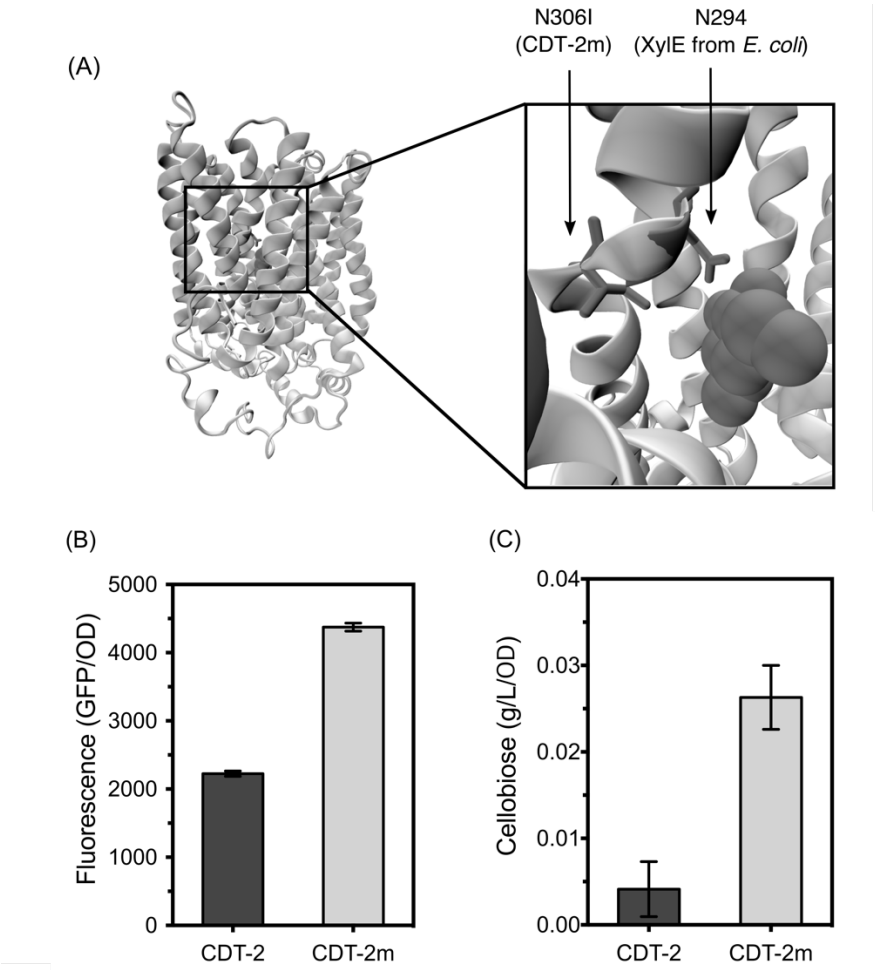

Figure 3.4 Amino acid change due to a point mutation in CDT-2 and relative expression level of CDT-2 wildtype and CDT-2 mutant with GFP tagging and intracellular cellobiose. Transporter homology model prediction of CDT-2 based on the Phyre2 online program (A). The arrow represents the mutation N306I in CDT-2 (left) and nearest glucose binding site (N294) site from alignment to *E. coli* XylE bound to glucose (PDB entry 4GBZ). Glucose is shown in VDW model. *S. cerevisiae* strains expressing only CDT-2-GFP or CDT-2m-GFP were cultured in SCD and fluorescence level was measured at stationary phase for relative expression level (B). Intracellular cellobiose of strains only expressing CDT-2 or CDT-2m were measured after culturing in the YPC medium until visible intracellular cellobiose is shown in both strains (C).

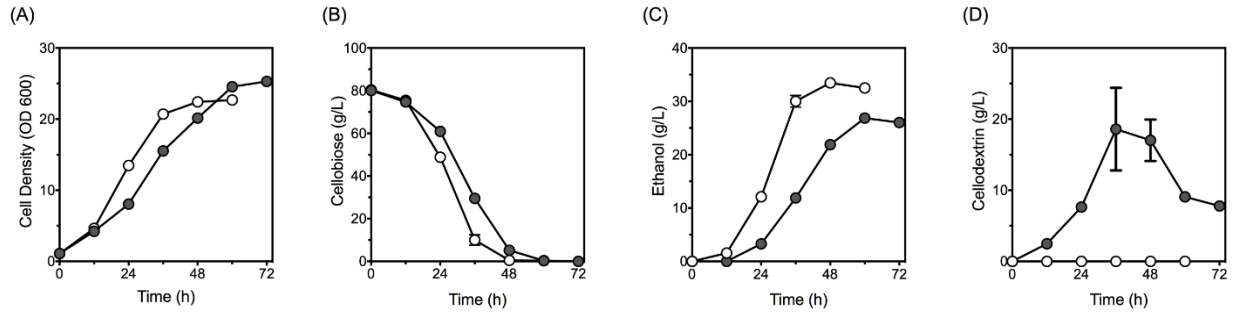

Figure 3.5 Comparison of fermentation profile by *S. cerevisiae* DBT-2m expressing the CDT-2 N306I and GH1-1 and *S. cerevisiae* DCT-2m expressing the CDT-2 N306I and CBP. Cell growth (A), cellobiose consumption (B), ethanol production (C) and cellodextrin accumulation (D) were compared. The DBT-2m and DCT-2m strains are represented in the gray circle and white circle, respectively.

Table 3.1 The list of plasmids and *S. cerevisiae* strains used in this study

Plasmids and strains	Relevant features	Sources and references
Plasmids		
pRS425PGK	*LEU2*, P_{PGK} -MCS- T_{CYC}, 2μ origin, Amp^r	[41]
pRS426PGK	*URA3*, P_{PGK} -MCS- T_{CYC}, 2μ origin, Amp^r	[41]
pRS425-SdCBP	*LEU2*, P_{PGK}-*Sdcbp*-T_{CYC}, 2μ origin, Amp^r	[45]
pRS425-gh1-1	*LEU2*, P_{PGK}-*gh1-1*-T_{CYC}, 2μ origin, Amp^r	[41]
pRS426-cdt-1	*URA3*, P_{PGK}-*cdt-1*-T_{CYC}, 2μ origin, Amp^r	[41]
pRS426-cdt-2	*URA3*, P_{PGK}-*cdt-2*-T_{CYC}, 2μ origin, Amp^r	[41]
pRS426-cdt-2-gfp	*URA3*, P_{PGK}-*cdt-2-gfp*-T_{CYC}, 2μ origin, Amp^r	This study
pRS426-mcdt-2-gfp	*URA3*, P_{PGK}-*cdt-2-gfp* N306I-T_{CYC}, 2μ origin, Amp^r	This study
Strains		
D452-2	*MATα leu2 his3 ura3 can1*	[97]
DCT-1	D452-2/ pRS425-SdCBP/pRS426-cdt-1	This study
DCT-2	D452-2/ pRS425-SdCBP/pRS426-cdt-2	This study
DCT-2m	D452-2/pRS425-SdCBP/pRS426-cdt2 N306I	This study
DBT-2	D452-2/pRS425-gh1-1/pRS426-cdt2-gfp	This study
DBT-2m	D452-2/pRS425-gh1-1/pRS426-cdt2-gfp N306I	This study

Table 3.2 Fermentation parameters of DCT1, DCT2, and DCT2m under oxygen-limited or anaerobic conditions

Strains	Oxygen-limited		Anaerobic	
	Y_{EtOH}[1]	P_{EtOH}[1]	Y_{EtOH}[1]	P_{EtOH}[1]
DCT-1	0.35 ± 0.00	0.26 ± 0.00	0.44 ± 0.00	0.09 ± 0.00
DCT-2	0.21 ± 0.00	0.07 ± 0.00	0.39 ± 0.00	0.03 ± 0.00
DCT-2m	0.42 ± 0.01	0.70 ± 0.01	0.45 ± 0.00	0.11 ± 0.00
DBT-2[2]	0.19 ± 0.00	0.11 ± 0.00	0.28 ± 0.00	0.13 ± 0.00
DBT-2m	0.33 ± 0.00	0.36 ± 0.00	0.32 ± 0.00	0.21 ± 0.00

[1] Fermentation parameters: Y_{EtOH}, ethanol yield (grams of ethanol per gram of sugar); P_{EtOH}, ethanol productivity (grams of ethanol per liter per hour) calculated at the end of fermentation

[2] Results referenced from Kim et al. [43]

CHAPTER IV: QTL Mapping Analysis for Enhanced Xylose Utilization in Engineered *Saccharomyces cerevisiae* [3]

4.1 Introduction

For efficient utilization of lignocellulosic sugars such as xylose, *Saccharomyces cerevisiae* strains should be engineered to express xylose assimilation pathway taken from native xylose-fermenting yeast such as *Scheffersomyces stipitis*. Previous studies successfully developed the xylose-fermenting yeasts by expressing xylose reductase (XR, encoded by *XYL1*), xylitol dehydrogenase (XDH, encoded by *XYL2*) and xylulose kinase (XK, encoded by *XYL3*) [30, 71, 72, 109]. Additionally, few genetic perturbations such as *PHO13* deletion allowed enhanced xylose fermentation [39, 78]. The efficiency of xylose fermentation remains to be less efficient compared to glucose fermentation.

Both rational and traditional combinatorial metabolic engineering have been employed to develop a strain with improved xylose-fermenting properties [77]. Many previous studies reported the successful application of both metabolic engineering approaches [78, 79]. Methodologies are often optimized for the monogenic effects focusing on a single gene effect on the desired phenotype. However, many observed phenotypes are complex (quantitative) traits, resulting from interactions of many genes. For example, xylose fermentation in yeast is a complex trait. A simple expression of the xylose-assimilating pathway in different yeast host strains result in different xylose fermentation pattern owing to the variance of the host strains. Current metabolic engineering approaches may be limited for determining complex traits. I hypothesized that QTL mapping analysis could be effective for identification of the genes responsible for robustness.

Traditional methodologies for identifying quantitative traits are depended on the two major factors: phenotypic (trait) evaluation and genotypic (genetic sequences) evaluation. Quantitative Trait Locus (QTL) mapping analysis is a widely accepted analysis used in various fields of study such as plant biology, medicine, and microbiology [80]. Many studies in metabolic engineering of microbes performed QTL mapping analysis that allowed identification genetic

[3] The content of this chapter is in preparation for submission. I performed the research with helps from Matthew Maurer, Jeffrey M. Skerker, Adam P. Arkin and Yong-Su Jin (director of the research)

targets for strain improvement [81-89]. The analysis allows linking statistically phenotypic and genotypic data for determining the genetic basis of the trait of interest. To qualify for QTL mapping analysis, two strains within the same species that differ genetically and phenotypically are required. The parental strains are then crossed to generate daughter cells that contain fractions of the genome from its parental strains. These individual progenies are evaluated for the trait of interest, and their genotype (sequence) data is obtained. For the genotypic evaluation, the differences such as single nucleotide polymorphisms (SNPs), indels, and transposable element locations are used as the marker [122, 123]. The sequences the individual progenies are mapped to the parental strains' genome as a reference and segregation pattern of the marker will be analyzed statistically for the association of the traits. Ideally, markers (i.e. SNPs) of the genetic sequences linked to the trait of interest will be highly segregated whereas unlinked markers will remain unsegregated [124].

Although QTL mapping analysis is a well-accepted tool for determining the genetic basis for a complex trait, there are a few problems with this method. The biggest limitation is the sample size of the progeny obtained from crossing parental strains. A sample size of the progeny is a critical factor that can determine the effectiveness of the QTL analysis result. A small number of the sample may result in failure of predicting the QTL associated with the trait [125]. Also, a large number of the sample may be extremely laborious to evaluate the traits and costly to sequence all of its genomes [124]. Regarding QTL analysis of the microorganisms, promising solutions to a sample size requires using bulk or large pools of segregants [126-131]. Instead of isolating each recombinant cell and using as each sample, the pool of recombinant individuals will be used for phenotyping and genotyping. Because the pool contains extremely varied recombinant individuals, the resulting QTL result will be more significant for predicting the correct QTL. Therefore, this study presents an extreme QTL (x-QTL) analysis of xylose fermentation in engineered *S. cerevisiae* to elucidate genetic interaction for enhanced xylose fermentation.

4.2 Materials and methods

Strains and Plasmids

All strains and plasmids used in the study are listed in Table 4.1. The mutant allele, *ura3-52*, from D452-2 [97] was introduced into both S288Cm and JAY291m strain for generating uracil auxotrophic strain. Strains were selected on SCD agar plates (synthetic complete media; 6.7 g/L yeast nitrogen base with ammonium sulfate, 0.79 g/L of complete supplement mixture with appropriate amino acid dropout (Bio 101, Vista, CA) and 20 g/L glucose) containing 1 g/L 5-fluoroorotic acid (5-FOA). Next, xylose-fermenting strains were constructed by integrating linearized pSR6 X123 plasmid [71] at *URA3* locus generating S288C X123 and JAY291 X123. The transformant was selected on SCD agar plate without uracil.

Fermentation experiments

To prepare yeast strains, yeast cells were cultivated in YPD medium (10 g/L yeast extract, 20 g/L peptone, and 20 g/L glucose) at 30°C and 250 rpm. Cells were harvested at late exponential phase by centrifugation and washed two times with sterile water. YPX medium (YP medium with appropriate concentrations of xylose) was used for main fermentation. All flask-scale fermentation experiments were performed in 50 mL culture using a 250 mL Erlenmeyer flask tightly covered with aluminum foil at 30°C and 100 rpm of rotation speed. Initial cell densities of all fermentation experiments were adjusted to OD_{600} of 1. All flask-scale fermentation experiments were performed in duplicates.

Analytical methods

Cell growth was monitored by measuring optical density (OD) at 600 nm using a UV-visible spectrophotometer (Biomate5, Thermo, Rochester, NY). Xylose, xylitol, and ethanol concentrations were determined by high-performance liquid chromatography (HPLC, Agilent Technologies 1200 Series, Mississauga, CA) equipped with a refractive index detector using a Rezex ROA-Organic Acid H^+ (8%) column (Phenomenex Inc., Torrance, CA). The column was eluted with 0.005 N of H_2SO_4 at a flow rate of 0.6 ml/min at 50°C.

Mating and recombinant segregant pool generation

Two parental strains, S288C X123 and JAY291 X123, were crossed to generate hybrid diploid strain SJ X123. Then SJ X123 strain was grown overnight in YPD 20 g/L at 30°C and 250 rpm. Cells were harvested (5mL, OD_{600} ~10), washed with sterile water twice and inoculated into 500 mL of sporulation media (10 g/L potassium acetate, 0.1 g/L yeast extract, 0.5 g/L glucose). Yeasts were sporulated at ambient temperature (~22°C), periodically monitoring for a

fraction of tetrad formation of the population by light microscopy. When ~70-80% of the culture was sporulated (~7 days), cells were harvested. Only *MATa* haploid was obtained by magic marker selection system, from the previously described method [127]. Harvested cultures were treated with Zymolyase and vortexed with glass beads to digest ascus and release ascospores. Then Zymolyase treated culture were diluted 100-fold and plated onto magic medium and incubated at 30°C until spores were germinated. Collected strains were suspended in 15% glycerol and stored at -80°C.

Serial subculture to enrich superior xylose-fermenting segregants

The pool of recombinant segregants obtained from mating two parental strains was activated in YPD for ~2 hours at 30°C. Initial cell density equal to an OD_{600} of 0.25 was inoculated in 50 mL of YP medium with 80 g/L of glucose or xylose using 250 mL Erlenmeyer flasks. When the sugar concentrations reached below 10 g/L, but not completely depleted, inoculum equivalent to an OD_{600} of 0.25 was collected and transferred to a new 50mL of YP medium with 80 g/L sugar. This step was repeated five times until xylose consumption rate was saturated. Initial pool population and enriched populations from each transfer were harvested for genomic DNA extraction to prepare for whole genome sequencing.

Whole genome sequencing of segregant population and QTL identification

Whole genome sequencing was performed by the University of Illinois at Urbana-Champaign Biotechnology Center, High-Throughput Sequencing and Genotyping Unit (Urbana, IL) using Illumina HiSeq 2500 platform to produced ~100bp paired ends. The reads were mapped to the S288C reference genome. Then the variant detection and filtering were performed as described previously [119], and about 46,000 segregating sites are used as a marker and mapped to S288C genome and calculated for the allele frequency.

CRISPR/Cas-based genome editing for strain engineering

CRISPR-Cas (Clustered Regularly Interspaced Short Palindromic Repeats/CRISPR-Associated Proteins) based genome editing system was for all strains engineering. Previously established technique in our lab was used [67, 132]. The pRS42N Cas9 plasmid was transformed into *S. cerevisiae* strain first then Cas9 carrying strain was used as host strain for further genetic modifications. Plasmid carrying guided RNA for targeting each QTL regions with the double stranded repairing donor DNA were transformed into Cas9 carrying strains. All

transformation method was adapted from PEG-LiAc high-efficiency yeast transformation method [133] and selected on yeast extract-peptone (YP) medium with 20 g/L of glucose and with appropriate antibiotic markers. All strains and plasmids used in the study are listed in Table 4.1.

Growth assay with BioscreenC

Yeast strains with a deletion in QTL or swapped allele was grown overnight in 5mL YPD medium, harvested, and washed twice with sterile water. Cell density equivalent to OD_{600} 0.01 was used in 200 µL YPX 40 g/L. The BioscreenC (Growth Curves USA, Piscataway, NJ 08854) was used to observe growth by monitoring OD_{600}. All strains were performed in triplicates.

4.3 Results

Construction of the two platform xylose-fermenting *S. cerevisiae* strains with a different genetic background

To perform QTL analysis of xylose-fermenting *S. cerevisiae*, two parental haploid strains S288C and JAY291 that are highly variant were selected. To ferment xylose in *S. cerevisiae*, xylose metabolic pathway consisting of *XYL1, XYL2,* and *XYL3* from *Scheffersomyces stipitis* were integrated. The resulting strains (S288C X123 and JAY291 X123) were then tested for xylose-fermenting capability. Initially, JAY291 X123 xylose fermentation was superior compared to S288C X123 strain. However, S288C X123 readily evolved every fermentation experiment performed at my hand. In the end, evolved strain was isolated from the culture. Then evolved S288C X123 strain was compared to JAY291 X123 strain (Figure 4.2A). With unknown mutation, xylose fermentation of the S288C X123 outperformed JAY291 X123. Overall growth, xylose consumption rate, ethanol production rate was enhanced as well as decreased xylitol accumulation, an undesirable byproduct of xylose fermentation. From the previous study, *PHO13* mutation allows rapid xylose fermentation [39]. Thus *PHO13* gene was sequenced to detect any mutations in the gene. No mutation was detected in *PHO13* sequence from the S288C X123. Based on the xQTL analysis method, the beneficial mutations will be enriched in selected progeny. Therefore, JAY291 X123 and evolved S288C X123 was used as two parental strains for xylose xQTL experiments.

Generation of the recombinant segregants from hybrid S288C X123 and JAY291 X123.

To perform xQTL mapping analysis, the first step is to generate a pool of recombinant segregants that exhibit shuffled genomes from the two parental strains, S288C X123 and JAY291 X123. Two parental strains were crossed to generate a hybrid diploid. Then the diploid strain was incubated in sporulation medium to induce sporulation. After successful formation of tetrads, the culture was harvested and treated to Zymolyase to remove the ascus surround the tetrad. Because the culture contains unsporulated diploids and both *MATa* and *MATalpha* haploids from tetrads, magic marker selection system was employed. Using mating type-specific induction of selective marker and using toxic homologs of amino acids (canavanine and thialysin) only one mating type will survive and kill the another mating type as well as diploids [134].

Enrichment of the segregant pool for selection of superior xylose fermenter.

The pool of haploid strains that have various recombinant genome from its parental strains was obtained. Then the pool was cultured in xylose conditions to obtain enriched culture consumes xylose at a faster rate. The pool was grown in 80 g/L of xylose to apply a strong selective pressure. Primarily, xylose consumption and ethanol production patterns were monitored to observe xylose fermentation rate enhancement (Figure 4.2B). When most the sugar was consumed during each batch of fermentation, a fraction of the population (the equivalent of cell density of OD_{600} 0.25) was inoculated into a fresh medium containing 80 g/L of xylose. This step was repeated until the good xylose-fermenting strains were saturated indicated by xylose consumption rate saturation (Figure 4.2B and C). A total of five rounds of subculturing was performed, and each batch constantly increased xylose consumption rate and ethanol productivity (Figure 4.2C). The original population of segregants and the fraction of the population at the end of each transfer was saved for further analysis. As a control, the same enrichment experiments with the initial batch of segregants were performed under 80 g/L of glucose for five transfers. The fraction of each batch from glucose enrichments was saved as well.

Whole genome sequencing of the enriched culture xQTL mapping analysis of the genome sequencing result

To map QTL for xylose fermentation, the genomic DNA from the parental strains (S288C X123 and JAY291 X123) and population from each round of fermentation were prepared for

whole genome sequencing. Illumina sequencing technology was used for the genome sequencing. The results were then used for xQTL mapping analysis. There are ~46,000 SNP differences between the two parental strains and used as a molecular marker to for QTL analysis. Variants were mapped to the S288C reference genome and calculated for the allele frequency as shown in Figure 4.3. Any enriched region during xylose fermentation from S288C X123 is indicated by allele frequency higher than 0.5 and lower than 0.5 if the region originates from JAY291 X123. About 25 potential QTL was identified among 9 of them showed highly significant QTLs (Table 4.2) and did not overlap with other QTL studies[131]. Also, marker segregation of mating type locus *MAT*, *CAN1,* and *LYP1* gene indicates the robustness of the selection of haploid strain used for the analysis.

Because genome mapping was primarily based on the S288C reference genome, sequence comparison to JAY291 was also performed. There are 11 unique genes exist in JAY291 but absent in S288C. To observe if any of these 11 genes are enriched, the coverage ratio or read-depth estimation was compared between the genome sequence from initial pool and xylose enriched pool. As shown in Figure 4.4, the coverage ratio remained ~1.0 for all 11 unique JAY291 genes.

Screening of the identified QTLs and allele swapping of the identified QTL region and elucidate genetic information of the enhanced xylose fermentation.

To determine the order of putative significance and to consider the ideal approach of the experiment, I utilized the allele frequency peak development with genomic information obtained from intermediate population during enrichment and the length of the QTLs (Table 4.1). I hypothesized that QTLs with a stronger link to the xylose fermentation would develop more rapidly during enrichment. Also, the shorter region will cover fewer genes that allow likelihood of finding a specific determinant for enhanced xylose fermentation. The QTL 1, 2 and 3 (Chr 4, Chr 8 and Chr 11) were tested initially, and all three regions are S288C favorable. The length of each region is 27.7 (Chr 4), 22.7 (Chr 8) and 18.3 Kbp (Chr 11) and divided into four sub-regions (~5-6 Kbp) to swap with another genome (S288C allele to JAY291, first). Deletion of each sub-region was also performed to observe any impact on the xylose fermentation. The cell density measurement using BioscreenC at 36 hours is presented in Figure 4.5. Deletion of the region did not impact growth on xylose except for sub-region 8-4 and 11-4 strain (Figure 4.5A).

However, the growth of 8-4 was recovered by swapping with the S288C allele. Also, swapping the region with 4-2 and 4-4 was detrimental to growth on xylose.

4.4 Discussion

S288C strain, a haploid prototrophic laboratory strain, was one of the first strains for which the full genome was sequenced. Also, it is widely used as a reference strain. JAY291 is a haploid strain derived from yeast isolated from Brazil ethanol plant origin. Its genome was recently sequenced and is available for use by researchers to utilize. As distant as the origins of the two strains, their genome is also highly variant (~46,000 SNP differences). From this information, I hypothesized xylose fermentation capability of the two strains would be different and S288C, and JAY291 can be good parental strains for QTL analysis. Initially, *XYL1, XYL2,* and *XYL3,* which are the minimal required genes for xylose utilization, was integrated into both S288C and JAY291 strains. Next, the resulting strains S288C X123 and JAY291 X123 were evaluated for xylose fermentation capability. Initially, S288C X123 was poorer xylose-fermenting strain compared to JAY291 X123. However, the strain readily evolved every time grown under xylose condition. So, evolved S288C X123 was isolated, and xylose fermentation pattern compared to JAY291 X123 (Figure 4.1A). Evolved S288C X123 exhibited better xylose fermentation compared to JAY291 X123. Previous studies showed mutation at *PHO13*, discovered by laboratory evolution, drastically improved xylose fermentation [39, 78]. Thus, the *PHO13* sequence of the evolved S288C X123 was examined, and no differences were detected. Because evolved S288C X123 and JAY291 X123 still exhibited different xylose fermentation, qualification as parental strains for QTL analysis was still valid.

To generate recombinant segregants, two parental strain were crossed, and the large population was sporulated. The resulting spores were selected on magic medium to obtain only one mating type haploids. Then, a fraction of the recombinant spores was enriched under 80 g/L of xylose. When xylose was depleted from the media, a fraction of the cells was transferred to the fresh xylose medium to saturate the population with superior xylose fermenters (Figure 4.2B and C). As a control, a fraction of the initial recombinant spores was ‘enriched’ under glucose. The genomic DNA from initial population, as well as population saved at each batch during enrichment, was sequenced (both glucose and xylose). Using ~46,000 SNP differences as a

molecular marker, the whole genome sequences were mapped to the S288C reference genome and calculated for allele frequency (Figure 4.3). The genome sequence of xylose enriched strains (red line) shows various unique peaks, indicating that regions were enriched, or conserved, during growth under xylose possibly favorable for xylose utilization. The 16 genes identified only in JAY291 strains were also examined. Read depth of xylose-enriched population was compared to the initial population, and there was not change in the coverage ratio. This data indicates none of the JAY291 unique genes are favorable for xylose fermentation.

Over ~20 possible QTL peaks were identified; however, nine most likely QTL regions were selected and listed in Table 4.1. QTL regions exceeding 200 Kbp or overlap with other QTL studies (likely to be enriched for QTL process, not xylose fermentation) were excluded. Most QTL regions were S288C favorable indicating S288C allele is favorable for xylose fermentation. Initially, the three shortest QTLs were examined due to increased likelihood of finding responsible genes for xylose fermentation (QTL 1-3, Chr 4, 11 and 8). Following the traditional method for QTL analysis, each QTL regions divided into 5-6 Kbp regions and swapped with the other allele. Additionally, deleting of the regions were studied (Figure 4.5). First, JAY291 X123 was used as a host. The deletion of each 5 Kbp fragments did not impact xylose fermentation Except for regions Δ8-4 and Δ11-4 (Figure 4.5A). The growth defect of Δ8-4 was recovered by swapping the region with S288C allele, indicating deletion in generally decreased growth fitness. On the other hand, surprisingly, swapping the region with S288C allele had a detrimental effect on strains 4-2 and 4-4. All QTL regions tested were S288C favorable, therefore, expressing S288C allele should be beneficial for xylose fermentation. Possibly, an S288C allele of 4-2 and 4-4 region brings negative interaction yielding inability to grow on xylose. No further QTL regions were performed due to lengthy QTL region and low likelihood of finding a xylose utilization enhancer gene.

This study attempted to overcome major challenges for developing optimal yeast strains xylose fermentation. Specifically, this project attempted to identify and understand the genetic element for beneficial phenotypes of xylose utilization in *S. cerevisiae*. Although successful QTL analysis was performed, results obtained from this project does not provide sufficient information for to elucidate possible factors crucial for xylose fermentation. Broad QTL region indicates very complex genetic. However, various genome sequences for xylose-fermenting strains were obtained. Perhaps, the different bioinformatic approach can be applied. For

example, gene duplication change during enrichment can be investigated. For example, the relative copy number of *URA3* locus, which was used for X123 cassette integration site, increased around 2-3 fold during enrichment. The data can indicate increased copy number of the X123 cassette, therefore increased xylose fermentation. Thus, although I did not find significant genetic players for xylose fermentation by QTL approach, the further bioinformatic approach is highly suggested.

4.5 Figures and tables

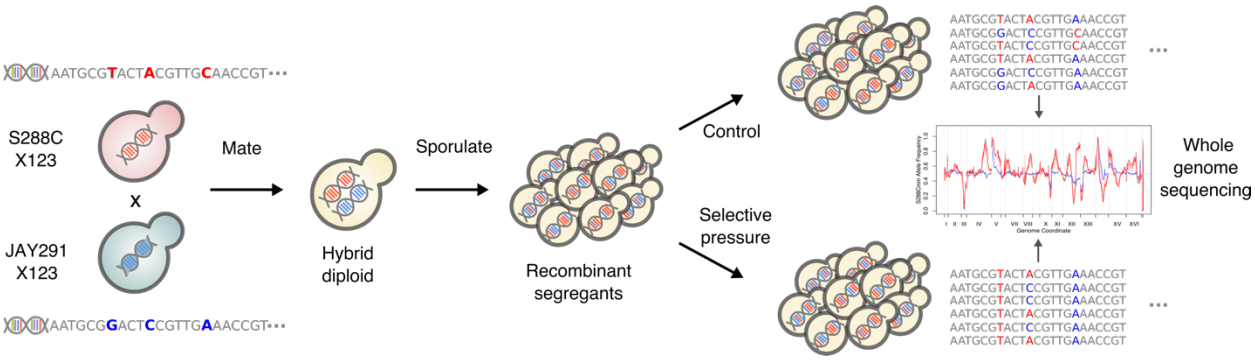

Figure 4.1 Schematic diagram for generating recombinant segregants for QTL plot generation. Two parental haploid strains, S288C X123 and JAY291 X123, are mated to obtain hybrid diploid. After sporulation, a pool recombinant segregants are generated. A sample of resulting recombinant segregants are used as a control, and another sample is enriched under a selective pressure (xylose). Control and selected pool of segregrant genomic DNA are sequenced in bulk and compared for QTL identification.

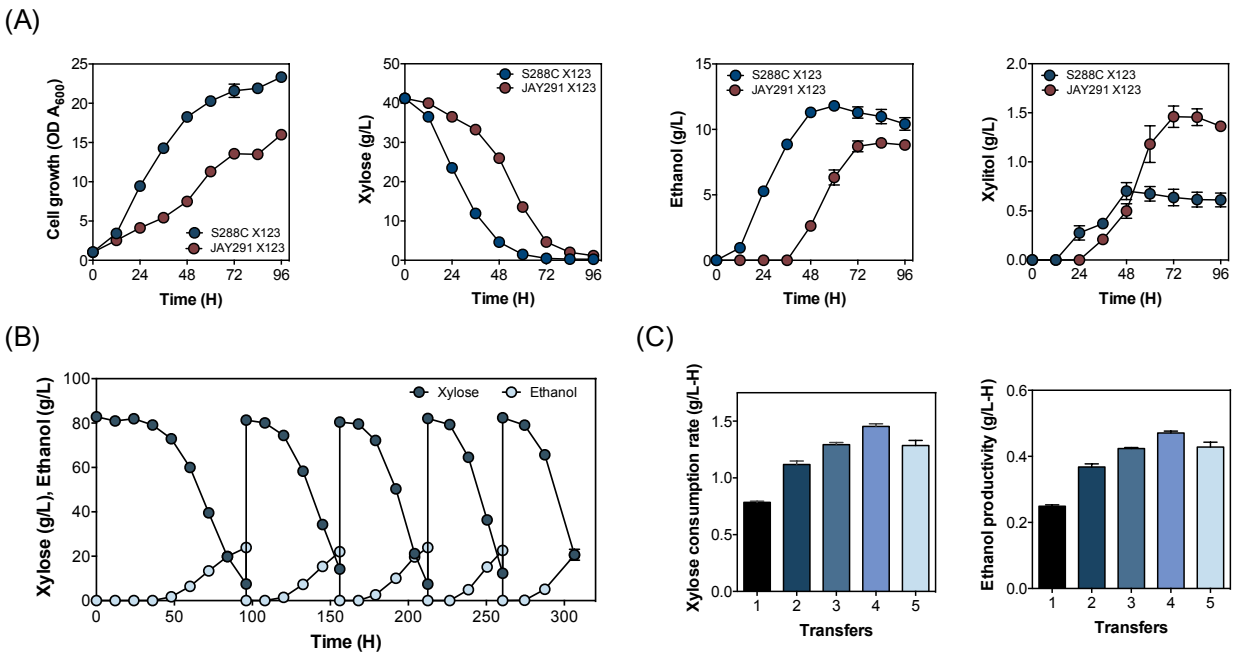

Figure 4.2 Xylose fermentation profile of two parental haploid strains and enrichment of resulting recombinant segregants under xylose-fermenting condition. (A) Xylose fermentation of S288C X123 and JAY291 X123 under 40 g/L of xylose. Cell growth, xylose consumption, ethanol production and xylitol accumulation pattern is shown in the first, second, third and fourth column, respectively. (B) Recombinant segregant pool resulting from crossing S288C X123 and JAY291 X23 and sporulation were enriched under 80 g/L of xylose for the selection of superior xylose-fermenting strain. Cells were harvested before xylose was depleted and transferred to fresh medium until xylose fermentation rate improvement was saturated. (C) Xylose consumption rate and ethanol productivity over each transfer were compared.

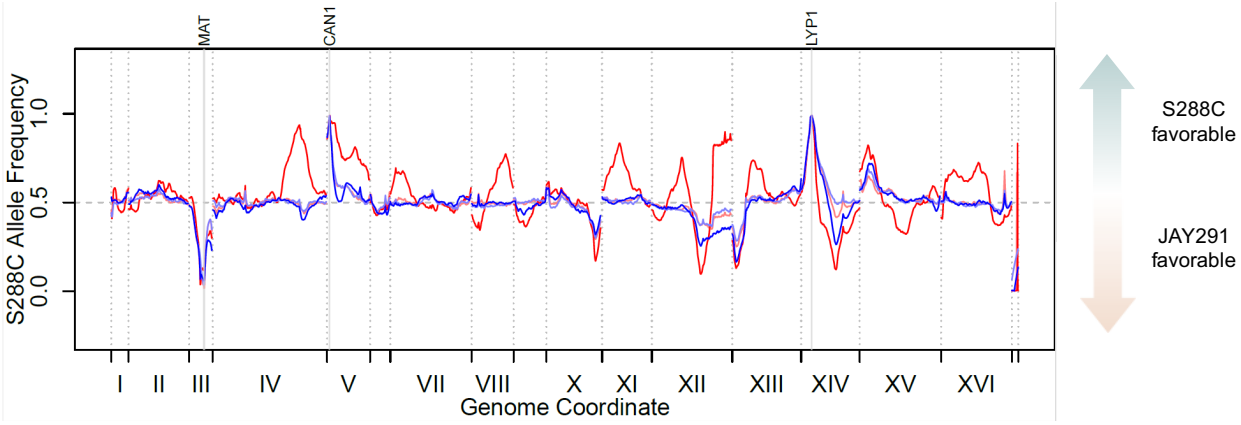

Figure 4.3 High-resolution genome mapping of faster xylose-fermenting QTLs. All sequenced genome was mapped to S288C as a reference. The light red line indicates the sequence of an initial pool of segregants and dark red indicates last xylose-enriched batch. Light blue and dark blue indicates an initial and final batch of the glucose enrichment used as a control. The selected QTLs and details are described in Table 4.2.

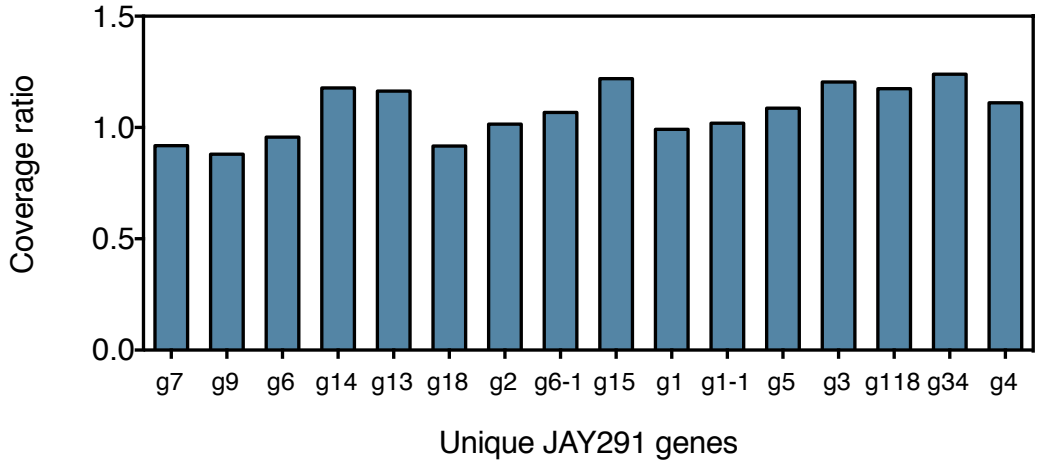

Figure 4.4 Coverage ratio of the genes unique to the JAY291 strain. The total to 16 genes' sequences read-depth of initial segregant pool and xylose enriched pool was compared.

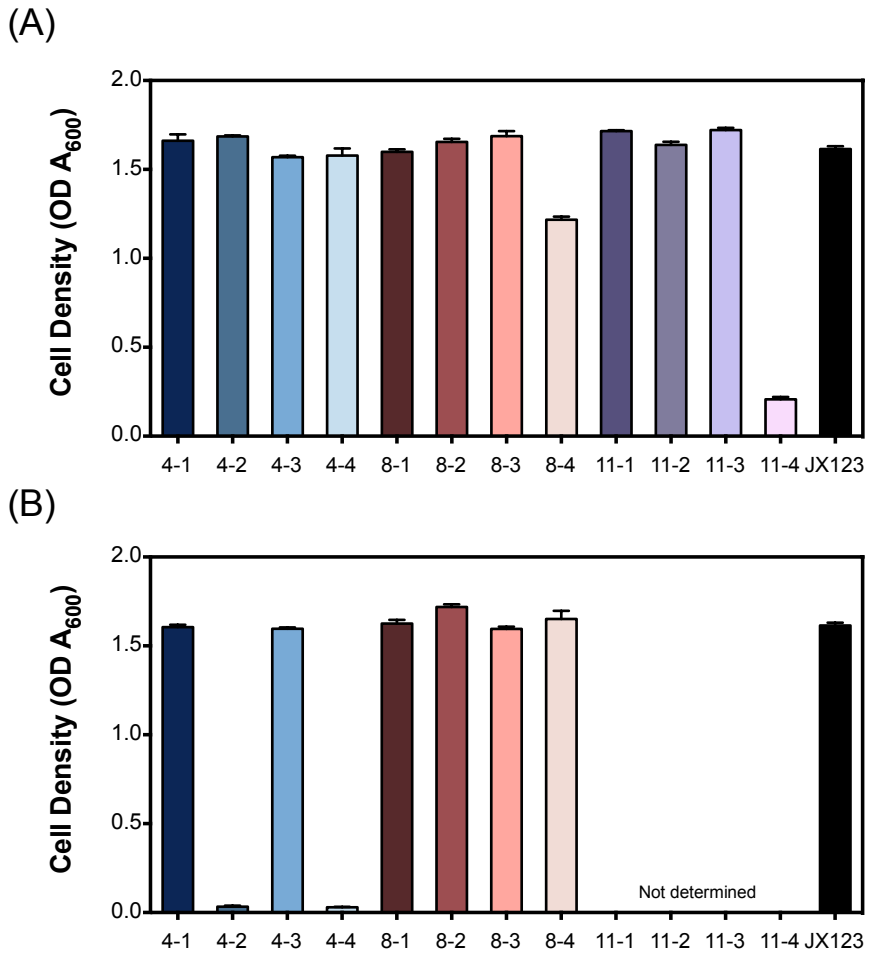

Figure 4.5 Growth on xylose by JAY291 X123 with selected QTL regions deleted (A) and swapped (B). The allele swapping of QTL from Chromosome 11 (swapped allele strains 11-1 - 11-4) was not tested. The OD_{600} measurements at 36 hours were compared.

Table 4.1 The list of plasmids and *S. cerevisiae* strains used in this study

Strain/Plasmid	Relevant characteristic(s)/Description	Source or Reference
Strains		
S288Cm	*MATα hoΔ::HphMX4 can1Δ::prSTE2-SpHIS5 lyp1Δ his3Δ1::NatMX4*	[131]
S288Cm-u	S288Cm strain with mutant allele of *ura3*	This study
S288C X123	S288Cm pSR6-X123 evolved	This study
JAY291m	*MAT*a *ho his3Δ::KanMX* NAT	[131]
JAY291m-u	JAY291m strain with mutant allele of *ura3*	This study
JAY291 X123	JAY291m pSR6-X123	This study
SJ X123	Resulting diploid by crossing S288CX123 and JAY291 X123	This study
D452-2	*MATα leu2 his3 ura3 can1*	This study
Plasmids		
pSR6-X123	pRS306 *TDHp-XYL1-TDH3t PGK1p-XYL2-PGK1t TDH2p-XYL3-TDH3t*	[71]

Table 4.2 List of identified QTLs from shortest to longest identified region.

QTL #	Chromosome	Peak position	Length (Kbp)	Favorability
1	XI	233377.9	18.3	S288C
2	VIII	455723.6	22.7	S288C
3	IV	1156577	27.7	S288C
4	XIII	282038.7	47	S288C
5	XVI	499815.2	47.1	S288C
6	II	102207.9	91.3	JAY291
7	XII	87601.8	151.4	JAY291
8	X	120219.8	166.9	S288C
9	IX	170002.7	209.7	JAY291

CHAPTER V: Enhanced Glucose and Galactose Fermentation by Engineered Yeast Harboring *TPS1* Deletion and Mutant *HXK2* [4]

5.1 Introduction

Saccharomyces cerevisiae is a traditional yeast, highly instrumental to brewing and bioethanol industries due to its superior glucose fermenting capability. Also, it is one of the intensively studied eukaryotic systems in molecular and cell biology, allowing advantages as a host for metabolic engineering of production of fuels and chemicals [135]. Although various strains can differ fermentation capability, *S. cerevisiae* strains prioritize utilization of glucose although it is capable of fermenting other sugars, creating glucose repression. During glucose repression, yeast inhibits the synthesis of enzymes involved in non-glucose utilization, gluconeogenesis, respiration and peroxisomal function and activate glucose fermentation related enzymes [136-138]. While glucose repression can be favorable for glucose fermentation to produce ethanol, it is a challenging barrier to overcome for non-glucose sugar utilization and chemical production by engineered yeast. For example, glucose repression can contribute to inefficient utilization of cellulosic sugars, containing both glucose and various other sugars. During mixed sugar fermentation, glucose will be used first then other sugars resulting in inefficient fermentation process [44, 72]. Thus, controlling and overcoming glucose repression should be addressed for efficient fuels and chemical production.

Glucose sensing starts with sensing extracellular glucose via Snf3/Rgt2 complex. The Snf3/Rgt2 complex act as a receptor for monitoring extracellular glucose concentration. Snf3 serve as a high-affinity glucose sensor inducing expression high-affinity hexose transporters (HXT 2 and 4) and Rgt2 act as a low-affinity glucose sensor inducing expression of low-affinity hexose transporter (HXT1 and 3). The Snf3/Rgt2 complex is also involved in the expression of genes such as *HXK2* and *MIG1* related to glucose metabolism repression [139]. The glucose signaling transduction also activates cAMP/PKA pathway, that regulates overall cellular physiology including growth, metabolism, stress response, etc. [136, 140]. Once glucose is transported into the cell, intracellular glucose sensing mechanism activates. Glucose-6-phosphate, produced by phosphorylating glucose by hexokinases (Hxk1, Hxk2, and Glk1) is

[4] The content of this chapter is in preparation for submission. I performed the research with helps from Jingjing Liu and Yong-Su Jin (director of the research)

required for intracellular glucose signaling affecting overall glycolytic flux rate. Snf1 protein kinase complex or yeast AMPK complex modifies transcription of various genes under stressful conditions (i.e. no available nutrient) (Figure 5.1) [140].

As illustrated in Figure 5.1, glucose repression mechanisms involve numerous genes related to sensing, signaling transduction, metabolism and stress responses. Although overall glucose repression mechanism is demonstrated, actual influence on glucose utilization is not well elucidated. Thus, this study investigates glucose fermentation capability of 50 gene targets selected based on their role in glucose sensing, signaling transduction, metabolism and stress responses. To evaluate the effect of each gene, the yeast deletion library strains were utilized. I found Δ*TPS1* with suppressor mutation changed glucose utilization pattern and aimed to elucidate phenotype changes caused in Δ*TPS1* with suppressor mutation strain.

5.2 Materials and methods

Strains and culture conditions

S. cerevisiae strains used in this study were summarized in Table 5.1. To create *TPS1* deletion strain, Δ*TPS1*::*KanMX* fragment from BY YKO Δ*TPS1* amplified and integrated to BY4742. Mating and tetrad dissection was used to create hybrid diploid and resulting progenies. To create mHXK2 strain, CRISPR/Cas-based genome editing was used. Yeast cells were routinely cultured in the Yeast extract-peptone and glucose or galactose (YPD or YPG, 10 g/L yeast extract, 20 g/L peptone, and 20 g/L glucose or galactose) medium to prepare initial inoculum at 30°C with 250 rpm agitation speed. Synthetic complete (SC, 6.7 g/L yeast nitrogen base with ammonium sulfate,0.79 g/L complete supplement mixture (CSM, (Bio 101, Vista, CA)) media and appropriate concentrations of glucose and galactose were used in fermentation experiments.

Plasmid construction

All primers, template plasmids, and constructed plasmids are listed in Table 1 and 2. The gene expressing plasmids used in this study are based on pRS series vectors with an antibiotic marker (Table 5.1, [141]). The guide RNA(gRNA) targeting *HXK2* was synthesized by gBlock from IDT Inc. The gBlocks for gRNAs were synthesized with the recognition site of each gene

and flanking sequences for *SacI* and *KpnI* restriction enzyme digestion. Then the gBlock and 42H vector plasmids were digested with *SacI* and *KpnI* enzyme. Resulting gBlocks and vectors were ligated and transformed into *E. coli* for plasmid amplification.

CRISPR/Cas-based genome editing for strain engineering

CRISPR-Cas (Clustered Regularly Interspaced Short Palindromic Repeats/CRISPR-Associated Proteins) based genome editing system was for all strains engineering. Previously established technique in our lab was used [67, 132]. The pRS42N Cas9 plasmid was transformed into *S. cerevisiae* strain first then Cas9 carrying strain was used as host strain for further genetic modifications. Plasmid carrying guided RNA for *HXK2* with the double stranded repairing donor DNA were transformed into Cas9 carrying strains. All transformation method was adapted from PEG-LiAc high-efficiency yeast transformation method [133] and selected on yeast extract-peptone (YP) medium with 20 g/L of glucose and with appropriate antibiotic markers. All strains and plasmids used in the study are listed in Table 5.1.

Fermentation experiments

To prepare yeast strains for fermentation experiments, yeast cells were cultivated in YPD medium at 30°C and 250 rpm. Cells were harvested at exponential phase by centrifugation and washed twice with sterile water. Flask-scale Fermentation experiments were performed in SC media with appropriate concentrations of glucose or galactose. All flask-scale fermentation experiments were performed in 50 mL culture using a 250 mL Erlenmeyer flask tightly covered with aluminum foil at 30°C and 100 rpm of rotation speed. Initial cell densities of all fermentation experiments were adjusted to OD_{600} of 1. All flask-scale fermentation experiments were performed in duplicates.

Analytical methods

Cell growth was monitored by measuring optical density (OD) at 600 nm using a UV-visible spectrophotometer (Biomate5, Thermo, Rochester, NY). Glucose, galactose, glycerol, and ethanol concentrations were determined by high-performance liquid chromatography (HPLC, Agilent Technologies 1200 Series, Mississauga, CA) equipped with a refractive index detector using a Rezex ROA-Organic Acid H^+ (8%) column (Phenomenex Inc., Torrance, CA). The column was eluted with 0.005 N of H_2SO_4 at a flow rate of 0.6 ml/min at 50°C.

Spot assay

Yeast strains were prepared by growth in 5mL of YPEthanol 20 g/L for two days, harvested, and washed twice with sterile water. Ten-fold serial dilution was made with water, and five µL of 10^{0}, 10^{-1}, 10^{-2}, 10^{-3}, 10^{-4} and 10^{-5} were spotted on YPD (glucose) or YPG (Galactose), and plates were incubated at 30°C for 2 days.

Mating and tetrad dissection experiment

BY YKO Δ*TPS1* and BY4741 were crossed to generate BY diploid. Then BY diploid strain was grown overnight in 5 mL of YPD 20 g/L at 30°C and 250 rpm. Cells were harvested (OD_{600} ~10), washed with sterile water twice and inoculated into 25 mL of sporulation media (10 g/L potassium acetate, 0.1 g/L yeast extract, 0.5 g/L glucose). Yeasts were sporulated for ~five days at ambient temperature (~22°C), periodically monitoring for a fraction of tetrad formation by light microscopy. Then approximately 1 x 10^{7} cells (~ 20 to 40% tetrad formation) were harvested and resuspended in 100 µL of sterile water and treated with two units of Zymolyase (E1006, Zymo Research) for 5 min to digest surrounding ascus. Then, another 100 µL cold water was added to stop the zymolyase reaction and kept in ice. Five µL of the tetrad containing solution was gently streaked on the center of YPD agar plate, and four ascospores were separated and placed apart from different cells using micromanipulator. After 2-3 day of incubation at 30°C, separated ascospores were obtained and confirmed by mating type locus PCR.

Whole genome sequencing and read mapping

The genomic DNA of BY YKO Δ*TPS1* and tetrad 1d (Δ*TPS1*::*KanMX,* m*HXK2*) were extracted to whole genome sequencing. Whole genome sequencing was performed by the University of Illinois at Urbana-Champaign Biotechnology Center, High-Throughput Sequencing and Genotyping Unit (Urbana, IL) using Illumina HiSeq 2500 platform. The reads were mapped to the S288C reference genome as described previously. CLC Genomic Workbench 7 was used to compare genome sequences of the BY YKO Δ*TPS1* and tetrad 1c.

5.3 Results

Glucose fermentation pattern comparison of 50 yeast knockout library

Initially, I selected 50 gene targets related to glucose sensing, signaling, metabolism and major stress response to starvation based on past research studies and its significance to glucose metabolism can be inferred (Figure 5.1 and Table 5.2). To screen for potential effects on the cellular metabolism of the 50 selected gene targets, I obtained BY4742 deletion library strains, derivative of S288C strains, that harbor each gene deleted by replacing KanMX cassette (BY YKO strains). To observed the deletion effect of each gene, glucose consumption pattern was compared first. To amplify the difference of glucose fermentation capability, minimal media (SC) with a high concentration of glucose (100 g/L) was used. The lethality of a gene knockout was not considered initially with an assumption that it will be indicated with poor or no glucose consumption. As shown in Figure 5.2A, total consumed glucose was compared to the control (BY4742 wildtype) and percent change was calculated. All 50 strains exhibited various patterns of glucose consumption. However, few genes had a significant difference from the control. For example, BY YKO Δ*TPS1* strain, as noted in figure 5.2A, had the highest positive percent change indicating more glucose consumption compared to the wildtype. To examine further, glucose fermentation pattern of BY YKO Δ*TPS1* was compared to the wildtype. Figure 5.2B first column shows that Δ*TPS1* strain completely consumed 100 g/L of glucose at a slightly faster rate and accumulated glycerol significantly (~ 13 g/L (Δ*TPS1*) vs. ~3 g/L (Wildtype)). However, *TPS1* deletion is reported to be a lethal under glucose condition [142, 143]. As I observed conflicting phenomena of what was already reported, in fact, enhanced glucose fermentation, I hypothesized the presence of suppressor mutation to overcome lethality of Δ*TPS1*.

Utilization of glucose and galactose by various Δ*TPS1* mutants

To confirm and evaluate Δ*TPS1* phenotype without the possibility of suppressor mutation, new ΔTPS1 strain (BY4742 Δ*TPS1*) was constructed by integration of KanMX cassette with *TPS1* upstream and downstream homology region. Then, growth tests on glucose and galactose, under both solid and liquid media conditions (Figure 5.4A and B) were performed with BY4742, BY4742 Δ*TPS1* and BY YKO Δ*TPS1* with potential suppressor mutation(s). According to previous studies, strains harboring ΔTPS1 cannot grow under glucose condition due to flux imbalance of upper and lower glycolysis [142, 143]. As expected, BY4742 grew on both galactose and glucose, and Δ*TPS1* only strain (clean mutant) grew under galactose but not glucose. Also, agreeing with earlier observation (Figure 5.2), BY YKO Δ*TPS1* with potential

suppressor mutation(s) grew under both galactose and glucose (Figure 5.4A and B). In general, BY YKO Δ*TPS1* with potential suppressor mutation had better sugar consumption under both glucose and galactose conditions.

Tetrad dissection and genome sequencing reveals one mutation is responsible for rescuing TPS1 lethality

After confirmation of Δ*TPS1* lethality under glucose and presence of unknown potential suppressor mutation(s) in BY YKO Δ*TPS1* strain, mating, and tetrad dissection were performed to find out how many mutations (genes) are potentially involved suppression of lethality. BY YKO Δ*TPS1* (*MATα*) as mated with another S288C-derived strain BY4741 (*MATa*). Then, resulting in hybrid diploid (BY diploid), cells were incubated under sporulation medium to induce tetrad formation. After tetrad had been obtained, each set of four haploid progenies were obtained by a micromanipulator. A total of 5 sets of tetrads was tested for the presence of Δ*TPS1*:: *KanMX* cassette under glycerol + G418 media, and growth under glucose and galactose. A representative tetrad set, 1a -1d, are shown in Figure 5.4C. Two haploids 1b and 1c were able to grow under glycerol + G418 condition indicating 1b and 1b harbors Δ*TPS1*:: *KanMX*. However, only 1c strain colonized under glucose agreeing with the phenotype of BY YKO Δ*TPS1* with potential suppressor mutation. Five tetrad sets showed similar phenotype (data not shown). Thus, the likelihood of observing the phenotype of BY YKO Δ*TPS1* with potential suppressor mutation is 1/4. By the general equation of phenotype of interest observed = one/ 2^n, where n is a number of factors (genes) involved, the n equals 2. The TPS1 deletion accounts for one, therefore, one other mutation is likely to be involved in rescuing *TPS1* deletion lethality.

To find which gene is involved for allowing growth under glucose with Δ*TPS1*, whole genome sequencing was performed. The genomes of BY YKO Δ*TPS1* and tetrad 1c were sequenced, and the reads were mapped to the S288C reference genome. The sequence alignment indicated a presence of single nucleotide change in *HXK2*, encoding for hexokinase 2 in yeast. To confirm, BY YKO Δ*TPS1* and tetrad 1a-1d *HXK2* gene was sequenced again, and BY YKO Δ*TPS1*, tetrad 1c and 1d had SNP changing amino acid sequence from Ser158 to Tyr158.

Enhanced glucose and galactose fermentation by Δ*TPS1* and m*HXK2* double mutant

Next, m*HXK2* (Ser158Tyr) was introduced in wildtype BY4742, and BY4742 Δ*TPS1* to observe the effect of m*HXK2* during glucose and galactose fermentation. As observed in Figure 5.5A, the introduction of m*HXK2* to Δ*TPS1* strain rescued the growth under glucose condition. Moreover, strains expressing m*HXK2* (BY m*HXK2* and BY Δ*TPS1* m*HXK2*) grew better and fermented glucose at a faster rate compared to the wildtype BY4742. Galactose fermentation was also performed (Figure 5.5B). Under Galactose condition, all strains BY4742, BY Δ*TPS1*, BY m*HXK2* and BY Δ*TPS1* m*HXK2* grew similarly (similar biomass accumulation). However, strains with Δ*TPS* (BY Δ*TPS1* and BY Δ*TPS1* m*HXK2*) had better galactose consumption followed by strain BY m*HXK2* and wildtype. Additionally, at 12 hours, all engineered strain, except for BY4742 strain started to grow indicating m*HXK2 or* Δ*TPS1* generally enhances galactose fermentation.

Expressing mHXK2 or both Δ*TPS1* m*HXK2* also enhanced mixed sugar utilization of glucose and galactose. Under glucose and galactose mixture, BY4742 consumed glucose rapidly but were not able to consume galactose after (Figure 5.6 first column). On the other hand, strains expressing both m*HXK2* or Δ*TPS1* m*HXK2* consumed glucose rapidly and even started to consume galactose before glucose was depleted. Due to poor growth on glucose, the Δ*TPS1* strain was excluded for mixed sugar fermentation experiments.

5.4 Discussion

The glucose sensing mechanism and metabolic network in yeast prioritize glucose utilization over any other sugars, creating glucose repression. Understanding the complex mechanism of glucose repression is proved to be difficult and can impose a challenging problem for metabolic engineering for production of fuels and chemicals. Thus, I attempted to screen 50 gene targets that might affect glucose fermentation. Targeted genes were selected based on previous literature and its function on glucose sensing, signaling, metabolism and major stress response to starvation (Table 5.2). To efficiently screen 50 gene targets, yeast deletion library was utilized [144]. By studying phenotype change by deletion, I might be able to elucidate mechanisms that affect glucose utilization directly. To my knowledge, no previous study reports glucose fermentation pattern comparison of many genes concurrently.

As expected, the 50 strains exhibited various glucose consumption pattern (Figure 5.2A). Some deletions lowered glucose consumption whereas some deletions enhanced glucose consumption. Particularly, Δ*TPS1* strain (BY YKO Δ*TPS1*) showed the best improvement in glucose consumption. When detailed glucose fermentation pattern of BY YKO Δ*TPS1* were examined, glucose consumption rate of BY YKO Δ*TPS1* was faster than BY4742 and significant glycerol production was observed (Figure 5.2B). Unexpectedly, however, the deletion of TPS1 gene is known to be lethal to the yeast due to its crucial role in glycolysis regulation [145, 146]. *TPS1* encodes for trehalose phosphate synthase, an enzyme converting glucose-6-phosphate to trehalose-6-phosphate. Trehalose-6-phosphate can further be converted to trehalose. However, trehalose-6-phophate also act as a regulatory molecule to control glycolysis. Energy consuming upper glycolysis is very rapid (glucose to fructose-1,6-bisphosphate) compared to the energy-generating lower glycolytic pathway (glyceraldehyde-3-phosphate to pyruvate). When upper and lower glycolytic pathways are not balanced, energy imbalance (shortage of ATP) can occur leading to lethality. Trehalose-6-phoshate prevents this by controlling the reaction rate of glucose to glucose-6-phosphate. Thus, deletion of *TPS1* is lethal to the cell. However, BY YKO Δ*TPS1* presented normal glycolytic pathway, if not faster (Figure 5.2). Therefore, I hypothesized presence of suppressor mutation in BY YKO Δ*TPS1* strain.

The phenotype of BY YKO Δ*TPS1* reveals that the potential suppressor mutation not only removes Δ*TPS1* but increase glucose utilization, or increase glycolytic flux (Figure 5.2B and Figure 5.4B). To confirm if unknown suppressor mutation increases glycolytic flux, growth under galactose was tested. Galactose utilization bypasses hexokinase step but metabolized via glycolysis from glucose-6-phosphate (Figure 5.3). If unknown suppressor mutation increases overall glycolytic flux, galactose utilization should also increase. As expected, galactose fermentation with BY YKO Δ*TPS1* increased compared to wildtype yeast indicating the unknown mutation increases overall glycolytic rate. However, Δ*TPS1* alone (BY4742 ΔTPS1) can also increase galactose fermentation slightly.

By whole genome sequencing, a mutation at *HXK2* (Ser158Tyr), a gene encoding for hexokinase two was identified. However, the interaction between *TPS1* and *HXK2* is already known, and my observation agrees with the previous study. The introduction of m*HXK2* to newly constructed Δ*TPS1* strain rescued the Δ*TPS1* lethality (Figure 5.5A). Interestingly, the

introduction of m*HXK2* to both wildtype and Δ*TPS1* strain increased the biomass accumulation and enhanced glucose fermentation rate. The mutation site of *HXK2*, Ser158, is known for phosphorylating site and reported mutation lowers overall enzyme activity. Thus, the introduction of m*HXK2* lowers overall efficiency of conversion of glucose to glucose-6-phosphate and may not cause an imbalance between upper and lower glycolytic pathway. Consequently, Δ*TPS1* is not lethal anymore when m*HXK2* is expressed. Also, nonlethal Δ*TPS1* mutant (with m*HXK2*) removes the regulation of hexokinase catalytic activity (by *HXK1* and *GLK1*). As a result, enhanced glucose fermentation is observed (Figure 5.5A). Galactose fermentation was also tested as previous observation (Figure 5.4B) indicated the mutation could increase overall glycolytic rate. Generally, m*HXK2* can mediate increased galactose utilization (indicated by m*HXK2* and m*HXK2* Δ*TPS1* strain), Δ*TPS1* was more effective in increasing galactose fermentation (indicated by Δ*TPS1* and m*HXK2* Δ*TPS1* strain) (Figure 5.5B).

The previous studies also reported that mutation at Ser158 also affects glucose signaling [147, 148]. Because galactose metabolic enzymes are strictly repressed by glucose repression, the introduction of m*HXK2* might remove the repression. Thus, mixed sugar (glucose and galactose) utilization was tested with the wildtype and m*HXK2* expressing strains (Figure 5.6). The wildtype strain (BY4742) consumed glucose rapidly. However, galactose was barely consumed. On the other hand, m*HXK2* expressing strains consumed glucose rapidly and started to consume galactose even before glucose was deleted. This result proves the m*HXK2* expression is beneficial to remove repression of galactose metabolism during the presence of glucose.

In summary, BY YKO Δ*TPS1* showed a significant change in glucose consumption from initial screening. Although combined effect with m*HXK2*, a change in glucose metabolism was observed and provided insights for glucose metabolism network. Additionally, Δ*TPS1* and m*HXK2* are beneficial for enhancing glucose or galactose fermentation. Especially, m*HXK2* removes glucose repression enabling glucose and galactose mixed sugar fermentation that can be advantages for utilizing milk sugar lactose (dimer of glucose and galactose). Although this study presents clear phenotype change due to genetic perturbation and followed by reasoning, the detailed mechanistic investigation was not performed. In the future, detailed investigation of Tps1 and mHxk2p interaction should be performed. Additionally, other deletion strains with a significant change in glucose consumption should be investigated.

5.5 Figures and tables

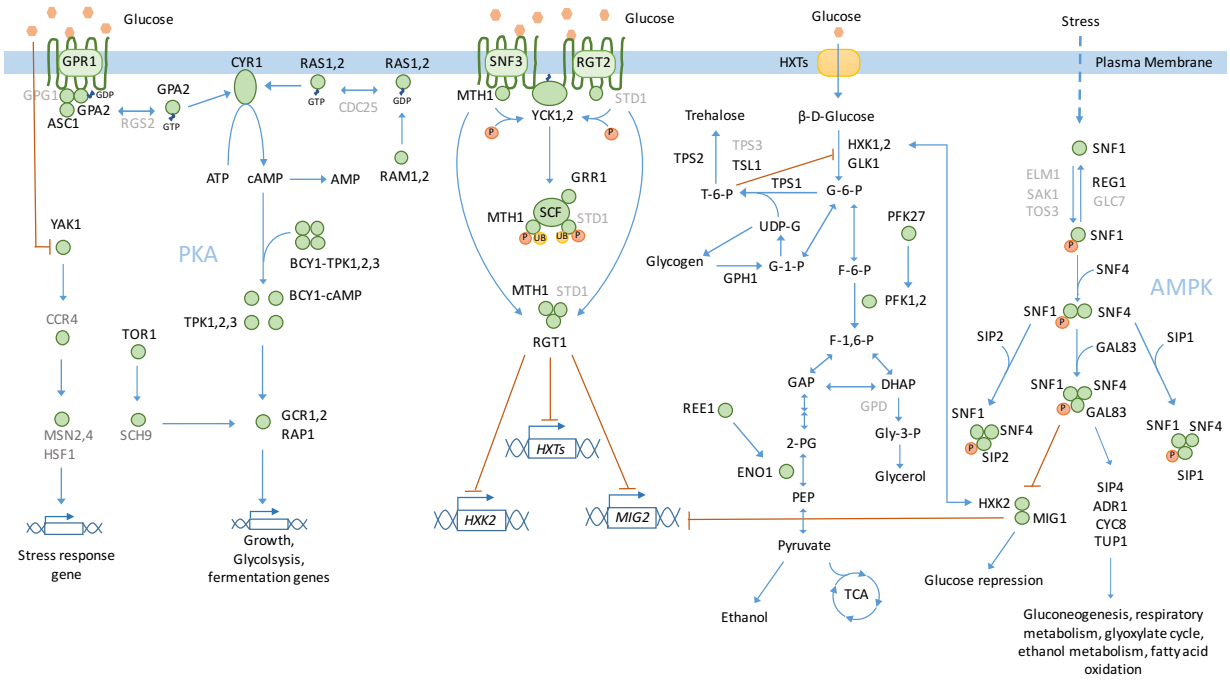

Figure 5.1 Schematic diagram of glucose metabolism and signaling transduction pathways [136]. PKA (cAMP-dependent protein kinase) transduction pathway, glucose sensing transduction pathway, glycolysis, and AMPK (AMP-activated protein kinase) transduction pathway is shown. Genes studied in this chapter is shown in black and did not study in gray. The blue line indicates a reaction and red line indicates inhibition. Orange circle with a letter 'p' indicates phosphate and yellow circle with 'UB' indicate ubiquitin.

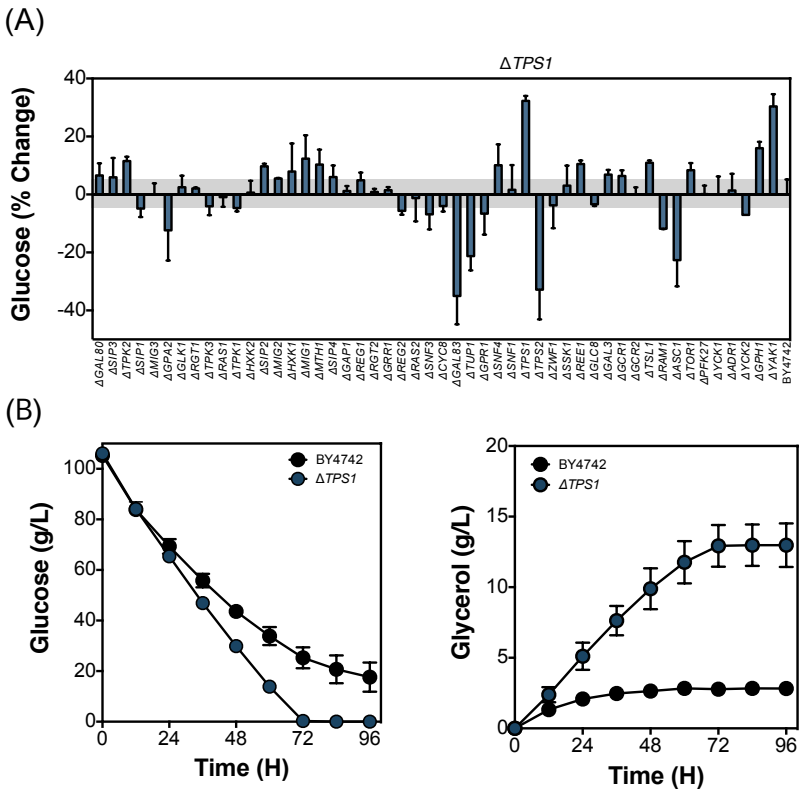

Figure 5.2 Fermentation capability of selected YKO strains. Total consumed glucose change (A) compared to wildtype (BY4742) is shown. (A) Total consumed glucose was calculated upon glucose depletion or ceased glucose consumption from SCD 100 g/L fermentation. Then percent change compares to BY4742 was calculated. Positive percent change indicates a higher amount of glucose consumption and negative percent change indicates a lower amount of glucose consumption compared to BY4742. Error range was determined by control strain BY4742 indicated by a gray area. (B) Glucose consumption and glycerol production pattern of BY4742 and BY YKO Δ*TPS1* was compared and indicated in a bar chart (A).

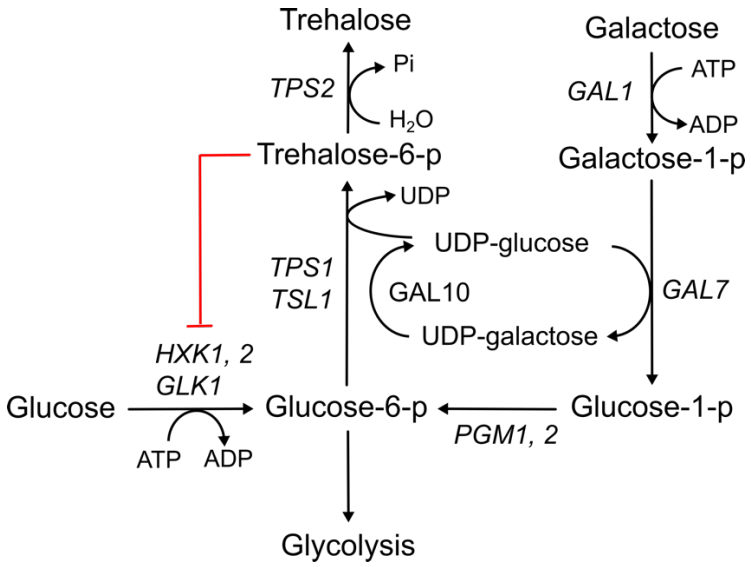

Figure 5.3 Schematic diagram of glucose and galactose metabolic pathway and role of *TPS1*. Galactose is converted to galactose-1-p by galactokinase (*GAL1*). Then galactose-1-phosphate uridyl transferase (*GAL7*) synthesizes galactose-1-p and UDP-D-glucose to glucose-1-phosphate and UDP-galactose. Glucose-1-p is converted to glucose-6-p by phosphoglucomutase (*PGM 1, 2*) and further metabolized by glycolysis. Glucose-6-p and UDP-D-glucose can be converted to trehalose-6-p by trehalose phosphate synthase (*TPS1*) and regulation by *TSL1*. Then trehalose-6-p can regulate the glycolytic reactions by controlling hexose kinase activity.

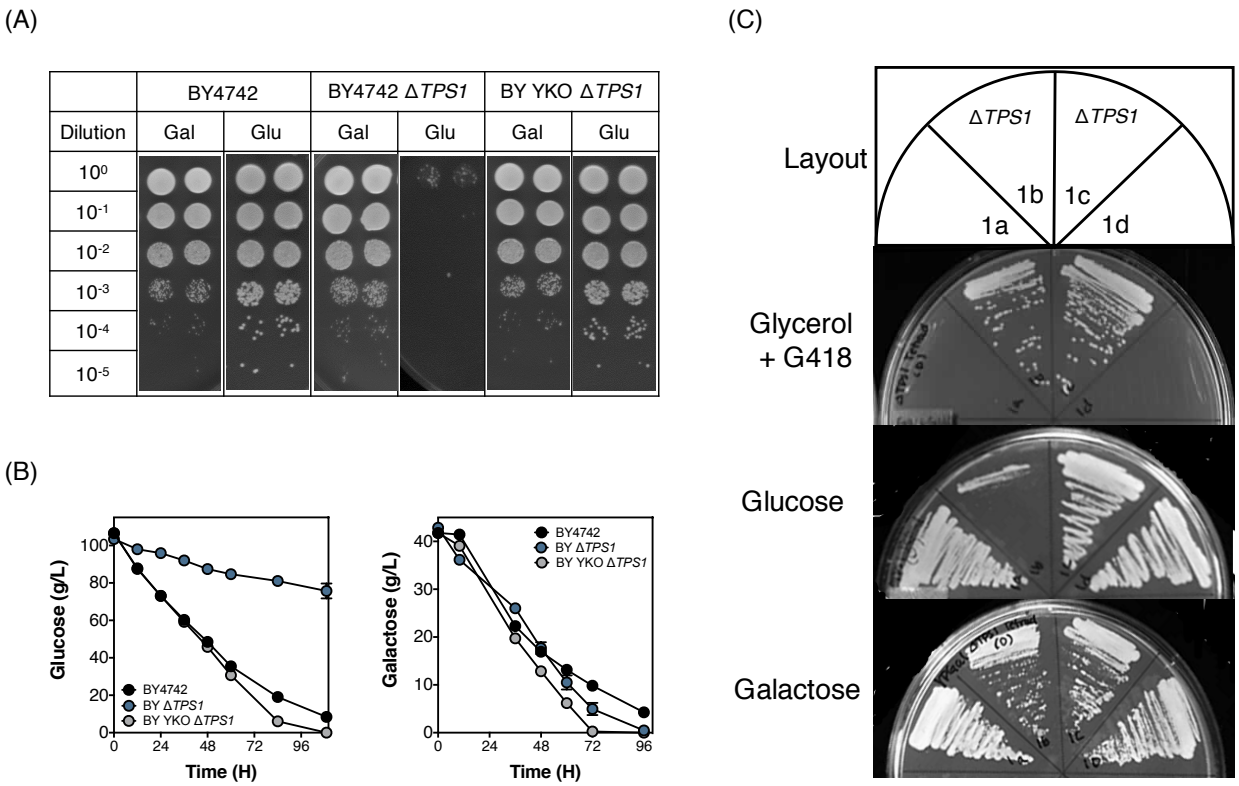

Figure 5.4 Growth on glucose and galactose by various mutants. (A-B) Growth YPD and YPG by spot assay or liquid media were compared between BY4742 (wildtype), BY4742 Δ*TPS1* and BY YKO Δ*TPS1*. (A) Colony formation after ~2 days of incubation was observed and (B) Sugar consumption pattern under liquid media was observed. (C) Growth test of haploid progenies from sporulation of hybrid BY diploid (BY YKO Δ*TPS1* x BY4741) and tetrad dissection on glycerol + G418, glucose, and galactose medium. The glycerol + G418 plate was used to indicate Δ*TPS1*::KanMX.

(A)

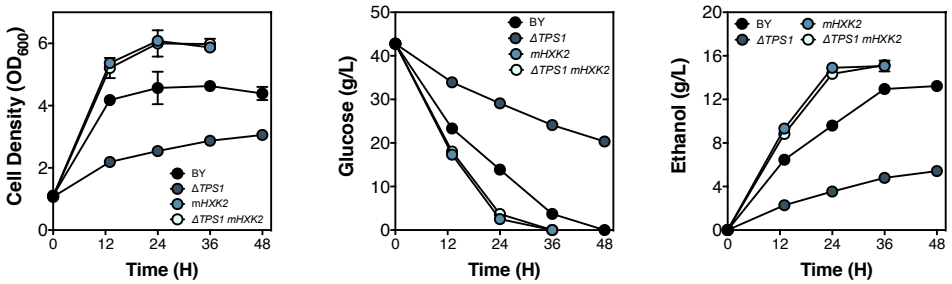

(B)

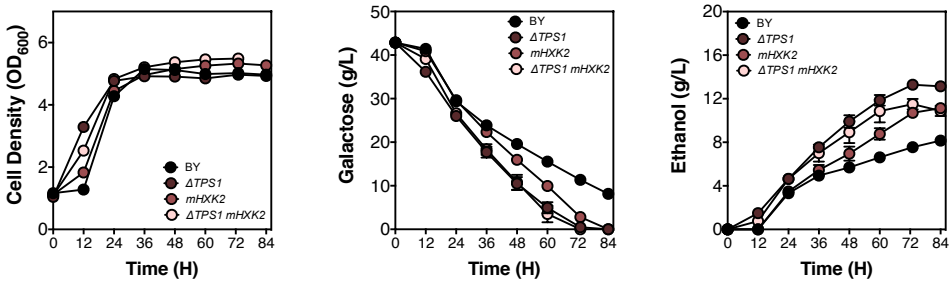

Figure 5.5 Glucose and galactose fermentation profiles of TPS1 and mHXK2 mutants. (A) Growth in glucose, glucose consumption and ethanol production patterns (first, second and third column, respectively) of BY4742, Δ*TPS1*, m*HXK2* and Δ*TPS1* m*HXK2* strains are compared and (B) growth on galactose, galactose consumption and ethanol productions are compared (first, second and third column, respectively) of BY4742, Δ*TPS1*, m*HXK2* and Δ*TPS1* m*HXK2* strains.

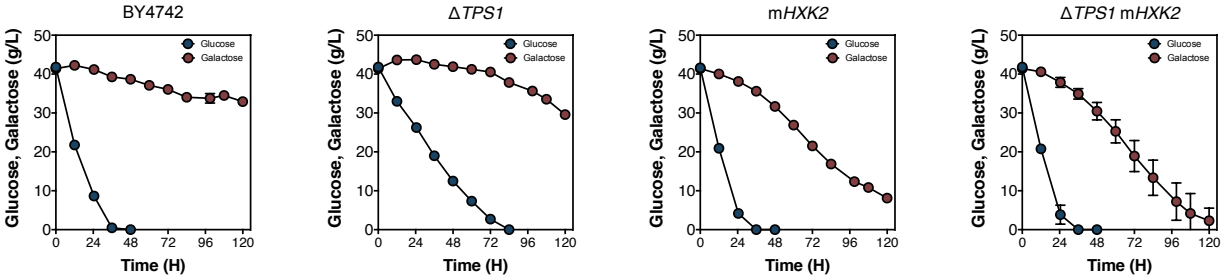

Figure 5.6 Glucose and galactose mixed sugar utilization pattern by BY4742, Δ*TPS1,* m*HXK2* and Δ*TPS1* m*HXK2* harboring strains (first, second and third column, respectively). A total of 80 g/L (40 g/L of glucose and 40 g/L galactose) sugar was used, and concentrations of each sugar were monitored.

Table 5.1 The list of plasmids and *S. cerevisiae* strains used in this study

Strain/Plasmid	Relevant characteristic(s)/Description	Source or Reference
Strains		
BY4742	*MATα leu2 his3 lys2 ura3*	[149]
BY4741	*MATa leu2 his3 met15 ura3*	[149]
BY YKO ΔTPS1	BY4742 Δ*TPS1*::*KanMX* from deletion library	[144]
BY diploid	Hybrid diploid of BY4741 and BY YKO ΔTPS1	This study
Tetrad 1a	Tetrad from BY diploid	This study
Tetrad 1b	Tetrad from BY diploid, Δ*TPS1*::*KanMX*	This study
Tetrad 1c	Tetrad from BY diploid, Δ*TPS1*::*KanMX.* m*HXK2*	This study
Tetrad 1d	Tetrad from BY diploid, m*HXK2*	This study
BY Δ*TPS1*	BY4742 Δ*TPS1*::*KanMX*	This study
BY m*HXK2*	BY4742 m*HXK2*	This study
BY Δ*TPS1* m*HXK2*	BY4742 Δ*TPS1*::*KanMX* m*HXK2*	This study
Plasmids		
pRS42N	NAT1 marker plasmid	EUROSCARF
pRS42H	HyB marker plasmid	EUROSCARF
pRS42N Cas9	P_{PGK} -MCS- T_{CYC}, Cas9 expression plasmid	[67]
pRS42K gRNA *HXK2*	*HXK2* gRNA plasmid	This study

Table 5.2 List of gene targets and a brief description.

Gene	Brief description (Information from yeastgenome.org)
ΔGAL80	Transcriptional regulator involved in the repression of GAL genes in the absence of galactose; inhibits transcriptional activation by Gal4p; inhibition relieved by Gal3p or Gal1p binding
ΔSIP3	Transcription cofactor; acts through interaction with DNA-bound Snf1p; C-terminal region has a putative leucine zipper motif; potential Cdc28p substrate; SIP3 has a paralog, YSP1, that arose from the whole genome duplication
ΔTPK2	cAMP-dependent protein kinase catalytic subunit; promotes vegetative growth in response to nutrients via the Ras-cAMP signaling pathway; partially redundant with Tpk1p and Tpk3p; localizes to P-bodes during stationary phase; relocalizes to the cytosol in response to hypoxia
ΔSIP1	Alternate beta-unit of the Snf1p kinase complex; may confer substrate specificity; vacuolar protein containing KIS (Kinase-Interacting Sequence) and ASC (Association with Snf1 kinase Complex) domains involved in protein interactions
ΔMIG3	Transcriptional regulator; partially nonfunctional in S288C strains but has a major role in catabolite repression and ethanol response in some other strains; involved in response to toxin agents; phosphorylation by Snf1p or the Mec1p pathway inactivates Mig3p, allowing induction of damage response genes
ΔGPA2	Nucleotide binding alpha subunit of the heterotrimeric G protein that interacts with the receptor Gpr1p has signaling role in response to nutrients; green fluorescent protein-fusion protein localizes to the cell periphery
ΔGLK1	Catalyzes the phosphorylation of glucose at C6 in the first irreversible step of glucose metabolism; one of three glucose phosphorylating enzymes; expression regulated by non-fermentable carbon sources
ΔRGT1	Glucose-responsive transcription factor; regulates expression of several glucose transporter genes in response to glucose; binds to promoters and acts both as a transcriptional activator and repressor
ΔTPK3	cAMP-dependent protein kinase catalytic subunit; promotes vegetative growth in response to nutrients via the Ras-cAMP signaling pathway; partially redundant with Tpk1p and Tpk2p; localizes to P-bodies during stationary phase
ΔRAS1	GTPase involved in G-protein signaling in adenylate cyclase activation; plays a role in cell proliferation; localized to the plasma membrane; relative distribution to the nucleus increases upon DNA replication stress
ΔTPK1	cAMP-dependent protein kinase catalytic subunit; promotes vegetative growth in response to nutrients via the Ras-cAMP signaling pathway; inhibited by regulatory subunit Bcy1p in the absence of cAMP; regulates Whi3p; partially redundant with Tpk2p and Tpk3p; phosphorylates pre-Tom40p, which impairs its import into mitochondria under non-respiratory conditions
ΔHXK2	Hexokinase isoenzyme 2; catalyzes phosphorylation of glucose in the cytosol; predominant hexokinase during growth on glucose; functions in the nucleus to repress expression of *HXK1* and *GLK1* and to induce expression of its own gene; phosphorylation/ dephosphorylation at serine-14 by protein kinase Snf1 and protein phosphatase Glc7p-Reg1p regulates nucleocytoplasmic shuttling of Hxk2p
ΔSIP2	One of three beta subunits of the Snf1 kinase complex; involved in response to glucose starvation; null mutants exhibit accelerated aging; N-myristoyl protein localized to the cytoplasm and the plasma membrane

Table 5.2. List of gene targets and a brief description continued.

Gene	Brief description (Information from yeastgenome.org)
Δ*MIG2*	Zinc finger transcriptional repressor; cooperates with Mig1p in glucose-induced repression of many genes; under low glucose conditions Mig2p re-localizes to mitochondrion, where it interacts with Ups1p and antagonizes mitochondrial fission factor, Dnm1p, indicative of a role in mitochondrial fusion or regulation morphology; regulates filamentous growth along with Mig2p in response to glucose depletion
Δ*HXK1*	Hexokinase isoenzyme 1; a cytosolic protein that catalyzes phosphorylation of glucose during glucose metabolism; expression is highest during growth on non-glucose carbon sources; glucose-induced repression involves hexokinase Hxk2p
Δ*MIG1*	Transcription factor involved in glucose repression; sequence specific DNA binding protein containing two Cys2His2 zinc finger motifs; regulated by the SNF1 kinase and the GLC7 phosphatase; regulates filamentous growth along with Mig2p in response to glucose depletion
Δ*MTH1*	Negative regulator of the glucose-sensing signal transduction pathway; required for repression of transcription by Rgt1p; interacts with Rgt1p and theSnf3p and Rgt2p glucose sensors; phosphorylated by Yck1p, triggering Mth1p degradation
Δ*SIP4*	C6 zinc cluster transcriptional activator that binds to the carbon source-responsive element (CSRE) of gluconeogenic genes; involved in the positive regulation of gluconeogenesis; regulated by Snf1p protein kinase; localized to the nucleus
Δ*GAP1*	General amino acid permease; Gap1p senses the presence of amino acid substrates to regulate localization to the plasma membrane when needed; essential for invasive growth
Δ*REG1*	Regulatory subunit of type 1 protein phosphatase Glc7p; involved in negative regulation of glucose-repressible genes; involved in regulation of the nucleocytoplasmic shuttling of Hxk2p
Δ*RGT2*	Plasma membrane high glucose sensor that regulates glucose transport; contains 12 predicted transmembrane segments and a long C-terminal tail required for induction of hexose transporters
Δ*GRR1*	F-box protein component of an SCF ubiquitin-ligase complex; modular substrate specificity factor which associates with core SCF (Cdc53p, Skp1p and Hrt1p/Rbx1p) to form the SCF (Grr1) Complex; SCF (Grr1) acts as a ubiquitin-protein ligase directing ubiquitination of substrates such as: Glc2p, Mks1p, Mth1p, Cln1p, Cln2p and Cln3p; involved in carbon catabolite repression, glucose-dependent divalent cation transport, glucose transport, morphogenesis, and sulfite detoxification
Δ*REG2*	Regulatory subunit of the Glc7p type-1 protein phosphatase; involved with Reg1p, Glc7p, and Snf1 in regulation of glucose-repressible genes, also involved in glucose-induced proteolysis of maltose permease
Δ*RAS2*	GTP-binding protein; regulates nitrogen starvation response, sporulation, and filamentous growth; farnesylation and palmitoylation required for activity and localization to plasma membrane
Δ*SNF3*	Plasma membrane low glucose sensor regulates glucose transport; contains 12 predicted transmembrane segments and a long C-terminal tail required for induction of hexose transporters; also, senses fructose and mannose
Δ*CYC8*	General transcriptional co-repressor; acts together with Tup1p; also acts as part of a transcriptional co-activator complex that recruits the SWI/SNF and SAGA complexes to promoters; can form the prion [OCT+]
Δ*GAL83*	One of three possible beta-subunits of the Snf1 kinase complex; allows nuclear localization of the Snf1 kinase complex in the presence of a nonfermentable carbon source; necessary and sufficient for phosphorylation of the Mig2p transcription factor in response to alkaline stress

Table 5.2. List of gene targets and a brief description continued.

Gene	Brief description (Information from yeastgenome.org)
Δ*TUP1*	General repressor of transcription; forms complex with Cyc8p, involved in the establishment of repressive chromatin structure through interactions with histones H3 and H4, appears to enhance expression of some genes
Δ*GPR1*	Plasma membrane G-protein coupled receptor (GPCR); interacts with the heterotrimeric G protein alpha subunit, Gpa2p, and with Plc1p; sensor that integrates nutritional signals with the modulation of cell fate via PKA and cAMP synthesis
Δ*SNF4*	Activating gamma subunit of the AMP-activated Snf1p kinase complex; additional subunits of the complex are Snf1p and a Sip1p/Sip2p/Gal83p family member; activates glucose-repressed genes, represses glucose-induced genes; role in sporulation, and peroxisome biogenesis; protein abundance increases in response to DNA replication stress
Δ*SNF1*	AMP-activated S/T protein kinase; forms a complex with Snf4p and members of the Sip1p/Sip2p/Gal83p family; required for transcription of glucose-repressed genes, thermotolerance, sporulation, and peroxisome biogenesis; regulates nucleocytoplasmic shuttling of Hxk2p; regulates filamentous growth and acts as a non-canonical GEF, activating Arf3p during invasive growth; SUMOylation by Mms21p inhibits its function and targets Snf1p for destruction via the Slx5-Slx8 Ub ligase
Δ*TPS1*	Synthase subunit of trehalose-6-P synthase/phosphatase complex; synthesizes the storage carbohydrate trehalose. Also found in a monomeric form; expression is induced by the stress response and repressed by the Ras-cAMP pathway; protein abundance increases in response to DNA replication stress and response to prolonged exposure to boric acid
Δ*TPS2*	Phosphatase subunit of the trehalose-6-P synthase/phosphatase complex; involved in synthesis of the storage carbohydrate trehalose; expression is induced by stress conditions and repressed by the Ras-cAMP pathway; protein abundance increases in response to DNA replication stress
Δ*ZWF1*	Glucose-6-phosphate dehydrogenase (G6PD); catalyzes the first step of the pentose phosphate pathway; involved in adapting to oxidative stress; protein abundance increases in response to DNA replication stress
Δ*SSK1*	Cytoplasmic phosphorelay intermediate osmosensor and regulator; part of a two-component signal transducer that mediates osmosensing via a phosphorelay mechanism; required for mitophagy; dephosphorylated form is degraded by the ubiquitin-proteasome system; potential Cdc28p substrate
Δ*REE1*	Cytoplasmic protein involved in the regulation of enolase (*ENO1*); mRNA expression is induced by calcium shortage, copper deficiency (via Mac1p) and the presence of galactose (via Gal4p); mRNA expression is also regulated by the cell cycle
Δ*GLC8*	Regulatory subunit of protein phosphatase 1 (Glc7p); involved in glycogen metabolism and chromosome segregation; proposed to regulate Glc7p activity via conformational alteration; protein abundance increases in response to DNA replication stress
Δ*GAL3*	Transcriptional regulator; involved in activation of the GAL genes in response to galactose; forms a complex with Gal80p to relieve Gal80p inhibition of Gal4p; binds galactose and ATP but does not have galactokinase activity

Table 5.2. List of gene targets and a brief description continued.

Gene	Brief description (Information from yeastgenome.org)
Δ*GCR1*	Transcriptional activator of genes involved in glycolysis; DNA-binding protein that interacts and functions with the transcriptional activator Gcr2p
Δ*GCR2*	Transcriptional activator of genes involved in glycolysis; interacts and functions with the DNA-binding protein Gcr1p
Δ*TSL1*	Large subunit of trehalose 6-phosphate synthase/phosphatase complex; Tps1p-Tps2p complex converts uridine-5'-diphosphoglucose and glucose 6-phosphate to trehalose; contributes to survival to acute lethal heat stress; mutant has aneuploidy tolerance; protein abundance increases in response to DNA replication stress
Δ*RAM1*	Beta subunit of the CAAX farnesyltransferase (FTase); this complex prenylates the a-factor mating pheromone and Ras proteins; required for the membrane localization of Ras proteins and a-factor
Δ*ASC1*	G-protein beta subunit and guanine dissociation inhibitor for Gpa2p; ortholog of RACK1 that inhibits translation; core component of the small (40S) ribosomal subunit; required to prevent frameshifting at ribosomes stalled at repeated CGA codons; regulates P-body formation induced by replication stress; represses Gcn4p in the absence of amino acid starvation
Δ*TOR1*	PIK-related protein kinase and rapamycin target; subunit of TORC1, a complex that controls growth in response to nutrients by regulating translation, transcription, ribosome biogenesis, nutrient transport, and autophagy; involved in meiosis
Δ*PFK27*	6-phosphofructo-2-kinase; catalyzes synthesis of fructose-2,6-bisphosphate; inhibited by phosphoenolpyruvate and sn-glycerol 3-phosphate, expression induced by glucose and sucrose, transcriptional regulation involves protein kinase A
Δ*YCK1*	Palmitoylated plasma membrane-bound casein kinase I (CK1) isoform; shares redundant functions with Yck2p in morphogenesis, proper septin assembly, endocytic trafficking, and glucose sensing; stabilized by Sod1p binding in the presence of glucose and oxygen, causing glucose repression of respiratory metabolism; involved in the phosphorylation and regulation of glucose sensor Rgt2p
Δ*ADR1*	Carbon source-responsive zinc-finger transcription factor; required for transcription of the glucose-repressed gene *ADH2*, of peroxisomal protein genes, and of genes required for ethanol, glycerol, and fatty acid utilization
Δ*YCK2*	Palmitoylated plasma membrane-bound casein kinase I (CK1) isoform; shares redundant functions with Yck1p in morphogenesis, proper septin assembly, endocytic trafficking, and glucose sensing; stabilized by Sod1p binding in the presence of glucose and oxygen, causing glucose repression of respiratory metabolism; involved in the phosphorylation and regulation of glucose sensor Rgt2p
Δ*GPH1*	Glycogen phosphorylase required for the mobilization of glycogen; non-essential; regulated by cyclic AMP-mediated phosphorylation; phosphorylation by Cdc28p may coordinately regulate carbohydrate metabolism and the cell cycle; expression is regulated by stress-response elements and by the HOG MAP kinase pathway
Δ*YAK1*	Serine-threonine protein kinase; component of a glucose-sensing system that inhibits growth in response to glucose availability; upon nutrient deprivation Yak1p phosphorylates Pop2p to regulate mRNA deadenylation, the co-repressor Crf1p to inhibit transcription of ribosomal genes, and the stress-responsive transcription factors Hsf1p and Msn2p; nuclear localization negatively regulated by the Ras/PKA signaling pathway in the presence of glucose

CHAPTER VI: Yeast to Rubber: Sustainable Production of Novel Polymers from Novel Molecule [5]

6.1 Introduction

Polymer industries account for the third largest manufacturing industry in the US and the world. Dominating polymers include polypropylene, polyvinylchloride, polystyrene, etc., that are typically used for making plastics [55, 150]. Due to high durability and inexpensiveness, plastics are very useful for human society and virtually used in every aspect of daily life. The demand for polymers synthesis, therefore, has been increasing. However, current polymers are typically derived from finite resources of petrochemicals [1, 2]. As predicted from current usage rate of fossil fuels, fossil fuels are likely to go extinct [3]. Thus, current polymer production is not sustainable. Additionally, current disposal rate of polymer-derived products presents certain environmental challenges. 'White pollution' involves the accumulation of plastic product in the environment [57]. It can impose detrimental effects in the environment due to its durability and practically difficult to regulate the production and disposal. Thus, biodegradable polymers synthesis that is both cost-effective and sustainable is desired, and scientific efforts to replace current petroleum-derived polymer production expanded greatly over last few decades [58, 151].

Recently, scientists turned to microbial engineering to utilize fermentation process for fuels and chemical production. Some of the visionaries include utilization of renewable resources and produce fuels and chemicals eventually replacing current fossil fuel-based processes. These efforts eventually led to utilizing fermentation products to synthesize bio-based, degradable polymers. The most noted examples include poly(lactide) (PLA) synthesis from fermentation product lactic acid, poly(butylene succinate) (PBS) from succinate and bio-polyethylene from ethanol [61, 152, 153]. However, despite successful polymer synthesis from renewable resources, inflexibility of these bio-based polymers cannot possibly accommodate all the existing plastic market requiring various characteristics. Consequently, need to diversify the

[5] The content of this chapter is in preparation for submission. I performed the research with helps from Camille Boucher, Suryang Kwak, Seong Oh Seo, Drs. Jingjing Liu, Damien Guironnet and Yong-Su Jin (director of the research).

polymer synthesis from non-fossil fuel system is desired. Particularly, as demonstrated with PLA and PBS synthesis, various monocarboxylic or dicarboxylic acid based polymer synthesis gained significant interests [58, 151]. Microorganisms naturally produce a variety of organic acids as their metabolic products and can be genetically engineered to improve production. Also, although all acids commonly share carboxyl group at the end of the chain, structures and chain lengths of each organic acid differ allowing variable characteristics of resulting polymers [154]. Due to these advantages, polymer synthesis from microbial organic acids is highly desirable.

Saccharomyces cerevisiae is a robust, instrumental yeast for baking, brewing and bioethanol production and signified as a model eukaryote in molecular and cellular biology. Extensive studies of *S. cerevisiae* allowed the establishment of the elaborate metabolic system, therefore, it may be an ideal candidate for genetically engineering to produce valuable fuels and chemicals. However, despite its well-known metabolism, their metabolite product accumulation other than alcoholic fermentation is relatively unknown. Hence, I investigated *S. cerevisiae* metabolites produced during fermentation under various conditions to identify potential monomer candidates for polymer synthesis. Among many metabolites, I observed significant amounts of 2-isopropylmalate (2-IPM) accumulation, an intermediate of leucine biosynthesis, during defined medium fermentation. I spotted the 2-IPM production only occurs with leucine auxotrophic strain, commonly used an auxotrophic marker in yeast for engineering purposes agreeing with previous studies [155]. The 2-IPM is a 4-carbon chain dicarboxylic acid with isopropyl group at alpha (second) carbon. I predicted the structure of 2-IPM is a suitable and novel monomer candidate for bio-based polymer synthesis. Thus, in this study, I metabolically engineered *S. cerevisiae* strain for overproduction of 2-IPM and demonstrated synthesis of bio-based polymer synthesis from 2-IPM. To my knowledge, this study is the first attempt for genetically engineering yeast to overproduce 2-IPM, and the attempted to synthesize polymer.

6.2 Materials and methods

Strains, medium and culture conditions

S. cerevisiae strains used in this study were summarized in Table 6.1. Yeast cells were routinely cultured in the Yeast extract-peptone and glucose (YPD, 10 g/L yeast extract, 20 g/L

peptone, and 20 g/L glucose) medium to prepare initial inoculum at 30°C with 250 rpm agitation speed. Various yeast defined medium (Yeast nitrogen base only (YNB), Synthetic complete (SC) and Verduyn medium [156]) were used in fermentation experiments. YNB medium contained 6.7 g/L yeast nitrogen base with ammonium sulfate, and SC medium contained 6.7 g/L yeast nitrogen base and 0.79 g/L complete supplement mixture (CSM) (Bio 101, Vista, CA). Modified Verduyn medium 15 g/L $(NH_2)_2SO_4$, 8.0 g/L KH_2PO_4, 3.0 g/L $MgSO_4$, 10 mL/L trace element and vitamin solution 12 mL/L. Trace element contained 15 g/L EDTA, 5.75 g/L $ZnSO_4$, 0.32 g/L $MnCl_2$, 0.50 g/L $CuCl_2$, 0.47 g/L $CoCl_2$, 0.48 g/L Na_2MoO_4, 2.9 g/L $CaCl_2$ and 2.8 g/L $FeSO_4$. Vitamin solution contained 0.05 g/L biotin, 1.0 g/L calcium pantothenate, 1.0 g/L nicotinic acid, 25.0 g/L *myo*-inositol, 1.0 g/L thiamine hydrochloride, 1.0 g/L pyridoxal hydrochloride and 0.2 g/L *p*-aminobenzoic acid [156]. pH of all media was adjusted to 5.8. leucine was added at 0.1 g/L for standard (1x) concentration otherwise indicated for supplemented concentration. Glucose was used as a carbon source for all yeast cultivation. To select yeast transformants carrying *NAT1, HyB, KanMX*, resistance gene, 120 μg/mL of nourseothricin, 300 μg/mL of Geneticin G418 and 300 μg/mL of hygromycin was used, respectively. *Escherichia coli* TOP10 was cultivated in the Luria-Bertani medium at 37°C with 250 rpm agitation speed, and 50 μg/mL of ampicillin was added for selection of plasmid-carrying cells.

Plasmid construction

All primers, template plasmids, and constructed plasmids are listed in Table 6.1, and 2. expressing plasmids used in this study are based on pRS series vectors with an antibiotic marker (Table 6.1, [141]). The guide RNA(gRNA) targeting *LEU1, LEU2, URE2*, *LEU4* and intergenic site (CS6, *S. cerevisiae* chromosome VII) were synthesized by gBlock from IDT Inc. or by PCR. The gBlocks for gRNAs were synthesized with the recognition site of each gene and flanking sequences for SacI and KpnI restriction enzyme digestion. Then gBlocks and pRS42K and 42H vector plasmids were digested with SacI and KpnI enzyme. Resulting gBlocks and vectors were ligated. The resulting ligated vectors and inserts were transformed into *E. coli* for plasmid amplification.

CRISPR/Cas-based genome editing for strain engineering

CRISPR-Cas (Clustered Regularly Interspaced Short Palindromic Repeats/CRISPR-Associated Proteins) based genome editing system was for all strains engineering. Previously established technique in our lab was used [67, 132]. The pRS42N Cas9 plasmid was transformed into *S. cerevisiae* strain first then Cas9 carrying strain was used as host strain for further genetic modifications. Plasmid carrying guided RNA for *LEU1, LEU2, LEU4, URE2* and intergenic site *CS6* with the double stranded repairing donor DNA were transformed into Cas9 carrying strains. All transformation method was adapted from PEG-LiAc high-efficiency yeast transformation method [133] and selected on yeast extract-peptone (YP) medium with 20 g/L of glucose and with appropriate antibiotic markers. All strains and plasmids used in the study are listed in Table 6.1 and primers are listed in Table 6.2.

Fermentation experiments

To prepare yeast strains for fermentation experiments, yeast cells were cultivated in YPD medium at 30°C and 250 rpm. Cells were harvested at exponential phase by centrifugation and washed two times with sterile water. Flask-scale Fermentation experiments were performed in SC, YNB and Verduyn media with 80 g/L glucose. All flask-scale fermentation experiments were performed in 50 mL culture using a 250 mL Erlenmeyer flask tightly covered with aluminum foil at 30°C and 100 rpm of rotation speed. Initial cell densities of all fermentation experiments were adjusted to OD_{600} of 1. All flask-scale fermentation experiments were performed in duplicates.

The glucose-limited fed-batch culture was conducted in BioFlo & CelliGen 310 fermentor (New Brunswick Scientific-Eppendorf, Enfield, CT, United States) with the 1-liter culture of modified Verduyn media and 40 g/L of glucose. Initial cell densities were adjusted to OD_{600} and pH was maintained at 5.8 with 5N NaOH. When glucose was depleted, feeding media solution was started containing: 9.0 g/L KH_2PO_4, 2.5 g/L $MgSO_4$, 3.5 g/L K_2SO_4, 0.28 g/L Na_2SO_4, 600 g/L glucose, 10mL/L trace element solution, 12mL/L vitamin solution [156] and 10 g/L Leucine. Feeding rate was adjusted accordingly to growth rate.

Analytical methods

Cell growth was monitored by measuring optical density (OD) at 600nm using a UV-visible spectrophotometer (Biomate5, Thermo, Rochester, NY). Glucose, acetate, 2-isopropyl malate and ethanol concentrations were determined by high-performance liquid

chromatography (HPLC, Agilent Technologies 1200 Series, Mississauga, CA) equipped with a refractive index detector using a Rezex ROA-Organic Acid H^+ (8%) column (Phenomenex Inc., Torrance, CA). The column was eluted with 0.005 N of H_2SO_4 at a flow rate of 0.6 mL/min at 50°C.

Purification of 2-IPM from fermentation broth

Solvent extraction and crystallization method adapted and modified from US Patent 4,407,953 [157] was used to purify 2-IPM. At the end of the fermentation, yeast cells were separated from the broth via centrifugation. The fermentation broth was concentrated by boiling and evaporating to about a fifth of its original volume. The pH of concentrated fermentation broth was adjusted to 1.5 with sulfuric acid then an equal volume of methyl ether ketone (MEK) was added. After a vigorous mixing, aqueous phase and solvent phase were separated by the separatory funnel, and 2-IPM remained in solvent phase. Extraction of 2-IPM with MEK was repeated one more time with remaining aqueous phase. The solvent phases were combined and allowed for evaporation until dissolved 2-IPM crystallized. 2-IPM crystals were separated and washed with ice-cold water until impurities were not detected.

Identification of 2-IPM by GC-MS

Gas chromatography-mass spectrometry was initially used for identification of 2-IPM. The 2-IPM is containing fermentation broth sample vacuum dried and derivatized by methoxyamination and silylation method as described previously [158]. 5 uL of methoxyamine hydrochloride in pyridine (40mg/mL) solution was added to 2-incubated at 30˚C and 400 rpm for 90 minutes. Then, 45uL of N-methyl-N-trimethylsilyl trifluoroacetamide (MSTFA) was added and incubated at 37˚C and 400 rpm for 30 minutes. The derivatized 2-IPM sample was analyzed by GC-MS (Agilent Technologies Inc., CA; 7890 Gas chromatography and 5975 MSD) and NIST library as well as a comparison to 2-IPM standard chemical (Sigma).

Polymer synthesis of 2-IPM

Purified 2-IPM was treated with acetic anhydride and sodium acetate for 3.5 hours, losing hydroxyl group at carbon 2 and producing cyclic form. Reaction method is used as previously described. [159]. Than 2-IPM anhydride monomer was reacted with epichlorohydrin to form polymers with catalysts in solvents at 45°C for about 15 hours. The method was adapted from a previous study [160].

6.3 Results

2-isopropylmalate (2-IPM) production by leucine auxotrophic strain

Initially, I performed glucose fermentation of *S. cerevisiae* strains under defined medium (SC) to observe the phenotypes and fermentation metabolite production. The prototrophic strain S288C and its auxotrophic derivative BY4742 was used for growth and analyses their fermentation metabolites. Overall, S288C had faster fermentation rate and higher biomass accumulation as compared to BY4742 strain under SC medium (data not shown). Overall metabolites were very similar but few significant differences in extracellular metabolite accumulation detected by HPLC. First, acetate production by BY4742 was notably higher than S288C. Secondly, unknown metabolite was detected by HPLC at retention time around 6.6 min only in BY4742 strain at a significant level (Figure 6.1A). To identify the unknown metabolite, I analyzed the fermentation broth sample of S288C and BY4742 with GC-MS. Initial analysis indicated 2-isopropylmalate (2-IPM) was a major difference between S288C and BY4742 strain. To confirm, the 2-IPM standard chemical analysis in HPLC and GC-MS was performed. Since 2-IPM is an intermediate of leucine biosynthetic pathway, the 2-IPM production is likely caused by leucine auxotrophy of BY4742 by Δ*LEU2* (Figure 6.2). However, metabolic pathway shows end-product of Δ*LEU2* is 3-isopropylmalate (3-IPM). To further confirm 2-IPM production, not the 3-IPM production I deleted each *LEU1* and *LEU2* in S288C (SL1 and SL2 strain, respectively) and compared for 2-IPM production. Figure 6.1C shows 2-IPM production occurs in both SL1 and SL2 strain.

Metabolic engineering of leucine auxotrophic strain for higher 2-IPM yield

After validating 2-IPM accumulation in Δ*LEU1* strain (SL1), I attempted to engineer the pathway of SL1 further to increase 2-IPM yield. The SL1 strain can accumulate ~0.5 g/L of 2-IPM fermenting 80 g/L of glucose (~0.007 g/g yield, Figure 6.1C), showing much room for improvement. First, I identified *URE2* as a target of deletion. The *URE2* gene in *S. cerevisiae* encodes Ure2p that plays an important role nitrogen catabolite repression transcriptional regulator. Thus, deletion of *URE2* will relieve the nitrogen catabolite repression during amino acid (leucine) supplemented medium [161]. As shown in Figure 6.3A, *URE2* deletion strain (SUL) produced higher 2-IPM yield compared to SL1 strain (~0.01 g/g vs. ~0.007 g/g).

Next, I targeted for increasing pyruvate flux to branched amino acid biosynthetic pathway and removal of leucine feedback inhibition. Although pyruvate is a key intermediate involved in several metabolic pathways and yet, native yeast mostly convert pyruvate into acetaldehyde to produce ethanol under fermentative growth condition. Thus, acetolactate synthase converting pyruvate to 2-aceto-lactate was targeted for overexpression (for example, *Bacillus subtilis AlsS* [162]). Also, yeast metabolism tightly regulates amino acid synthesis by feedback regulation. To remove leucine feedback inhibition, *LEU4* was targeted to mutate leucine feedback inhibition residue (Asp578) as previous research identified [163]. Each and both *BsAlsS* and m*LEU4* (Asp578 changed to Tyr578) were introduced into SUL strain resulting in SUAL (SUL strain overexpressing *BsAlsS*), SULL (SUL strain with m*LEU4*) and SUALL (SUL strain overexpressing *BsAlsS* and m*LEU4*) strains. Unexpectedly, SUAL and SULL strain did not increase in 2-IPM yield (Figure 6.3A). In fact, SULL strain yielded lower 2-IPM compared to before the introduction of m*LEU4* strain. However, the strain harboring both *BsAlsS* and m*LEU4* had a two-fold increase in 2-IPM yield achieving highest 2-IPM production among all engineered strains in this study. The 2-IPM productivity patterns were consistent to 2-IPM yield, showing genetic manipulation increased 2-IPM generally improved overall production as well (Figure 6.3A and B).

Fermentation condition optimization for large scale fermentation and purification of 2-IPM

2-IPM production further enhanced as fermentation conditions were optimized. How yeast cells cognize the environment, as nutrient-limited or nutrient-rich, especially nitrogen sources, can be important for producing amino acid-related products. Thus, different defined media with best 2-IPM producing strain (SUALL) were tested for 2-IPM production. SC medium, YNB medium and Verduyn medium varying nitrogen source, vitamin, trace elements and amino acids were tested with an equal amount of leucine supplementation. As shown in Figure 6.3C, YNB and Verduyn media had 1.5-fold higher 2-IPM yield (0.03 g/g) compared to SC medium (0.02 g/g). Although both YNB and Verduyn media showed similar yield, however, the 2-IPM productivity of Verduyn was higher illustrating that 2-IPM production is most efficient under Verduyn medium. Next, different concentrations of leucine supplementation were tested. With 0.1 g/L as a 1x standard, concentrations of 0.1x, 0.5, 1x and 2x Leucine supplementation were tested with Verduyn media. Overall, increasing leucine concentration resulted in higher yield

and productivity (Figure 6.3C and D). In sum, SUALL strain with Verduyn media, 2x leucine supplementation resulted in highest yield and productivity.

After 2-IPM overproducing strains was developed, and optimization of fermentation conditions was accomplished, I performed large-scale fermentation (starting at 1 L) to tightly control the fermentation parameters such as pH, aeration, and agitation. For batch phase, Verduyn medium with 20 g/L glucose and 2x leucine supplementation was used. The cell density equivalent of OD 1 was inoculated. Once glucose from batch phase depleted, limited-glucose fed-batch phase started by feeding concentrated glucose solution by tubes. Cell density and glucose accumulation were carefully monitored to minimize overfeeding glucose solution thus preventing alcoholic fermentation. At the end of fermentation, ~25 g/L of 2-IPM was produced with a culture volume of ~1.5 L with a cell volume of ~100 mL. This result illustrates 2-IPM at industrial scale is achievable.

Because there was no 2-IPM product available to purchase at large scale, at the end of fermentation, the broth was harvested for purification. The produced 2-IPM was purified using solvent extraction by MEK and crystallization. To obtain high purity 2-IPM for polymer synthesis, several washing steps were performed yielding ~15 g/L of 2-IPM in the end.

Polymer synthesis using 2-IPM

Based on previous work of malic acid polymerization, 2-IPM was tested for polymer synthesis with a similar strategy. First, 2-IPM was dehydrated to lose hydroxyl group at carbon 2 and become cyclic form to produce 2-IPM anhydride monomer. Two isomers can present depending on the location of the double bond (isopropyl group chain or in the ring). Then 2-IPM anhydride monomer can react with epichlorohydrin to form polymers at 45°C with a catalyst for 15 hours. The reaction steps and 2-IPM polymeric structures are illustrated in Figure 6.5.

6.4 Discussion

The use engineered microorganisms as a microbial cell factory has been widely adapted producing fuels and chemicals envisioning to replace fossil fuel-based production. Recently, the idea of extended to synthesize polymers from bio-based chemicals. However, to successfully replace current polymer industries, various types of polymer synthesis must be established.

Here I demonstrate overproduction of 2-isopropylmalic acid (2-IPM), an intermediate of leucine biosynthesis by engineered *S. cerevisiae* and synthesis of the novel polymer using 2-IPM.

The native yeast strains can synthesize 2-IPM but do not accumulate at high amounts 2-IPM. However, with leucine auxotrophy (Δ*LEU2* or Δ*LEU1*), yeast can accumulate 2-IPM under glucose fermentation with the minimal medium. Additionally, when yeast accumulates 2-IPM, higher acetate is observed as a signature due to acetyl group of acetyl-CoA is required to produce 2-IPM. Anticipating the value of 2-IPM as new monomer material for polymer synthesis, I attempted to overproduce 2-IPM by metabolic engineering strategy. The native yeast metabolic system tightly regulates amino acid biosynthetic pathway via feedback regulation and nitrogen catabolic repression network (Figure 6.2). Also, most sugars are metabolized via glycolysis and converted to ethanol under fermentative condition. Thus, several genes were identified as a target of genetic manipulation to remove feedback regulation, nitrogen catabolite repression (NCR) and increase carbon flux toward 2-IPM synthesis.

During culturing of yeast, yeast perceives growth environment as either nutritious or starving, depending on nitrogen source availability and quality. Then, via NCR, nitrogen catabolic genes are amino acid biosynthesis either activated or repressed. *URE2*, one of the global NCR transcriptional regulator, was first targeted for deletion to remove NCR. *URE2* inhibits *GLN3* and GCN4 transcription under rich nitrogen source which activates genes that are subject to NCR and amino acid biosynthesis. Thus, I hypothesized deletion of *URE2* would result in activation of *GLN3* and *GCN4* consequently activating amino acid biosynthesis (leucine biosynthesis) and improve 2-IPM production in leucine auxotrophic strain (SL1). As expected, the Δ*URE2* in SL1 strain (SUL) increased 2-IPM yield and productivity by ~1.4 fold (Figure 6.3A and B).

With the removal of NCR, increasing pyruvate flux toward leucine biosynthetic pathway and removal of leucine feedback inhibition was considered. Because native yeast produces ethanol from pyruvate as a major product, increasing pyruvate flux into leucine biosynthetic pathway (branched amino acid pathway) is necessary. The heterologous acetolactate synthase from *Bacillus subtilis* (*BsAlsS*) with constitutive promoter was introduced to SUL strain to avoid any transcriptional regulation if native acetolactate synthase (*ILV2*). For the removal of leucine feedback inhibition, a SNP was introduced to native *LEU4* resulting in a change of amino acid Asp578 to Tyr578 (m*LEU4*) as the previous study already reported. The *LEU4* gene also

encodes for 2-IPM synthase converting 2-keto-isovalerate to 2-IPM. Each *BsAlsS* and m*LEU4* were introduced into SUL strain (SUAL and SULL, respectively) to observe the effect on 2-IPM production. Unexpectedly, when *BsAlsS* or m*LEU4* was introduced, 2-IPM production did not improve (Figure 6.3 A and B). *BsAlsS* did not change the yield not the productivity of 2-IPM, and the introduction of m*LEU4* decreased in 2-IPM production. I speculated increasing pyruvate flux had did not help in increasing 2-IPM production because leucine feedback inhibition is present making conversion of 2-keto-isovalerate to 2-IPM limiting reaction. Likewise, removal of feedback inhibition did not improve 2-IPM production likely due not enough carbon flux toward leucine biosynthetic pathway achieved. Hence, both *BsAlsS* and m*LEU4* were introduced to SUL strain (SUALL) to observe synergistic effect to overproduce 2-IPM. The 2-IPM yield improved significantly (~2-fold increase in yield and productivity from SUL strain, Figure 6.3A and B). These data show both 'push and pull' was necessary to achieve desired product formation.

After optimizing yeast strains for 2-IPM production, fermentation condition optimization was performed with best 2-IPM producing strain. Three conditions varying nutrient composition were used (SC, YNB and Verduyn, composition listed in materials and method). Verduyn media showed the best 2-IPM production increasing in both yield and productivity (Figure 6.3C and D). SC media contains other amino acid mixture whereas YNB and Verduyn media do not. As a result, shown in Figure 6.2C, the 2-IPM yield of SC medium lower compared to YNB and Verduyn media. This is an indirect evidence of the presence of remaining nitrogen catabolite repression other than genes regulated by *URE2.* Also, 2-IPM productivities were higher with SC and Verduyn medium compared to YNB medium. This result show 2-IPM productivities depend on nutrient availability. To further optimize, different leucine concentration supplementation was tested. Because 2-IPM producing strains are leucine auxotrophic, higher leucine supplementation increased 2-IPM yield and productivities in general. In sum, Verduyn media with 2x leucine supplementation showed best 2-IPM yield and productivity (0.033 g/g and 0.11 g/L/H).

To illustrate 2-IPM production at industrial scale, limited glucose fed-batch fermentation using bioreactor was performed. Tightly controlling fermentation parameters, maintaining pH at 5.8 and high aeration to prevent alcoholic fermentation much as possible, 25 g/L of 2-IPM was achieved (Figure 6.4B). After illustrating overproduction of 2-IPM by engineered yeast,

purification of 2-IPM from fermentation broth was attempted. Due to low demand of the chemical, 2-IPM was unavailable for large-scale purchase that is necessary for investigating polymer synthesis by 2-IPM. Using solvent extraction by MEK and crystallization, I obtained 15 g/L of 2-IPM powder with 99% purity. The resulting high-pure 2-IPM was then dehydrated to form anhydride monomer and polymerized with an epoxide. The predicted characteristics of the 2-IPM based polymer are a biodegradable elastomer. Further 2-IPM-derived polymer characterization is currently under investigation.

In conclusion, I successfully overproduced 2-IPM by metabolically engineering yeast from initial 2-IPM accumulation observation. To my knowledge, this is first report attempting to engineering yeast strains to overproduce 2-IPM. Further, 2-IPM was successfully purified with high purity, and polymer synthesis was attempted. Detailed 2-IPM-derived polymer characterization is currently under investigation. With success of 2-IPM-derived polymer synthesis, I anticipate various application can be achieved possibly replacing part of the current petrochemical production of polymer.

6.5 Figures and tables

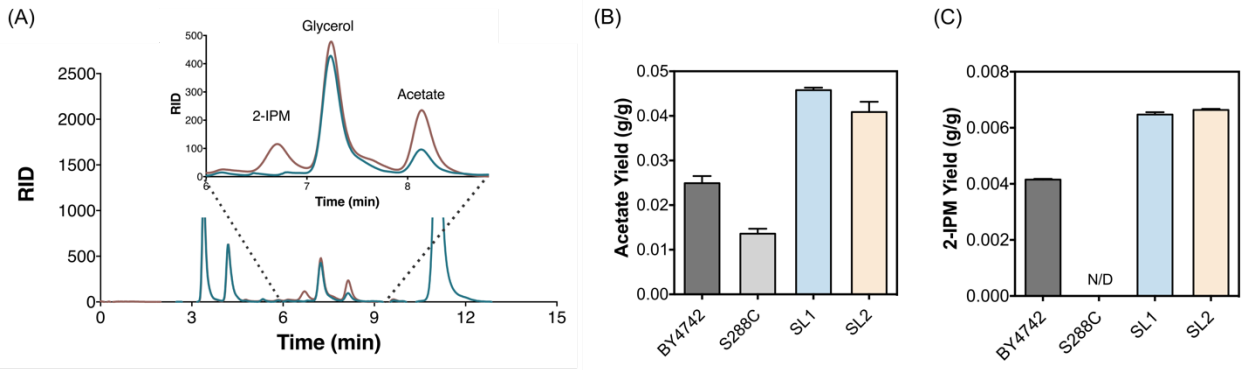

Figure 6.1 Identification and confirmation of 2-IPM accumulation by leucine auxotrophic strains. (A) HPLC chromatogram comparison of BY4742 (leucine auxotroph, red line) and S288C (prototroph, green line) after glucose depletion. Acetate (B) and 2-IPM (C) yield from 80 g/L glucose show. BY4742, S288C, SL1 and SL2 strains were compared. (N/D: not detected).

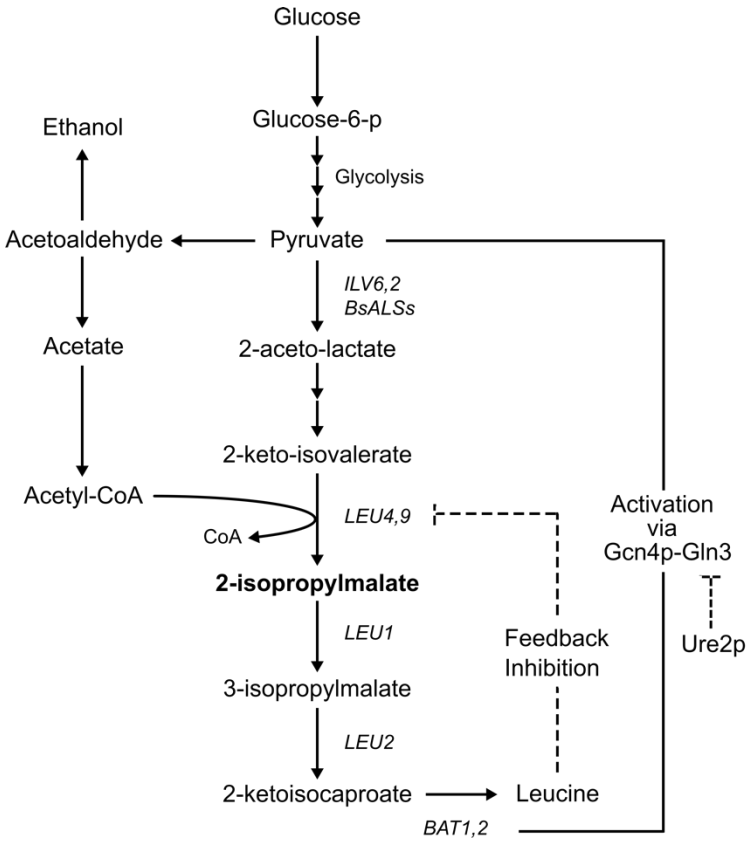

Figure 6.2 Leucine biosynthesis pathway from glucose. Glucose is first converted to pyruvate via glycolysis. Pyruvate can be converted to acetaldehyde for ethanol or acetate production for ethanol and acetate production and 2-aceto-lactate entering leucine biosynthetic pathway. Acetate is converted to acetyl-CoA which combines with 2-keto-isovalerate to produce 2-IPM. Inhibitory regulation is shown by a dotted line, and activation regulation is shown with solid line. *LEU2*, 3-isopropylmalate dehydrogenase; *LEU1*, isopropylmalate isomerase; *URE2*, nitrogen catabolite repression transcriptional regulator; *ILV2,6*, acetolactate synthase, and regulatory unit; *BsALSs*, Bacillus subtilis acetolactate synthase; *LEU4,9* 2-isopropylmalate synthase.

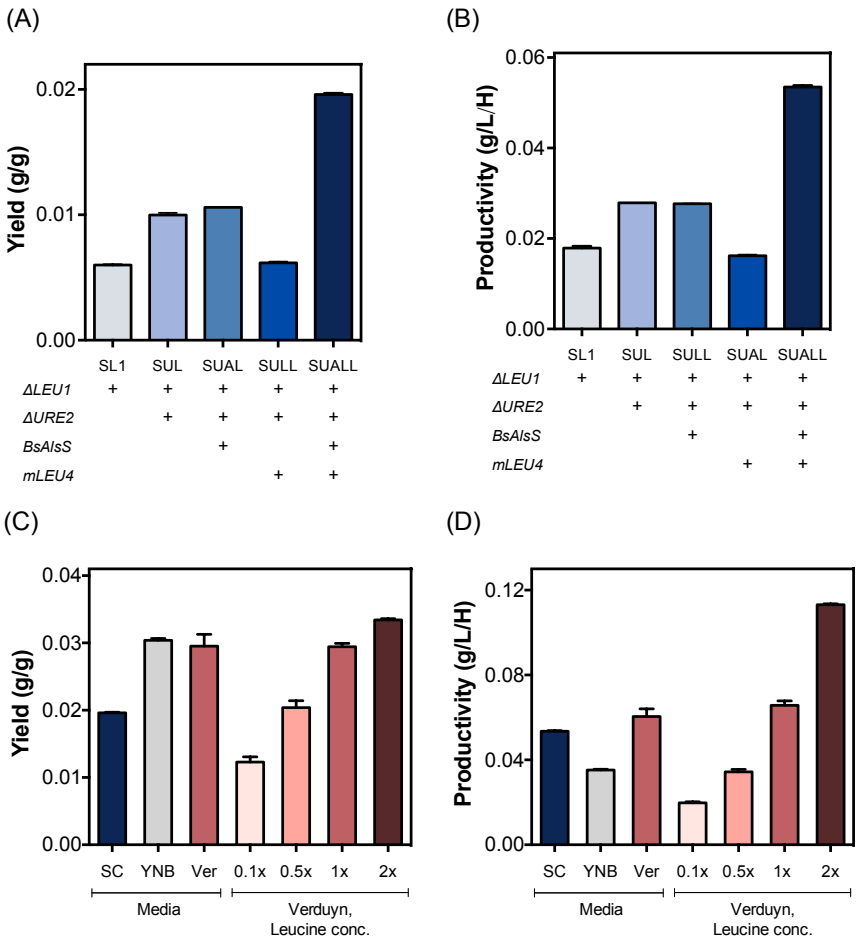

Figure 6.3 Fermentation profiles of engineered strains and different fermentation media conditions. (A-B) 2-IPM yield (A) and productivity (B) of all engineered strains for improving 2-IPM production. SL1, SUL, SUAL, SULL and SUALL strains were compared under SC medium with 80 g/L glucose. (C-D) Different defined medium fermentations were compared for improved 2-IPM yield (C) and productivity (D). SC, YNB and Verduyn media and different concentrations of leucine supplementation were tested with SUALL strain.

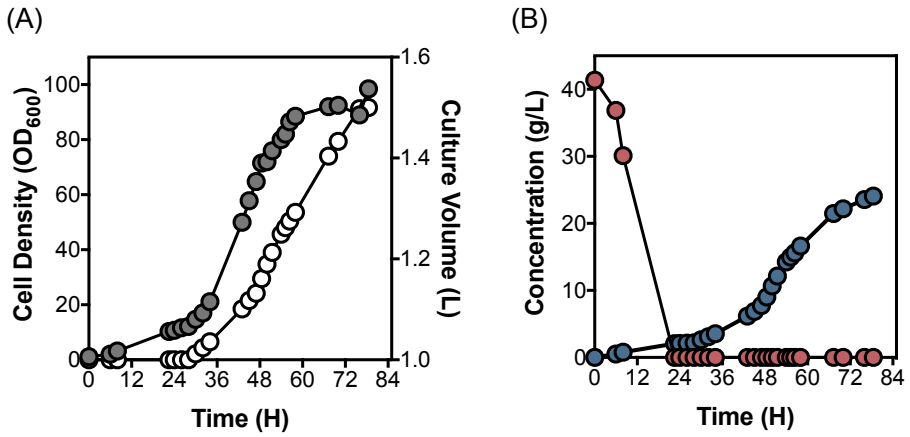

Figure 6.4 Yields, productivities, and yield and productivity comparison of 2-IPM accumulation. All engineered strains and different fermentation medium conditions were compared. (A)Yields and (B) productivities of 2-IPM were calculated based on the amount of consumed glucose and last time point of fermentation. (C) Yield and productivities (from (A and B)) were compared together for 2-IPM production improvement by a different strategy.

1) 2-IPM Anhydride synthesis

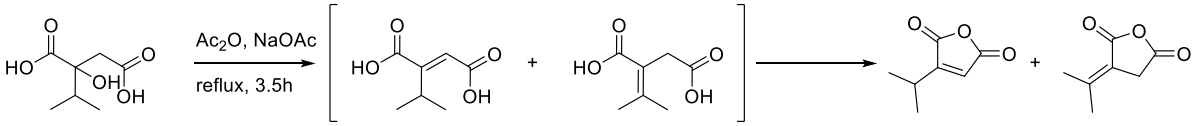

2) Polymerization of 2-IPM anhydride with epoxides

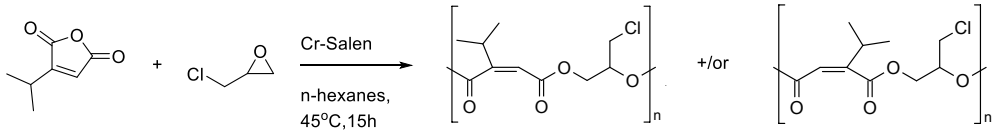

Figure 6.5 Polymerization steps using 2-IPM as a starting material. 2-IPM Anhydride monomer can be synthesized by dehydration with acetic anhydride and sodium acetate losing hydroxyl group at carbon 2 and closing to for cyclic form. Then 2-IPM anhydride monomer was reacted with epichlorohydrin to form polymers.

Table 6.1 The list of plasmids and *S. cerevisiae* strains used in this study

Strain/Plasmid	Relevant characteristic(s)/Description	Source or Reference
BY4742 strains		
BY	BY4742 *MATα leu2 his3 lys2 ura3*	
S288C strains		
S288C	*MATα*	
SL2	*MATα* Δ*LEU2*	This study
SL1	*MATα* Δ*LEU1*	This study
SUL	*MATα* Δ*LEU1* Δ*URE2*	This study
SUAL	*MATα* Δ*LEU1* Δ*URE2 CS6::BsAlsS*	This study
SULL	*MATα* Δ*LEU1* Δ*URE2 mLEU4*	This study
SUALL	*MATα* Δ*LEU1* Δ*URE2 mLEU4 CS6::BsAlsS*	This study
Plasmids		
pRS405	*LEU2*, 2μ origin, Amp^r plasmid	EUROSCARF
pRS42N	NAT1 marker plasmid	EUROSCARF
pRS42K	KanMX marker plasmid	EUROSCARF
pRS42H	HyB marker plasmid	EUROSCARF
pRS42N Cas9	P_{PGK} -MCS- T_{CYC}, Cas9 expression plasmid	[67]
pRS42K gRNA *URE2*	*URE2* gRNA plasmid	This study
pRS42H gRNA *LEU2*	*LEU2* gRNA plasmid	[67]
pRS42H gRNA *LEU1*	*LEU1* gRNA plasmid	This study
pRS42K gRNA *LEU4*	*LEU4* gRNA plasmid	This study
pRS42H gRNA *CS6*	CS6 intergenic site gRNA plasmid	This study
pRS426 *BsAlsS*	pRS426 GPDp-*alsS*-CYC1t	[162]

Table 6.2 Primers used in this study

Primers	Sequence	Description
JIN4360	AGCAATATATATATATATATTTCAAGGATATACCATTCTACATAAACGCCAGGTTGTGTC	*ΔLEU2* donor
JIN4361	TAAAGTTTATGTACAAATATCATAAAAAAAGAGAATCTTTGACACAACCTGGCGTTTATG	
JIN4318	TGGTTAGCAATCGTCTTACTTTCTAACT	*ΔLEU2* confirm
JIN4321	TCTACGGTAGCAGGTAAGTTGAAAAT	
JIN5419	GGGAAAAGGCTGTTGCCTACGTTTTAGAGCTAGAAATAGCAAG	*LEU1* gRNA
JIN5420	GTAGGCAACAGCCTTTTCCCGATCATTTATCTTTCACTGCGGA	
JIN5421	TTTTGTCGCTATCGATTTTTATTATTTGCTGTTTTAAATCCATAAACGCCAGGTTGTGTC	*ΔLEU1* donor
JIN5422	CATGTTATTGACGCCAGGTTTGGACGTTGTTTTTCACTGTGACACAACCTGGCGTTTATG	
JIN5423	CTTATTTAAACAGCAGAACTTAACT	*ΔLEU1* confirm
JIN5424	TATAAACTTCATCAATGATGTTATA	
JIN3739	GATATACCCTTTTCTCTCACGTTTTAGAGCTAGAAATAGCAAG	*URE2* gRNA
JIN3740	GTGAGAGAAAAGGGTATATCGATCATTTATCTTTCACTGCGGA	
JIN3743	GTTTTTCATTTTTTGTTATTAGTCATATTGTTTTAAGCTGCAAATTAAGTTGTACACCAAAGGCTGCTTTAAAAAC	*ΔURE2 donor*
JIN3744	ACATACCCTTATAACCTTCTTTTCCTCCTTCTTCTTTCTTTCTTGTTTTTAAAGCAGCCTTTGGTGTACAACTTAA	
JIN3716	GAATACCGACTGTTGTCTGG	*ΔURE2* confirm
JIN3717	CATATCTCGACATCAATCG	
JIN5425	TGAAGAATCACCGACATCTT GTTTTAGAGCTAGAAATAGCAAG	*LEU4* gRNA
JIN5426	TGAAGAATCACCGACATCTTGTTTTAGAGCTAGAAATAGCAAG	
JIN5427	AAGATGTCGGTGATTCTTCAGATCATTTATCTTTCACTGCGGA	*mLEU4* donor
JIN5428	CGTAATGCCGACAACGAAAAGGCCTACAAATGGGGTGTAGGTGTCTCAGAATATGTCGGT	
JIN4319	TCTACGGTAGCAGGTAAGTTGAAAAT	*mLEU4* confirm
JIN4320	TTCTAGCGCCGTTCAAGACCAT	
SOO587	AACCTCGAGGAGAAGTTTTTTTACCCCTCTCCACAGATCCAGGAAACAGCTATGACCATG	CS6 intergenic site-M13
SOO588	TAATTAGGTAGACCGGGTAGATTTTTCCGTAACCTTGGTGTCTGTAAAACGACGGCCAGT	
SOO595	GTCTGCCGAAATTCTGTG	CS6 site integration confirm
SOO596	CGGTCAGAAAGGGAAATG	

Chapter VII: Potential Applications of 2-IPM: Novel Skin-Brightening Agent[6]

7.1 Introduction

Skin-brightening agents are highly demanded in cosmetic industries especially in skin-care products due to driving force of desiring for brighter and clearer skin. Skin-care products containing skin-brightening agents can be readily found in the market and the demand it is increasing. In severe cases, skin-brightening agents demanded to treat abnormal hyperpigmentations such as melasma or any other forms of melanin hyperpigmentation. Responding to this high demand, many skin-brightening agents were discovered in past few decades. For example, arbutin, a naturally occurring beta-D-glucopyranoside of hydroquinone is known for its effectiveness for skin depigmentation capability [164]. However, recent studies proposed potential carcinogenicity of beta-arbutin [165, 166]. Thus, usage of beta-arbutin in cosmetic products in Europe is prohibited. Thus, increasing number of studies are investigating to discover novel skin- brightening agents.

The primary mechanism of skin-brightening is to inhibit melanin synthesis. To do this, rate-limiting tyrosinase enzyme inhibition is effective to control the melanin production. Tyrosinase is a copper-containing enzyme, which requires copper ion as a cofactor. Consequently, lowering copper ion availability can effectively inhibit tyrosinase activity [167-169]. Therefore, organic acids, generally metal chelators, can be used as the novel skin-brightening agent. Also, effectively chelate copper ions and inhibit tyrosinase activity, organic acids should be transported into the cell where melanin synthesis takes place [170]. However, organic acids cannot be transported into the readily due to the dependence of pH and polarity. Hence, the skin-brightening agent should be able to enter the cell and inhibit the tyrosinase activity.

A previous study (**Chapter VI**) reports overproduction of 2-isopropylmalate (2-IPM) from engineered yeast. The 2-IPM is producing yeast accumulated 2-IPM up to 25 g/L during fermentation. From this result, I inferred superior cell permeability of 2-IPM compared to other

[6] The content of this chapter is in preparation for submission. I performed the research with helps from Ji Hye Kim, Nam Joo Kang and Yong-Su Jin (director of the research).

organic acids. Thus, this study investigates the skin-brightening capability of 2-IPM by examining tyrosinase inhibitory activity in both *in vitro* and *in vivo* system.

7.2 Material and Method

In vitro tyrosinase inhibition assay

The sample solutions (Arbutin, malic acid, and 2-IPM) was dissolved in sterile pure water and prepared to have final concentrations of 50, 40, 30, 20, 10mM. Following ingredients were added to each well to 96 well microplate in order of 220 µL 0.1M phosphate buffer (pH 6.5), 20 µL sample solution or buffer as a control 40 µL mushroom tyrosinase and 40 µL 1.5 mM tyrosine. The microplate was incubated at 37°C for 20 minutes, and the absorbance at 490nm using microplate reader was recorded.

Intracellular detection of 2-IPM and malic acid

To test cell permeability of 2-IPM and malic acid, yeast S288C was used. 100mM of 2-IPM and malic acid solutions, adjusting pH to 4.0, 5.0 and 6.0 were prepared in a buffer. Cell density equivalent to OD_{600} 20 was inoculated to 2mL solutions and incubated at 30°C with 250 rpm agitation speed for ~10 hours until both 2-IPM and malic acid concentrations were detected.

Cytotoxicity of 2-IPM

Effect of 2-IPM on cell viability of B16F10 (ATCC® CRL-6475™) cells was tested. 2-IPM concentrations of 0, 0.5, 1, 2, 4, 8, and 10 mM were used. 2-IPM samples were treated for ~five days, and cell viability was calculated by % viable cells to the untreated group.

α-MSH-induced melanogenesis

To all B16F10 cell samples**,** 100 nM of α-MSH was treated to induce melanogenesis. Then 100 or 200 µM Arbutin or 1, 2, or 4 mM 2-IPM was treated. Samples were incubated for five days. Both intracellular and extracellular melanin was observed and recorded.

7.3 Results

To observe potentials of 2-IPM as a depigmenting agent, *in vitro* tyrosinase inhibitory activity was tested. As a positive control, arbutin was used, and as a structural control to 2-IPM, malate was used. Although tyrosinase inhibitory activity was observed in all samples, the inhibitory activity of arbutin was superior compared to malate and 2-IPM in any concentrations (Figure 7.1). The inhibitory effect of malate and 2-IPM was similar. Although overall tyrosinase inhibitory activity was lower with 2-IPM, I hypothesized 2-IPM can be still effective based on previous speculations of 2-IPM structure and cell permeability. To observe relative cell permeability, laboratory yeast strain, S288C was incubated with 100mM of 2-IPM or malate or water at different pH. Then, cells were harvested, lysed for intracellular 2-IPM or malate detection. As shown in Figure 7.2, 2-IPM had significantly higher 2-IPM accumulation compared to malate.

After *in vitro* tyrosinase inhibition was measured, *in vivo* test was performed with mouse skin melanoma cell, B16F10. First, cytotoxicity of 2-IPM was tested. B16F10 cells were treated with 2-IPM concentration ranging 0-10 mM. The cell viability was compared to untreated group and % cell viability was calculated. 2-IPM did not show cell cytotoxicity up at four mM. However, the toxicity started to show from 8- 10 mM displayed at lower cell viability (Figure 7.3). Thus, 2-IPM concentration from 8 mM and higher was excluded from the further experiments. Next, the effect of 2-IPM on α-MSH-induced melanogenesis in B16F10 cells was observed (Figure 7.4). B16F10 cells can produce melanin only with α-MSH induction. Thus, treating the cell with α-MSH and sample of interest can illustrate effects of melanin synthesis by various samples. The first and second column shows α-MSH induction is necessary for melanin synthesis. Arbutin was treated with 100 or 200 μM as a control. At both concentrations, extracellular melanin concentration decreased, but intracellular melanin decreased significantly only with 200 μM. For 2-IPM samples, 1, 2 and four mM concentrations were tested. At one mM, melanin synthesis by α-MSH induced B16F10 was not inhibited indicated by high melanin synthesis. However, both 2 and four mM showed significant reduction of melanin contents (Figure 7.4).

7.4 Discussion

As demand to find novel skin-brightening agents are increasing, I investigated the potential skin-brightening effect of 2-IPM by observing tyrosinase inhibitory activity in this study. From the *in vitro* tyrosinase inhibitory activity assay, 2-IPM showed some inhibitory activity as shown in Figure 7.1. However, compared to the positive control, arbutin, 2-IPM had significantly lower tyrosinase inhibitory activity at all concentrations tested. Additionally, malate (malic acid) was used as a structural control to 2-IPM, and tyrosinase inhibitory of 2-IPM and malate was similar.

Although tyrosinase activity of 2-IPM was lower than the positive control arbutin, I hypothesized 2-IPM still can be a good skin-brightening agent. A previous study (**Chapter VI**) reports overproduction of 2-IPM in engineered yeast up to 25 g/L indicating secretion of 2-IPM is not a limiting. Typically, transport of charged molecules such as organic acids heavily depended on surrounding pH and known as one of the bottlenecks for overproducing in the microbial system. However, 2-IPM production in yeast had no apparent inhibition of secretion. Thus, cell permeability of 2-IPM can be better compared to other organic acids. It is advantageous to have better permeability as a skin-brightening agent because tyrosinase activity or melanin synthesis occurs inside the cell. To test relative cell permeability, yeast cells were inoculated in either 2-IPM and malic acid at various pH ranges, and intracellular accumulation was observed. As shown in Figure 7.3, intracellular 2-IPM accumulation was superior compared to malic acid at any given pH. The result indicates 2-IPM has relatively good cell permeability.

Next, *in vivo* tyrosinase inhibition activity assay was performed by measuring extracellular and intracellular melanin contents of the B16F10 cells. Four mM of 2-IPM was tested as the highest sample concentration due to a possible cell cytotoxicity with concentrations higher than four mM (Figure 7.3). At a 2-IPM concentration of 2 mM, both extracellular and intracellular melanin concentration decreased demonstrating effective inhibition 2-IPM on melanogenesis. Although the effective 2-IPM dose compared to arbutin was about 10-fold higher, arbutin is potentially carcinogenic (Figure 7.4). In Europe, for example, prohibited usage of arbutin in any cosmetic products. Thus, I compared other commonly known skin-brightening agents in the literature. Though various system and concentration were used, common skin-whitening agents such as ascorbic acid derivatives (Ethyl ascorbyl ether, ascorbyl glucoside, magnesium ascorbyl phosphate, ascorbyl tetraisopalmiate, etc.) and niacinamide,

had an effective concentration typically ranging from around 100 μM to 30 mM for ascorbic acid derivatives and 1 mM to 5 mM for niacinamide [171-174]. Therefore, 2-IPM is a competitive compared to ascorbic acid derivatives and niacinamide as a skin-brightening agent.

In summary, I investigated the potential of 2-IPM as a novel skin-brightening agent. Due to superior relative cell permeability, 2-IPM can be an effective skin-whitening agent, and effective doses are comparable to current commercialized skin-brightening agents. Thus, further investigation of skin-brightening effect on human skins should be pursued, and I anticipate 2-IPM as an active ingredient in skin-care products in the future.

7.5 Figures and tables

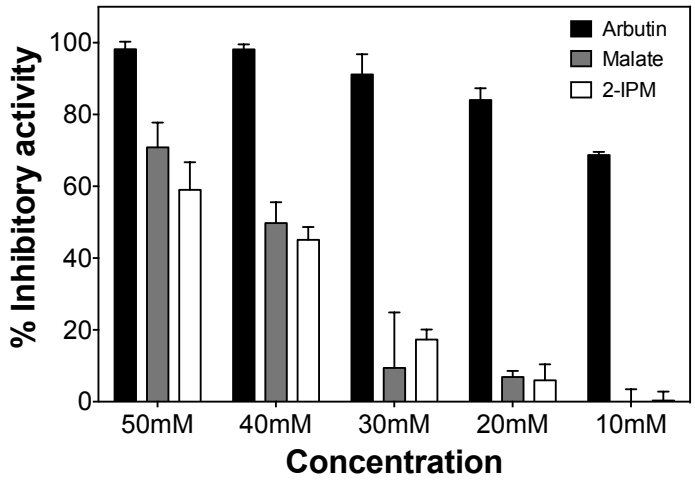

Figure 7.1 Tyrosinase inhibitory activity of arbutin, malate, and 2-IPM. Various concentrations of chemicals were tested.

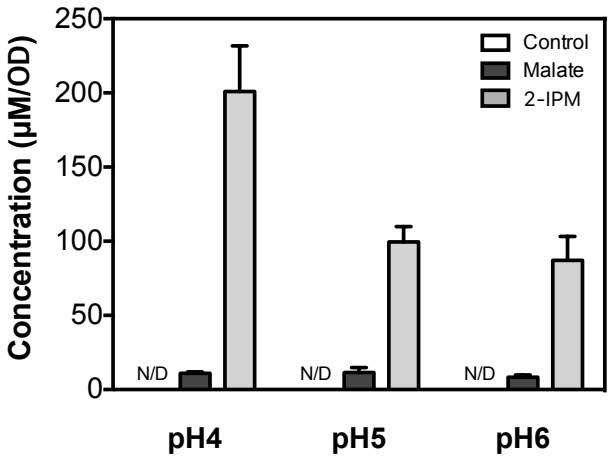

Figure 7.2 Intracellular detection of 2-IPM and malate. Strains were incubated with either water, malate or 2-IPM at various pH ranges then measured the intracellular accumulation of 2-IPM.

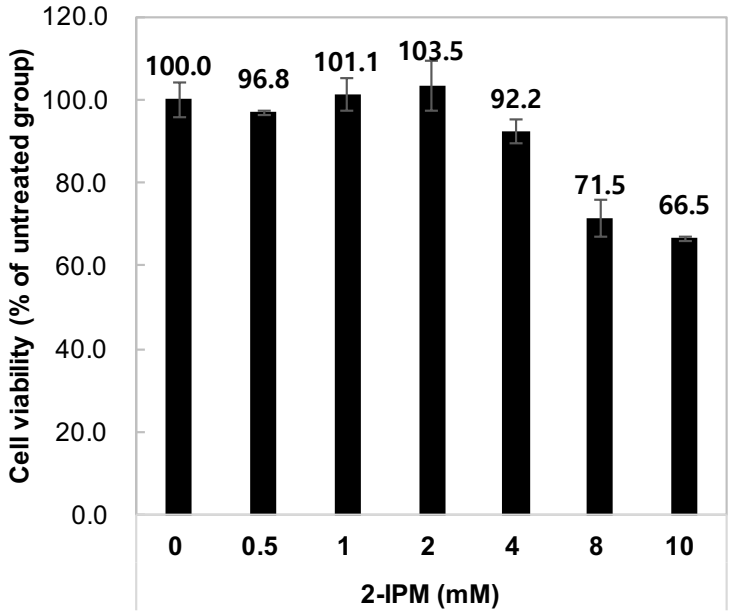

Figure 7.3 Cytotoxicity of 2-IPM on B16F10 cell. Various concentrations of 2-IPM were tested for cell viability, calculated by a fraction of viable cells compared to untreated group.

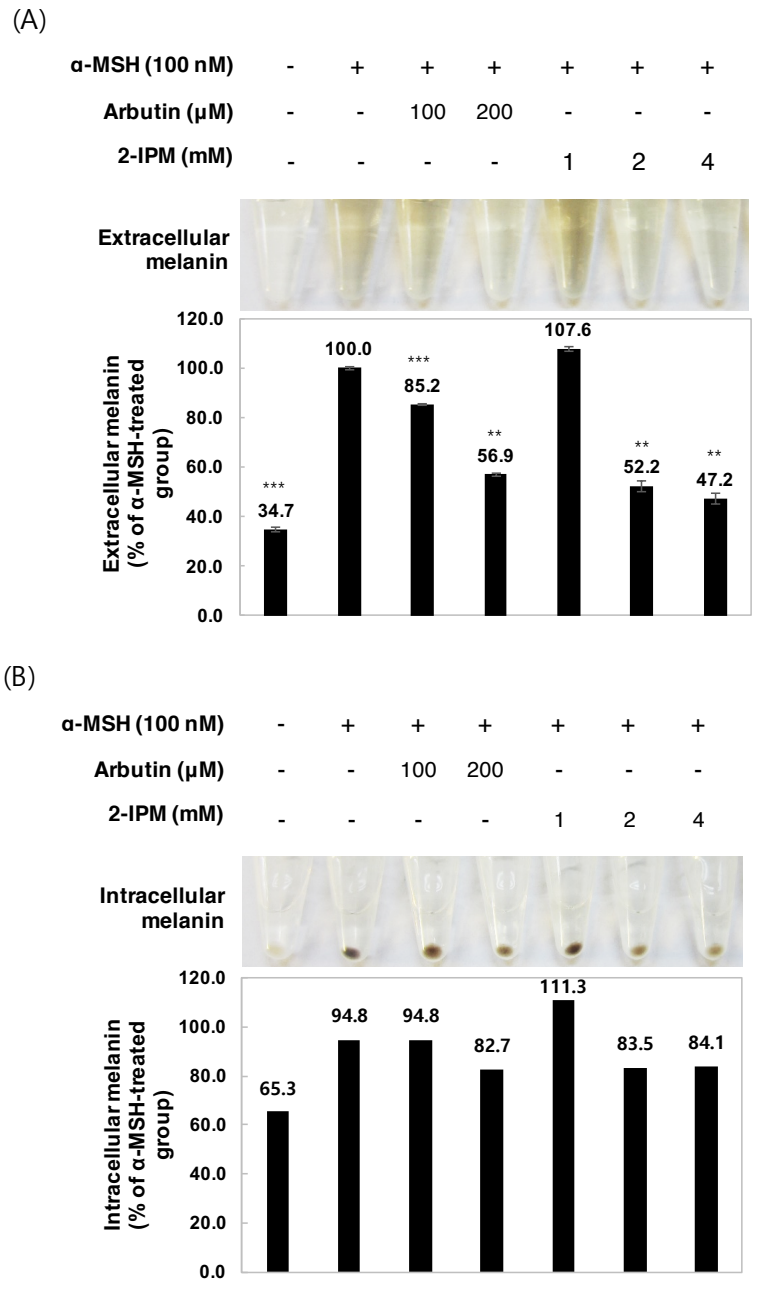

Figure 7.4 Effect of 2-IPM on α-MSH-induced melanogenesis in B16F10 cells. Cells were induced for melanogenesis by α-MSH and treated with either arbutin or 2-IPM. After five days of incubation, extracellular (A) and intracellular (B) melanin was measured.

Chapter VIII: Summary and Future Studies

8.1 Summary

Microbial engineering to produce valuable fuels and chemicals have been gained considerable attention as a sustainable alternative solution to current energy and chemical synthesis. To make this option sustainable, feasible, and environmentally friendly, it is essential to develop an engineered microbial strain that can utilize renewable feedstocks such as lignocellulosic biomass. Lignocellulosic biomass can be broken down to several sugars (mainly xylose and cellobiose) that can be used for microbial fermentations. However, cellobiose and xylose cannot be assimilated by the industrial microorganisms, such as traditional industrial yeast *Saccharomyces cerevisiae.* To utilize cellobiose or xylose for the fuel and chemical production by *S. cerevisiae* strains, heterologous expression of cellobiose or xylose metabolizing genes are required. Thus, the initial study of this dissertation investigates on developing optimal yeast strains for utilizing renewable resources (cellobiose, xylose, and galactose) and underlying mechanism for efficient fermentation.

First, the cellobiose fermentation in engineered *S. cerevisiae* was investigated (**Chapter II**). *S. cerevisiae* can be engineered to ferment cellobiose by expressing a cellodextrin transporter and cellobiose hydrolyzing enzyme. Two cellodextrin transporters (CDT-1 and CDT-2) were previously identified in *N. crassa*, but their kinetic properties and efficiency for cellobiose fermentation have not been studied in detail. In this study, CDT-1 and CDT-2, which are hypothesized to transport cellodextrin with distinct mechanisms, were introduced into *S. cerevisiae* along with an intracellular β-glucosidase (BGL). Cellobiose transport assays with the resulting strains indicated that CDT-1 is a proton symporter while CDT-2 is a simple facilitator. A strain expressing CDT-1 and GH1-1 (DBT-1) showed faster cellobiose fermentation than the strain expressing CDT-2 and GH1-1 (DBT-2) under various culture conditions with different medium compositions and aeration levels. While CDT-2 is expected to have energetic benefits, the expression levels and kinetic properties of CDT-1 in *S. cerevisiae* appears to be optimum for cellobiose fermentation. These results suggest CDT-1 is a more effective cellobiose transporter than CDT-2 for engineering *S. cerevisiae* to ferment cellobiose.

However, regardless of enhanced cellobiose fermentation by CDT-1, I investigated CDT-2 transporter further due to its potential advantage (**Chapter II**). Heterologous expression of

cellobiose metabolizing enzymes requires extra energy for *S. cerevisiae.* The passive CDT-2 transporter does not require energy whereas active CDT-1 transporter requires energy. This suggests that the CDT-2 might be engineered to provide energetic benefits over the active transporter in cellobiose fermentation. I, therefore, attempted to improve cellobiose transporting activity of CDT-2 through laboratory evolution. Nine rounds of a serial subculture of *S. cerevisiae* expressing CDT-2 and cellobiose phosphorylase (less ATP-requiring enzyme compared to BGL), on cellobiose led to the isolation of an evolved strain capable of fermenting cellobiose to ethanol 10-fold faster than the original strain. After sequence analysis of the isolated CDT-2, a single point mutation on CDT-2 (N306I) was revealed to be responsible for enhanced cellobiose fermentation. Also, the engineered strain expressing the mutant CDT-2 with cellobiose phosphorylase showed a higher ethanol yield than the engineered strain expressing CDT-1 and intracellular β-glucosidase under anaerobic conditions, suggesting that CDT-2 coupled with cellobiose phosphorylase may be better choices for efficient production of cellulosic ethanol with the engineered yeast.

After investigation of cellobiose fermentation, xylose fermentation in *S. cerevisiae* was studied in **Chapter IV**. Previously, improved xylose-fermenting *S. cerevisiae* strains were developed. However, the efficiency of xylose utilization can be improved further. With an assumption that xylose fermentation phenotype is complex, QTL analysis approach was taken. Two strains harboring different xylose fermentation capability (S288C X123 and JAY291 X123), were crossed and recombinant segregants were obtained. The pool of segregants was grown under xylose condition to enrich the superior xylose fermenters. Then the whole genome of the population was mapped, and QTL analysis was performed. Although clear QTL peaks were identified, however, genes affecting xylose fermentation were not discovered.

In **Chapter V**, enhanced glucose and galactose fermentation were achieved by screening and investigating the 50 gene targets related to glucose sensing, signaling transduction, metabolism and stress responses. Initially, Δ*TPS1* strains showed enhanced glucose and galactose fermentation. However, this observation led to the prediction of presence suppressor mutation because previous research reported lethality of Δ*TPS1* under glucose condition. By whole genome sequencing, I found one mutation at *HXK2* (mHXK2) rescued the Δ*TPS1* lethality. Also, m*HXK2* changed the glucose repression phenotype. In the end, both

m*HXK2* and Δ*TPS1* allowed enhanced glucose or galactose utilization and mixed sugar fermentation.

The second part of this dissertation focuses on the production of value-added chemicals. Specifically, novel organic acid production was investigated (**Chapter VI**). 2-isopropylmalate (2-IPM), an intermediate of leucine biosynthesis, was observed by leucine auxotrophic strain. Because organic acids are highly valuable to the industries for their diverse usage, *S. cerevisiae* strain was metabolically engineered to overproduce 2-IPM. Δ*LEU1* was required to accumulate 2-IPM initially, *URE2* was deleted to remove nitrogen catabolite repression, a mutation at *LEU4* was introduced to remove leucine feedback inhibition, and *BsAlsS* was expressed for enhanced pyruvate flux to leucine biosynthetic pathway. The resulting engineered strains produced 25 g/L glucose under limited glucose fed batch fermentation. There is no apparent usage of 2-IPM. Thus, potential applications were investigated to synthesize biodegradable polymer and skin-brightening agent (**Chapter VII**).

8.2 Future research directions

Although this dissertation provides advances in using engineered yeast to produce value-added fuels and chemicals, major barriers remain to achieve efficient microbial platform. The efficiency of renewable sugars (cellobiose, xylose, and galactose) utilization is still not as efficient compared to conventional glucose fermentation. Also, renewable sugars are derived from pretreating lignocellulosic or marine biomass which generates fermentation inhibitors during hydrolysis process. Engineered yeasts fermenting renewable sugars should be able to tolerate the inhibitors.

One of the specific future research that can be achieved is re-investigation of xylose genome sequences from QTL analysis (**Chapter IV**). With different bioinformatics tool, different aspects of the data can be analyzed such as gene amplifications that occurred during enrichment, etc. Secondly, 2-IPM production can be improved (**Chapter VI**). With finding promising applications of 2-IPM, higher production demand can be anticipated. For instance, 2-IPM overproducing strains can be further engineered to consume renewable sugars. With these goals achieved, efficient production of bio-based production from renewable resources can be achieved in the future.

REFERENCE

1. Hubbert, M.K. *Nuclear energy and the fossil fuel*. in *Drilling and production practice*. 1956. American Petroleum Institute.
2. Escobar, J.C., et al., *Biofuels: environment, technology and food security.* Renewable and sustainable energy reviews, 2009. **13**(6): p. 1275-1287.
3. Nigam, P.S. and A. Singh, *Production of liquid biofuels from renewable resources.* Progress in energy and combustion science, 2011. **37**(1): p. 52-68.
4. Berg, P. and A. Boland, *Analysis of ultimate fossil fuel reserves and associated co2 emissions in ipcc scenarios.* Natural resources research, 2014. **23**(1): p. 141-158.
5. Davis, S.C., K.J. Anderson-Teixeira, and E.H. DeLucia, *Life-cycle analysis and the ecology of biofuels.* Trends in plant science, 2009. **14**(3): p. 140-146.
6. Dessler, A. and L.S.C. Theater, *The science of climate change.* 2002.
7. Friedlingstein, P., et al., *Persistent growth of CO2 emissions and implications for reaching climate targets.* Nature geoscience, 2014. **7**(10): p. 709-715.
8. Jarboe, L.R., et al., *Metabolic engineering for production of biorenewable fuels and chemicals: contributions of synthetic biology.* BioMed Research International, 2010. **2010**.
9. Ro, D.-K., et al., *Production of the antimalarial drug precursor artemisinic acid in engineered yeast.* Nature, 2006. **440**(7086): p. 940-943.
10. Saxena, R., et al., *Microbial production of 1, 3-propanediol: recent developments and emerging opportunities.* Biotechnology advances, 2009. **27**(6): p. 895-913.
11. Jakočiūnas, T., M.K. Jensen, and J.D. Keasling, *CRISPR/Cas9 advances engineering of microbial cell factories.* Metabolic engineering, 2016. **34**: p. 44-59.
12. Jones, C.S. and S.P. Mayfield, *Algae biofuels: versatility for the future of bioenergy.* Current opinion in biotechnology, 2012. **23**(3): p. 346-351.
13. Wei, N., J. Quarterman, and Y.-S. Jin, *Marine macroalgae: an untapped resource for producing fuels and chemicals.* Trends in biotechnology, 2013. **31**(2): p. 70-77.
14. Mohanty, A., M. Misra, and L. Drzal, *Sustainable bio-composites from renewable resources: opportunities and challenges in the green materials world.* Journal of Polymers and the Environment, 2002. **10**(1-2): p. 19-26.
15. Abbott, D.A., et al., *Metabolic engineering of Saccharomyces cerevisiae for production of carboxylic acids: current status and challenges.* FEMS yeast research, 2009. **9**(8): p. 1123-1136.
16. Goldemberg, J., *Ethanol for a sustainable energy future.* science, 2007. **315**(5813): p. 808-810.
17. Farrell, A.E., et al., *Ethanol can contribute to energy and environmental goals.* Science, 2006. **311**(5760): p. 506-508.
18. Pimentel, D., et al., *Food versus biofuels: environmental and economic costs.* Human ecology, 2009. **37**(1): p. 1-12.
19. Viikari, L., J. Vehmaanperä, and A. Koivula, *Lignocellulosic ethanol: from science to industry.* Biomass and Bioenergy, 2012. **46**: p. 13-24.
20. Foust, T.D., et al., *An economic and environmental comparison of a biochemical and a thermochemical lignocellulosic ethanol conversion processes.* Cellulose, 2009. **16**(4): p. 547-565.
21. Schmer, M.R., et al., *Net energy of cellulosic ethanol from switchgrass.* Proceedings of the National Academy of Sciences, 2008. **105**(2): p. 464-469.

22. Almeida, J.R., et al., *Increased tolerance and conversion of inhibitors in lignocellulosic hydrolysates by Saccharomyces cerevisiae.* Journal of chemical technology and biotechnology, 2007. **82**(4): p. 340-349.
23. Holden, H.M., I. Rayment, and J.B. Thoden, *Structure and function of enzymes of the Leloir pathway for galactose metabolism.* Journal of Biological Chemistry, 2003. **278**(45): p. 43885-43888.
24. Kim, S.R., et al., *Simultaneous co-fermentation of mixed sugars: a promising strategy for producing cellulosic ethanol.* Trends in biotechnology, 2012. **30**(5): p. 274-282.
25. Kötter, P. and M. Ciriacy, *Xylose fermentation by Saccharomyces cerevisiae.* Applied microbiology and biotechnology, 1993. **38**(6): p. 776-783.
26. Tantirungkij, M., et al., *Construction of xylose-assimilating Saccharomyces cerevisiae.* Journal of Fermentation and Bioengineering, 1993. **75**(2): p. 83-88.
27. Ho, N.W., Z. Chen, and A.P. Brainard, *Genetically engineered Saccharomycesyeast capable of effective cofermentation of glucose and xylose.* Applied and Environmental Microbiology, 1998. **64**(5): p. 1852-1859.
28. Jin, Y.-S., et al., *Conversion of xylose to ethanol by recombinant Saccharomyces cerevisiae containing genes for xylose reductase and xylitol dehydrogenase from Pichia stipitis.* Journal of microbiology and biotechnology, 2000. **10**(4): p. 564-567.
29. Eliasson, A., et al., *The xylose reductase/xylitol dehydrogenase/xylulokinase ratio affects product formation in recombinant xylose-utilising Saccharomyces cerevisiae.* Enzyme and Microbial Technology, 2001. **29**(4): p. 288-297.
30. Jin, Y.-S., et al., *Optimal growth and ethanol production from xylose by recombinant Saccharomyces cerevisiae require moderate D-xylulokinase activity.* Applied and Environmental Microbiology, 2003. **69**(1): p. 495-503.
31. Yu, S., H. Jeppsson, and B. Hahn-Hägerdal, *Xylulose fermentation by Saccharomyces cerevisiae and xylose-fermenting yeast strains.* Applied microbiology and biotechnology, 1995. **44**(3-4): p. 314-320.
32. Meinander, N.Q., I. Boels, and B. Hahn-Hägerdal, *Fermentation of xylose/glucose mixtures by metabolically engineered Saccharomyces cerevisiae strains expressing XYL1 and XYL2 from Pichia stipitis with and without overexpression of TAL1.* Bioresource technology, 1999. **68**(1): p. 79-87.
33. Hahn-Hägerdal, B., et al., *Metabolic engineering for pentose utilization in Saccharomyces cerevisiae*, in *Biofuels*. 2007, Springer. p. 147-177.
34. Verho, R., et al., *Engineering redox cofactor regeneration for improved pentose fermentation in Saccharomyces cerevisiae.* Applied and Environmental Microbiology, 2003. **69**(10): p. 5892-5897.
35. Kuyper, M., et al., *High-level functional expression of a fungal xylose isomerase: the key to efficient ethanolic fermentation of xylose by Saccharomyces cerevisiae?* FEMS yeast research, 2003. **4**(1): p. 69-78.
36. Kuyper, M., et al., *Metabolic engineering of a xylose-isomerase-expressing Saccharomyces cerevisiae strain for rapid anaerobic xylose fermentation.* FEMS yeast research, 2005. **5**(4-5): p. 399-409.
37. Zhou, H., et al., *Xylose isomerase overexpression along with engineering of the pentose phosphate pathway and evolutionary engineering enable rapid xylose utilization and ethanol production by Saccharomyces cerevisiae.* Metabolic engineering, 2012. **14**(6): p. 611-622.
38. Walfridsson, M., et al., *Xylose-metabolizing Saccharomyces cerevisiae strains overexpressing the TKL1 and TAL1 genes encoding the pentose phosphate pathway*

enzymes transketolase and transaldolase. Applied and environmental microbiology, 1995. **61**(12): p. 4184-4190.
39. Kim, S.R., et al., *Deletion of PHO13, encoding haloacid dehalogenase type IIA phosphatase, results in upregulation of the pentose phosphate pathway in Saccharomyces cerevisiae.* Applied and environmental microbiology, 2015. **81**(5): p. 1601-1609.
40. Xu, H., et al., *PHO13 deletion-induced transcriptional activation prevents sedoheptulose accumulation during xylose metabolism in engineered Saccharomyces cerevisiae.* Metabolic engineering, 2016. **34**: p. 88-96.
41. Galazka, J.M., et al., *Cellodextrin transport in yeast for improved biofuel production.* Science, 2010. **330**(6000): p. 84-86.
42. Ha, S.-J., et al., *Single amino acid substitutions in HXT2. 4 from Scheffersomyces stipitis lead to improved cellobiose fermentation by engineered Saccharomyces cerevisiae.* Applied and environmental microbiology, 2013. **79**(5): p. 1500-1507.
43. Kim, H., et al., *Analysis of cellodextrin transporters from Neurospora crassa in Saccharomyces cerevisiae for cellobiose fermentation.* Applied microbiology and biotechnology, 2014. **98**(3): p. 1087-1094.
44. Ha, S.-J., et al., *Engineered Saccharomyces cerevisiae capable of simultaneous cellobiose and xylose fermentation.* Proceedings of the National Academy of Sciences, 2011. **108**(2): p. 504-509.
45. Ha, S.-J., et al., *Energetic benefits and rapid cellobiose fermentation by Saccharomyces cerevisiae expressing cellobiose phosphorylase and mutant cellodextrin transporters.* Metabolic engineering, 2013. **15**: p. 134-143.
46. Li, S., et al., *Overcoming glucose repression in mixed sugar fermentation by co-expressing a cellobiose transporter and a β-glucosidase in Saccharomyces cerevisiae.* Molecular BioSystems, 2010. **6**(11): p. 2129-2132.
47. Bohlin, C., et al., *A comparative study of hydrolysis and transglycosylation activities of fungal β-glucosidases.* Applied microbiology and biotechnology, 2013. **97**(1): p. 159-169.
48. Yoon, J.J., et al. *Production of polysaccharides and corresponding sugars from red seaweed*. in *Advanced Materials Research*. 2010. Trans Tech Publ.
49. Siso, M.G., *The biotechnological utilization of cheese whey: a review.* Bioresource Technology, 1996. **57**(1): p. 1-11.
50. Timson, D.J., *Galactose metabolism in Saccharomyces cerevisiae.* Dyn Biochem Process Biotechnol Mol Biol, 2007. **1**(1): p. 63-73.
51. Ostergaard, S., et al., *Physiological studies in aerobic batch cultivations of Saccharomyces cerevisiae strains harboring the MEL1 gene.* Biotechnology and bioengineering, 2000. **68**(3): p. 252-259.
52. Ostergaard, S., et al., *Increasing galactose consumption by Saccharomyces cerevisiae through metabolic engineering of the GAL gene regulatory network.* Nature biotechnology, 2000. **18**(12): p. 1283-1286.
53. Lee, K.S., et al., *Improved galactose fermentation of Saccharomyces cerevisiae through inverse metabolic engineering.* Biotechnology and bioengineering, 2011. **108**(3): p. 621-631.
54. Hong, K.-K., et al., *Unravelling evolutionary strategies of yeast for improving galactose utilization through integrated systems level analysis.* Proceedings of the National Academy of Sciences, 2011. **108**(29): p. 12179-12184.
55. Matar, S. and L.F. Hatch, *Chemistry of petrochemical processes*. 2001: Gulf Professional Publishing.

56. Kolb, H.C., M. Finn, and K.B. Sharpless, *Click chemistry: diverse chemical function from a few good reactions.* Angewandte Chemie International Edition, 2001. **40**(11): p. 2004-2021.
57. Jambeck, J.R., et al., *Plastic waste inputs from land into the ocean.* Science, 2015. **347**(6223): p. 768-771.
58. Nonato, R., P. Mantelatto, and C. Rossell, *Integrated production of biodegradable plastic, sugar and ethanol.* Applied Microbiology and Biotechnology, 2001. **57**(1-2): p. 1-5.
59. Ishida, N., et al., *The effect of pyruvate decarboxylase gene knockout in Saccharomyces cerevisiae on L-lactic acid production.* Bioscience, biotechnology, and biochemistry, 2006. **70**(5): p. 1148-1153.
60. Turner, T.L., et al., *Lactic acid production from xylose by engineered Saccharomyces cerevisiae without PDC or ADH deletion.* Applied microbiology and biotechnology, 2015. **99**(19): p. 8023-8033.
61. Auras, R.A., et al., *Poly (lactic acid): synthesis, structures, properties, processing, and applications*. Vol. 10. 2011: John Wiley & Sons.
62. Yan, D., et al., *Construction of reductive pathway in Saccharomyces cerevisiae for effective succinic acid fermentation at low pH value.* Bioresource technology, 2014. **156**: p. 232-239.
63. Agren, R., J.M. Otero, and J. Nielsen, *Genome-scale modeling enables metabolic engineering of Saccharomyces cerevisiae for succinic acid production.* Journal of industrial microbiology & biotechnology, 2013. **40**(7): p. 735-747.
64. Otero, J.M., et al., *Industrial systems biology of Saccharomyces cerevisiae enables novel succinic acid cell factory.* PloS one, 2013. **8**(1): p. e54144.
65. Bailey, J.E., *Toward a science of metabolic engineering.* Science, 1991. **252**(5013): p. 1668-1675.
66. Ran, F.A., et al., *Genome engineering using the CRISPR-Cas9 system.* Nature protocols, 2013. **8**(11): p. 2281-2308.
67. Zhang, G.-C., et al., *Construction of a Quadruple Auxotrophic Mutant of an Industrial Polyploid Saccharomyces cerevisiae Strain by Using RNA-Guided Cas9 Nuclease.* Applied and Environmental Microbiology, 2014. **80**(24): p. 7694-7701.
68. Liu, Y., et al., *Global metabolite profiling and diagnostic ion filtering strategy by LC–QTOF MS for rapid identification of raw and processed pieces of Rheum palmatum L.* Food chemistry, 2016. **192**: p. 531-540.
69. Shen, Y., et al., *Quantitative metabolic network profiling of Escherichia coli: An overview of analytical methods for measurement of intracellular metabolites.* TrAC Trends in Analytical Chemistry, 2016. **75**: p. 141-150.
70. Stephanopoulos, G. and A.J. Sinskey, *Metabolic engineering—methodologies and future prospects.* Trends in biotechnology, 1993. **11**(9): p. 392-396.
71. Kim, S.R., et al., *High expression of XYL2 coding for xylitol dehydrogenase is necessary for efficient xylose fermentation by engineered Saccharomyces cerevisiae.* Metabolic engineering, 2012. **14**(4): p. 336-343.
72. Kim, S.R., et al., *Strain engineering of Saccharomyces cerevisiae for enhanced xylose metabolism.* Biotechnology advances, 2013. **31**(6): p. 851-861.
73. Chen, R., *Enzyme engineering: rational redesign versus directed evolution.* Trends in biotechnology, 2001. **19**(1): p. 13-14.
74. Sauer, U., *Evolutionary engineering of industrially important microbial phenotypes*, in *Metabolic engineering*. 2001, Springer. p. 129-169.

75. Petri, R. and C. Schmidt-Dannert, *Dealing with complexity: evolutionary engineering and genome shuffling.* Current opinion in biotechnology, 2004. **15**(4): p. 298-304.
76. Woolston, B.M., S. Edgar, and G. Stephanopoulos, *Metabolic engineering: past and future.* Annual review of chemical and biomolecular engineering, 2013. **4**: p. 259-288.
77. Nevoigt, E., *Progress in metabolic engineering of Saccharomyces cerevisiae.* Microbiology and Molecular Biology Reviews, 2008. **72**(3): p. 379-412.
78. Kim, S.R., et al., *Rational and evolutionary engineering approaches uncover a small set of genetic changes efficient for rapid xylose fermentation in Saccharomyces cerevisiae.* PloS one, 2013. **8**(2): p. e57048.
79. Alper, H., K. Miyaoku, and G. Stephanopoulos, *Construction of lycopene-overproducing E. coli strains by combining systematic and combinatorial gene knockout targets.* Nature biotechnology, 2005. **23**(5): p. 612-616.
80. Liu, B.H., *Statistical genomics: linkage, mapping, and QTL analysis*. 1997: CRC press.
81. Kruglyak, L. and E.S. Lander, *A nonparametric approach for mapping quantitative trait loci.* Genetics, 1995. **139**(3): p. 1421-1428.
82. Brem, R.B. and L. Kruglyak, *The landscape of genetic complexity across 5,700 gene expression traits in yeast.* Proceedings of the National Academy of Sciences of the United States of America, 2005. **102**(5): p. 1572-1577.
83. Marullo, P., et al., *Single QTL mapping and nucleotide-level resolution of a physiologic trait in wine Saccharomyces cerevisiae strains.* FEMS yeast research, 2007. **7**(6): p. 941-952.
84. Hirasawa, T., C. Furusawa, and H. Shimizu, *Saccharomyces cerevisiae and DNA microarray analyses: what did we learn from it for a better understanding and exploitation of yeast biotechnology?* Applied microbiology and biotechnology, 2010. **87**(2): p. 391-400.
85. Dikicioglu, D., P. Pir, and S.G. Oliver, *Predicting complex phenotype–genotype interactions to enable yeast engineering: Saccharomyces cerevisiae as a model organism and a cell factory.* Biotechnology journal, 2013. **8**(9): p. 1017-1034.
86. Wilkening, S., et al., *An evaluation of high-throughput approaches to QTL mapping in Saccharomyces cerevisiae.* Genetics, 2014. **196**(3): p. 853-865.
87. Swinnen, S., J.M. Thevelein, and E. Nevoigt, *Genetic mapping of quantitative phenotypic traits in Saccharomyces cerevisiae.* FEMS yeast research, 2012. **12**(2): p. 215-227.
88. den Haan, R., et al., *Engineering Saccharomyces cerevisiae for next generation ethanol production.* Journal of chemical technology and biotechnology, 2013. **88**(6): p. 983-991.
89. Hu, X., et al., *Genetic dissection of ethanol tolerance in the budding yeast Saccharomyces cerevisiae.* Genetics, 2007. **175**(3): p. 1479-1487.
90. Shapouri, H. and M. Salassi, *The economic feasibility of ethanol production from sugar in the United States*. 2006: United States Department of Agriculture.
91. Wyman, C.E., *What is (and is not) vital to advancing cellulosic ethanol.* TRENDS in Biotechnology, 2007. **25**(4): p. 153-157.
92. Kumar, R., S. Singh, and O.V. Singh, *Bioconversion of lignocellulosic biomass: biochemical and molecular perspectives.* Journal of industrial microbiology & biotechnology, 2008. **35**(5): p. 377-391.
93. Haki, G. and S. Rakshit, *Developments in industrially important thermostable enzymes: a review.* Bioresource Technology, 2003. **89**(1): p. 17-34.
94. Lynd, L.R., et al., *Microbial cellulose utilization: fundamentals and biotechnology.* Microbiology and molecular biology reviews, 2002. **66**(3): p. 506-577.

95. Shen, Y., et al., *Simultaneous saccharification and fermentation of acid-pretreated corncobs with a recombinant< i> Saccharomyces cerevisiae</i> expressing β-glucosidase.* Bioresource Technology, 2008. **99**(11): p. 5099-5103.
96. Sikorski, R.S. and P. Hieter, *A system of shuttle vectors and yeast host strains designed for efficient manipulation of DNA in Saccharomyces cerevisiae.* Genetics, 1989. **122**(1): p. 19-27.
97. Hosaka, K., et al., *A dominant mutation that alters the regulation of INO1 expression in Saccharomyces cerevisiae.* Journal of biochemistry, 1992. **111**(3): p. 352-358.
98. Ha, S.J., et al., *Engineered Saccharomyces cerevisiae capable of simultaneous cellobiose and xylose fermentation.* Proceedings of the National Academy of Sciences, 2011. **108**(2): p. 504-509.
99. Cussler, E., R. Aris, and A. Bhown, *On the limits of facilitated diffusion.* Journal of membrane science, 1989. **43**(2): p. 149-164.
100. Postma, E., W. Alexander Scheffers, and J.P. Van Dijken, *Kinetics of growth and glucose transport in glucose-limited chemostat cultures of Saccharomyces cerevisiae CBS 8066.* Yeast, 1989. **5**(3): p. 159-165.
101. Santos, E., et al., *Uptake of sucrose by Saccharomyces cerevisiae.* Archives of biochemistry and biophysics, 1982. **216**(2): p. 652-660.
102. Weusthuis, R.A., et al., *Energetics and kinetics of maltose transport in Saccharomyces cerevisiae: a continuous culture study.* Applied and environmental microbiology, 1993. **59**(9): p. 3102-3109.
103. Bhat, K.M., J.S. Gaikwad, and R. Maheshwari, *Purification and characterization of an extracellular β-glucosidase from the thermophilic fungus Sporotrichum thermophile and its influence on cellulase activity.* Microbiology, 1993. **139**(11): p. 2825-2832.
104. Park, T.-H., et al., *Substrate specificity and transglycosylation catalyzed by a thermostable β-glucosidase from marine hyperthermophile Thermotoga neapolitana.* Applied microbiology and biotechnology, 2005. **69**(4): p. 411-422.
105. Nombela, C., C. Gil, and W.L. Chaffin, *Non-conventional protein secretionin yeast.* Trends in microbiology, 2006. **14**(1): p. 15-21.
106. Giuliani, F., A. Grieve, and C. Rabouille, *Unconventional secretion: a stress on GRASP.* Current opinion in cell biology, 2011. **23**(4): p. 498-504.
107. Spiro, S. and J.R. Guest, *Adaptive responses to oxygen limitation in< i> Escherichia coli</i>.* Trends in biochemical sciences, 1991. **16**: p. 310-314.
108. Hahn-Hägerdal, B., et al., *Bio-ethanol–the fuel of tomorrow from the residues of today.* Trends in biotechnology, 2006. **24**(12): p. 549-556.
109. Jin, Y.-S., et al., *Improvement of xylose uptake and ethanol production in recombinant Saccharomyces cerevisiae through an inverse metabolic engineering approach.* Applied and environmental microbiology, 2005. **71**(12): p. 8249-8256.
110. Katahira, S., et al., *Ethanol fermentation from lignocellulosic hydrolysate by a recombinant xylose-and cellooligosaccharide-assimilating yeast strain.* Applied microbiology and biotechnology, 2006. **72**(6): p. 1136-1143.
111. Lau, M.W. and B.E. Dale, *Cellulosic ethanol production from AFEX-treated corn stover using Saccharomyces cerevisiae 424A (LNH-ST).* Proceedings of the National Academy of Sciences, 2009. **106**(5): p. 1368-1373.
112. Zhang, Y.H.P. and L.R. Lynd, *Toward an aggregated understanding of enzymatic hydrolysis of cellulose: noncomplexed cellulase systems.* Biotechnology and bioengineering, 2004. **88**(7): p. 797-824.

113. Ha, S.-J., et al., *Continuous co-fermentation of cellobiose and xylose by engineered Saccharomyces cerevisiae.* Bioresource technology, 2013. **149**: p. 525-531.
114. Sadie, C.J., et al., *Co-expression of a cellobiose phosphorylase and lactose permease enables intracellular cellobiose utilisation by Saccharomyces cerevisiae.* Applied microbiology and biotechnology, 2011. **90**(4): p. 1373-1380.
115. van Maris, A.J., et al., *Alcoholic fermentation of carbon sources in biomass hydrolysates by Saccharomyces cerevisiae: current status.* Antonie Van Leeuwenhoek, 2006. **90**(4): p. 391-418.
116. Kelley, L.A., et al., *The Phyre2 web portal for protein modeling, prediction and analysis.* Nature protocols, 2015. **10**(6): p. 845-858.
117. Humphrey, W., A. Dalke, and K. Schulten, *VMD: visual molecular dynamics.* Journal of molecular graphics, 1996. **14**(1): p. 33-38.
118. Lian, J., et al., *Directed evolution of a cellodextrin transporter for improved biofuel production under anaerobic conditions in Saccharomyces cerevisiae.* Biotechnology and bioengineering, 2014. **111**(8): p. 1521-1531.
119. Ryan, O.W., et al., *Selection of chromosomal DNA libraries using a multiplex CRISPR system.* Elife, 2014. **3**: p. e03703.
120. Znameroski, E.A., et al., *Evidence for transceptor function of cellodextrin transporters in Neurospora crassa.* Journal of Biological Chemistry, 2014. **289**(5): p. 2610-2619.
121. Ha, S.-J., et al., *Cofermentation of cellobiose and galactose by an engineered Saccharomyces cerevisiae strain.* Applied and environmental microbiology, 2011. **77**(16): p. 5822-5825.
122. Casa, A.M., et al., *The MITE family Heartbreaker (Hbr): molecular markers in maize.* Proceedings of the National Academy of Sciences, 2000. **97**(18): p. 10083-10089.
123. Gupta, P. and S. Rustgi, *Molecular markers from the transcribed/expressed region of the genome in higher plants.* Functional & integrative genomics, 2004. **4**(3): p. 139-162.
124. Miles, C. and M. Wayne, *Quantitative trait locus (QTL) analysis.* Nature Education, 2008. **1**(1): p. 208.
125. Beavis, W.D., *QTL analyses: power, precision, and accuracy.* Molecular dissection of complex traits, 1998. **1998**: p. 145-162.
126. Brauer, M.J., et al., *Mapping novel traits by array-assisted bulk segregant analysis in Saccharomyces cerevisiae.* Genetics, 2006. **173**(3): p. 1813-1816.
127. Ehrenreich, I.M., et al., *Dissection of genetically complex traits with extremely large pools of yeast segregants.* Nature, 2010. **464**(7291): p. 1039-1042.
128. Magwene, P.M., J.H. Willis, and J.K. Kelly, *The statistics of bulk segregant analysis using next generation sequencing.* PLoS Comput Biol, 2011. **7**(11): p. e1002255.
129. Liti, G. and E.J. Louis, *Advances in quantitative trait analysis in yeast.* PLoS Genet, 2012. **8**(8): p. e1002912-e1002912.
130. Takagi, H., et al., *QTL-seq: rapid mapping of quantitative trait loci in rice by whole genome resequencing of DNA from two bulked populations.* The Plant Journal, 2013. **74**(1): p. 174-183.
131. Maurer, M.J., et al., *QTL-guided metabolic engineering of a complex trait.* ACS Synthetic Biology, 2016.
132. Tsai, C.S., et al., *Rapid and marker-free refactoring of xylose-fermenting yeast strains with Cas9/CRISPR.* Biotechnology and bioengineering, 2015. **112**(11): p. 2406-2411.
133. Gietz, R.D. and R.H. Schiestl, *High-efficiency yeast transformation using the LiAc/SS carrier DNA/PEG method.* Nature protocols, 2007. **2**(1): p. 31-34.

134. Tong, A.H.Y., et al., *Systematic genetic analysis with ordered arrays of yeast deletion mutants.* Science, 2001. **294**(5550): p. 2364-2368.
135. Zhang, G.-C., et al., *Combining C6 and C5 sugar metabolism for enhancing microbial bioconversion.* Current opinion in chemical biology, 2015. **29**: p. 49-57.
136. Carlson, M., *Glucose repression in yeast.* Current opinion in microbiology, 1999. **2**(2): p. 202-207.
137. Celenza, J.L. and M. Carlson, *A yeast gene that is essential for release from glucose repression encodes a protein kinase.* Science, 1986. **233**: p. 1175-1181.
138. Trumbly, R., *Glucose repression in the yeast Saccharomyces cerevisiae.* Molecular microbiology, 1992. **6**(1): p. 15-21.
139. Kuttykrishnan, S., et al., *A quantitative model of glucose signaling in yeast reveals an incoherent feed forward loop leading to a specific, transient pulse of transcription.* Proceedings of the National Academy of Sciences, 2010. **107**(38): p. 16743-16748.
140. Wilson, W.A., S.A. Hawley, and D.G. Hardie, *Glucose repression/derepression in budding yeast: SNF1 protein kinase is activated by phosphorylation under derepressing conditions, and this correlates with a high AMP: ATP ratio.* Current Biology, 1996. **6**(11): p. 1426-1434.
141. Mumberg, D., R. Müller, and M. Funk, *Yeast vectors for the controlled expression of heterologous proteins in different genetic backgrounds.* Gene, 1995. **156**(1): p. 119-122.
142. Teusink, B., et al., *The danger of metabolic pathways with turbo design.* Trends in biochemical sciences, 1998. **23**(5): p. 162-169.
143. van Heerden, J.H., et al., *Lost in transition: start-up of glycolysis yields subpopulations of nongrowing cells.* Science, 2014. **343**(6174): p. 1245114.
144. Brachmann, C.B., et al., *Designer deletion strains derived from Saccharomyces cerevisiae S288C: a useful set of strains and plasmids for PCR-mediated gene disruption and other applications.* YEAST-CHICHESTER-, 1998. **14**: p. 115-132.
145. Eastmond, P.J. and I.A. Graham, *Trehalose metabolism: a regulatory role for trehalose-6-phosphate?* Current opinion in plant biology, 2003. **6**(3): p. 231-235.
146. Ernandes, J.R., et al., *During the initiation of fermentation overexpression of hexokinase PII in yeast transiently causes a similar deregulation of glycolysis as deletion of Tps1.* Yeast, 1998: p. 255-269.
147. KRAAKMAN, L.S., et al., *Structure–function analysis of yeast hexokinase: structural requirements for triggering cAMP signalling and catabolite repression.* Biochemical journal, 1999. **343**(1): p. 159-168.
148. Behlke, J., et al., *Hexokinase 2 from Saccharomyces cerevisiae: regulation of oligomeric structure by in vivo phosphorylation at serine-14.* Biochemistry, 1998. **37**(34): p. 11989-11995.
149. Winston, F., C. Dollard, and S.L. Ricupero-Hovasse, *Construction of a set of convenient Saccharomyces cerevisiae strains that are isogenic to S288C.* Yeast, 1995. **11**(1): p. 53-55.
150. Miller, S.A., *Sustainable polymers: opportunities for the next decade*. 2013, ACS Publications.
151. Tsui, A., Z.C. Wright, and C.W. Frank, *Biodegradable polyesters from renewable resources.* Annual review of chemical and biomolecular engineering, 2013. **4**: p. 143-170.
152. Xu, J. and B.H. Guo, *Poly (butylene succinate) and its copolymers: research, development and industrialization.* Biotechnology journal, 2010. **5**(11): p. 1149-1163.

153. Morschbacker, A., *Bio-ethanol based ethylene.* Journal of Macromolecular Science®, Part C: Polymer Reviews, 2009. **49**(2): p. 79-84.
154. Xiong, M., et al., *Scalable production of mechanically tunable block polymers from sugar.* Proceedings of the National Academy of Sciences, 2014. **111**(23): p. 8357-8362.
155. Sai, T., *α-Isopropylmalic Acid Accumulation by Leucine-requiring Yeast Mutants.* Agricultural and Biological Chemistry, 1968. **32**(4): p. 522-524.
156. van Hoek, W., et al., *Fermentative Capacity in High-Cell-Density Fed-Batch Cultures of Bakers' Yeast.* Fermentative Capacity in Aerobic Cultures of Bakers' Yeast, 2000: p. 89.
157. DeZeeuw, J.R. and I. Stasko, *Fermentation process for production of alpha-isopropylmalic acid*. 1983, Google Patents.
158. Kim, S., et al., *Evaluation and optimization of metabolome sample preparation methods for Saccharomyces cerevisiae.* Analytical chemistry, 2013. **85**(4): p. 2169-2176.
159. Meador, M.A.B., et al., *On the oxidative degradation of nadic endcapped polyimides: I. Effect of thermocycling on weight loss and crack formation.* High Performance Polymers, 1996. **8**(3): p. 363-379.
160. DiCiccio, A.M. and G.W. Coates, *Ring-opening copolymerization of maleic anhydride with epoxides: a chain-growth approach to unsaturated polyesters.* Journal of the American Chemical Society, 2011. **133**(28): p. 10724-10727.
161. Courchesne, W.E. and B. Magasanik, *Regulation of nitrogen assimilation in Saccharomyces cerevisiae: roles of the URE2 and GLN3 genes.* Journal of bacteriology, 1988. **170**(2): p. 708-713.
162. Kim, S.-J., et al., *Production of 2, 3-butanediol by engineered Saccharomyces cerevisiae.* Bioresource technology, 2013. **146**: p. 274-281.
163. Oba, T., et al., *Asp578 in LEU4p is one of the key residues for leucine feedback inhibition release in sake yeast.* Bioscience, biotechnology, and biochemistry, 2005. **69**(7): p. 1270-1273.
164. Maeda, K. and M. Fukuda, *Arbutin: mechanism of its depigmenting action in human melanocyte culture.* Journal of Pharmacology and Experimental Therapeutics, 1996. **276**(2): p. 765-769.
165. Blaut, M., et al., *Mutagenicity of arbutin in mammalian cells after activation by human intestinal bacteria.* Food and chemical toxicology, 2006. **44**(11): p. 1940-1947.
166. McGregor, D., *Hydroquinone: an evaluation of the human risks from its carcinogenic and mutagenic properties.* Critical reviews in toxicology, 2007. **37**(10): p. 887-914.
167. Korner, A. and J. Pawelek, *Mammalian tyrosinase catalyzes three reactions in the biosynthesis of melanin.* Science, 1982. **217**(4565): p. 1163-1165.
168. Lerner, A.B., et al., *Mammalian tyrosinase: preparation and properties.* Journal of Biological Chemistry, 1949. **178**(1): p. 185-195.
169. Masuda, M., et al., *Skin lighteners: An overview of the skin-lightening market in Japan, including an introduction to two new active ingredients.* Cosmetics and toiletries, 1996. **111**(10): p. 65-77.
170. Mishima, Y., Y. Oyama, and M. Kurimoto, *Skin-whitening agent*. 1993, Google Patents.
171. Shimada, Y., et al., *Effects of ascorbic acid on gingival melanin pigmentation in vitro and in vivo.* Journal of periodontology, 2009. **80**(2): p. 317-323.
172. Austria, R., A. Semenzato, and A. Bettero, *Stability of vitamin C derivatives in solution and topical formulations.* Journal of pharmaceutical and biomedical analysis, 1997. **15**(6): p. 795-801.

173. Ma, H.J., et al., *Efficacy of quantifying melanosome transfer with flow cytometry in a human melanocyte–HaCaT keratinocyte co-culture system in vitro.* Experimental dermatology, 2010. **19**(8).
174. Hakozaki, T., et al., *The effect of niacinamide on reducing cutaneous pigmentation and suppression of melanosome transfer.* British Journal of Dermatology, 2002. **147**(1): p. 20-31.